AFCRL-63-157

TECHNICAL REPORT 400-76

THE EXACT SYNTHESIS OF DISTRIBUTED RC NETWORKS

Ralph W. Wyndrum, Jr.

NEW YORK UNIVERSITY
COLLEGE OF ENGINEERING
DEPARTMENT OF ELECTRICAL ENGINEERING
Laboratory for Electroscience Research

University Heights
New York 53, New York

THIRD SCIENTIFIC REPORT

Contract AF 19(628)-379
Project 5628
Task 562801

May 1963

Prepared
for

AIR FORCE CAMBRIDGE RESEARCH LABORATORIES
OFFICE OF AEROSPACE RESEARCH
UNITED STATES AIR FORCE
BEDFORD, MASSACHUSETTS

NOTICE

Requests for additional copies by Agencies of the Department of Defense, their contractors, and other Government agencies should be directed to the:

DEFENSE DOCUMENTATION CENTER (DDC)
ARLINGTON HALL STATION
ARLINGTON 12, VIRGINIA

Department of Defense contractors must be established for DDC services or have their "need-to-know" certified by the cognizant military agency of their project or contract.

All other persons and organizations should apply to the:

U. S. DEPARTMENT OF COMMERCE
OFFICE OF TECHNICAL SERVICES
WASHINGTON 25, D. C.

ACKNOWLEDGEMENT

The research reported herein received partial sponsorship from both the Air Force Cambridge Research Laboratories, under contract AF 19(628)-379, and the American Machine and Foundry Corporation. This assistance is gratefully acknowledged.

ABSTRACT

The research reported in this thesis is devoted to the development of network synthesis techniques which are exact and applicable to distributed RC functions. Complex variable transformations are introduced which greatly simplify the representation and use of the hyperbolic complex frequency functions of distributed RC structures. Realizability conditions are given for the existence of distributed RC driving point and transfer functions, and the actual synthesis techniques are described in detail. Examples of the methods introduced herein are verified by experimental data.

TABLE OF CONTENTS

LIST OF ILLUSTRATIONS

CHAPTER ONE

AN INTRODUCTION TO DISTRIBUTED RC NETWORKS

1.0 Introduction

Common objectives in the use of microminiature network techniques are to increase system reliability, to lower cost, and to reduce overall network size by orders of magnitude. An attractive possibility for achieving these aims is the use of distributed circuitry, i.e., electrical networks made of three or more homogeneous layers. To date, mathematical and physical complexity have restricted the distributed network designer to simple RC distributed networks, hereafter referred to as $\overline{RC}$ networks. Such circuits do not require interconnecting leads, as do lumped elements, thus decreasing size and greatly increasing operational reliability. Network deposition on a masked substrate can be accomplished by several physical and chemical techniques.[1,2,9]

1.1 Summary of Previous Research

Although a large body of papers[1-3,7-14] have discussed the $\overline{RC}$ network problem, comparatively few significant results applicable to the synthesis of such networks with prescribed characteristics have been obtained. Present design procedures require the designer to consider a large number of previously analyzed $\overline{RC}$ circuits,[1,2,3] and match the desired characteristic with those available. Often, the problem in commercial microelectronics is solved with small discrete elements, and a concurrent loss of packing density and reliability.

As more information becomes available concerning $\overline{RC}$ lines, these elements have greater appeal for practical microelectronics. The characteristics of an $\overline{RC}$ line, an incremental section of which is shown in Fig. 1-1, have not been determined for arbitrary density functions r(x) and c(x). The differential equation for the $\overline{RC}$ line voltage and current have been solved[4,5,6,7,21] for special cases. The simplest case occurs when r and c are independent of distance x, i.e., the uniform $\overline{RC}$ ($\overline{URC}$) line of Fig. 1-2. If r(x) is proportional to e^{kx} and c(x) is inversely proportional to e^{kx}, i.e., the exponential $\overline{RC}$ ($\overline{ERC}$) line of Fig. 1-3, another class of solutions[9] has been derived. From both classes the Z parameters of a length L of $\overline{RC}$ line may be obtained.

Truncation techniques to approximate a finite pole-zero pattern by a distributed network with an infinite number of poles and zeros have been applied in special cases.[9,12-15] These methods are fruitful where dominant poles exist near the $j\omega$ axis, and poles far removed from the axis may be neglected. Potential analogs may be used to adjust the pole-zero locations for the desired responses along the $j\omega$ axis. If no dominant poles exist, such cut-and-try techniques are tedious, and of limited application.

Computers have been used to find frequency characteristics for particular $\overline{RC}$ configurations, such as $\overline{URC}$ and $\overline{ERC}$ notch filters of Fig. 1-4. Computer solutions are necessary, since these networks involve complicated hyperbolic transfer functions.[8,9] Control of the notch frequency by a single element, independent of the $\overline{RC}$ network, has been suggested by Castro.[1] The network structure and design curves have been given by Wyndrum.[10]

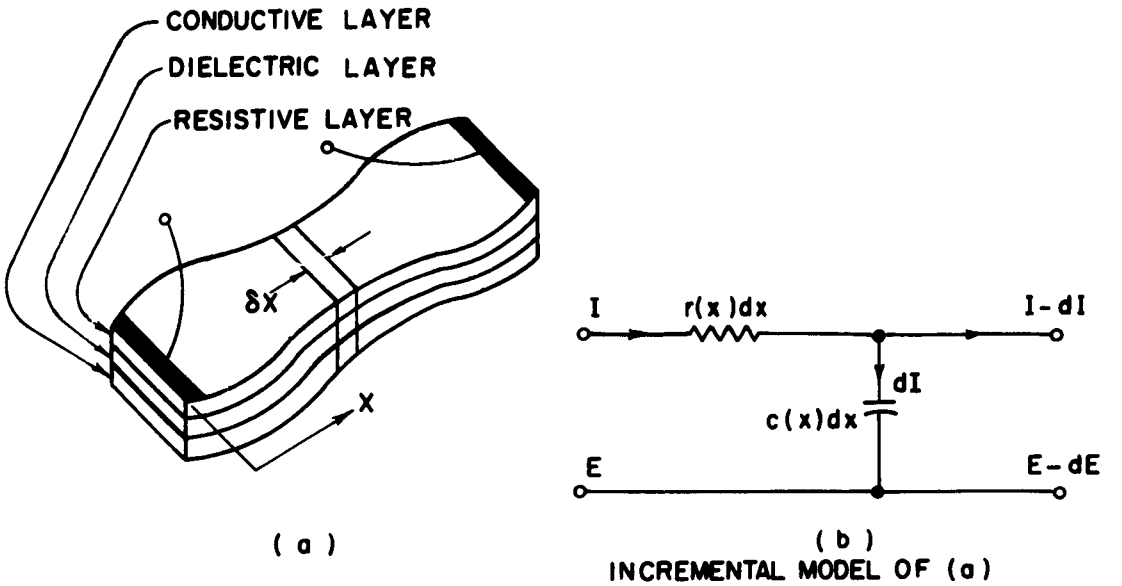

FIG. 1-1

$\overline{RC}$ LINE WITH ARBITRARY GEOMETRY

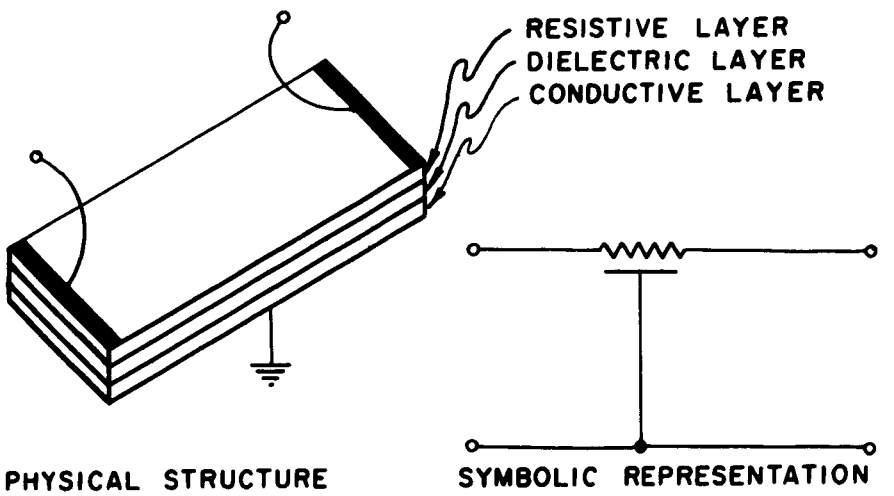

FIG. 1-2

UNIFORM $\overline{RC}$ LINE

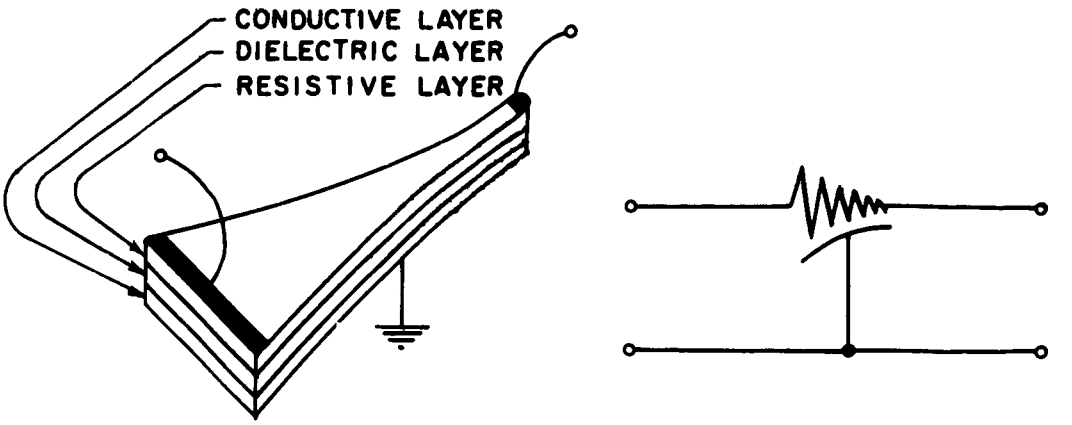

PHYSICAL STRUCTURE SYMBOLIC REPRESENTATION

FIG. 1-3

EXPONENTIAL $\overline{RC}$ LINE

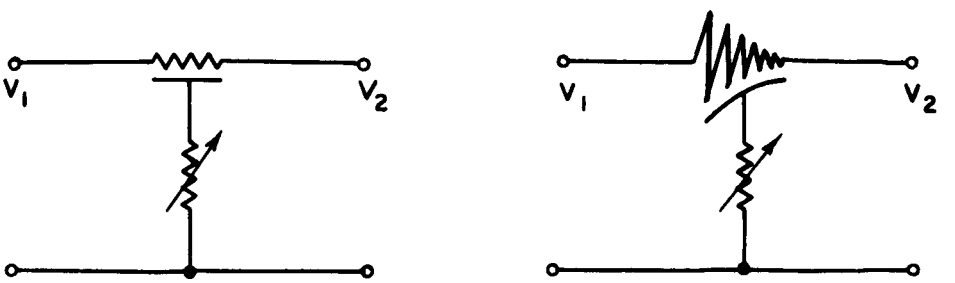

(a)
U$\overline{RC}$ FILTER

(b)
E$\overline{RC}$ FILTER

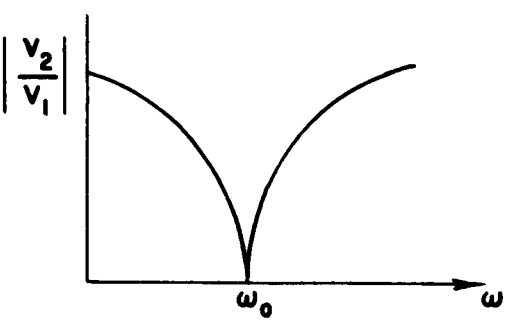

(c)
TYPICAL GAIN FUNCTION

FIG. 1-4

NOTCH FILTERS

1.2 Mathematical Model of the $\overline{RC}$ Segment

An incremental model of the $\overline{RC}$ line is depicted in Fig. 1-1. The differential equations for E and I, assuming signal transmission in the x direction only, arise from

$$\frac{dE}{dx} = r(x)\ I \tag{1}$$

$$\frac{dI}{dx} = sc(x)\ E\ . \tag{3}$$

Combination of (1) and (2) yields

$$E'' - (r'/r)\ E' - scrE = 0 \tag{3}$$

$$I'' - (c'/c)\ I' - scrI = 0 \tag{4}$$

where the prime indicates differentiation with respect to x. When (3) and (4) are solved for a finite line length, with prescribed terminal conditions as done in Appendix II for the $\overline{URC}$ line, the two-port $\overline{RC}$ segment Z-parameters may be found.

Since the incremental $\overline{RC}$ line voltages and currents are in general functions of x, y and time, they must be solved for as a two dimensional field problem. The partial differential equations, subject to the proper boundary conditions, are derived in Appendix II. Boundary conditions suitable to a rectangular geometry with uniform cross section are then applied and the potential and current density functions are found. The thickness of the dielectric is assumed to be very small, as discussed in Appendix II.

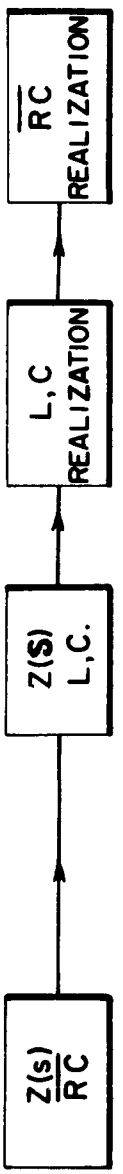

FIG. 1-5

SYNTHESIS PROCEDURE

If $r(x)$ and $c(x)$ have constant value, R_o and C_o, respectively, the solutions of (3) and (4) are exponential functions of x. These solutions exist when the line is of uniform cross section. For this case,

$$z_{11} = z_{22} = \frac{R_o \coth \sqrt{sR_oC_oL^2}}{\sqrt{sR_oC_o}} \tag{5}$$

and

$$z_{12} = z_{21} = \frac{R_o \operatorname{csch} \sqrt{sR_oC_oL^2}}{\sqrt{sR_oC_o}} \tag{6}$$

1.3 Proposed $\overline{RC}$ Synthesis Technique

The research reported in this dissertation develops $\overline{RC}$ synthesis techniques which are exact, analytic, and suitable for wide-band design. Conformal, positive-real transformations permit hyperbolic $\overline{RC}$ network functions to be expressed as ratios of polynomials of finite order. The method employed herein derives its strength from the large body of realization techniques available for lumped networks. In particular, a lumped LC synthesis method is also shown to be an $\overline{RC}$ method. Carried over to the $\overline{RC}$ embodiment, certain LC techniques are found preferable to others. The general procedure involves a transformation from the s-plane to the S plane, illustrated in Fig. 1-5.

1.4 Summary of Accomplishments

Chapter Two is devoted to the mathematical characterization of the uniform $\overline{RC}$ ($U\overline{RC}$) segment which is the building block for later synthesis techniques. The hyperbolic frequency functions associated with $U\overline{RC}$ networks are investigated, and a transformation is introduced which

simplifies the representation of such functions. This transformation is the basis for the synthesis techniques in the remainder of this dissertation.

Additionally in Chapter Two, a four layer $\overline{RCR}$ network is suggested, and mathematically characterized. The $\overline{URCR}$ network is shown to possess frequency characteristics which are related to those of the $\overline{URC}$ network by a single transformation.

Chapter Three discusses the analytical representation of $\overline{RC}$ network functions in the original complex frequency plane of definition (the s plane). These representations occur as ratios of polynomials which are rational in $e^{a\sqrt{s}}$, with the foreknowledge that under the transformation to the S plane (see Fig. 1-5), namely

$$e^{a\sqrt{s}} = \frac{1 + S}{1 - S}$$

the resulting expressions are rational in S. The hyperbolic functional description is motivated by the knowledge that uniform $\overline{RC}$ networks are exactly characterized by hyperbolic network functions with an infinity of poles and zeros.

In Chapter Four, the material of Chapters Two and Three are employed to derive realizability conditions on $\overline{RC}$ driving point immittances in terms of the exponential polynomials. Methods are described to attain any realizable $\overline{RC}$ driving point immittance as a practical, one-piece cascade of segments of $\overline{RC}$ line; the characteristics of each segment are prescribed by the synthesis technique using Richard's Theorem.

Chapter Five extends the techniques of Chapter Four to transfer function synthesis. Since cascaded $\overline{RC}$ structures inherently possess all of their transmission zeros at infinity, a modification of the cascade structure is introduced to achieve finite transmission zeros. Stubs are employed at prescribed intervals along the in-line cascade. Realizability conditions outline the classes of functions achieved by this technique in terms of the exponential polynomials interpreted in Chapter Three.

Chapter Six considers the problems of building practical $\overline{RC}$ networks by the methods described in earlier chapters. The design of a low pass filter with prescribed cutoff characteristics illustrates the proper use of the exponential polynomials to approximate a given plot of gain versus frequency.

Chapter Seven summarizes the conclusions resulting from this research.

CHAPTER TWO

THE MATHEMATICAL CHARACTERIZATION OF $\overline{RC}$ FUNCTIONS

2.0 Introduction

In this chapter the two-port parameters of the several distributed network segments to be employed in future chapters are derived. Upon completion of the representation of $\overline{URC}$ networks, a conformal transformation is suggested. By definition of a new complex frequency variable, $S = \tanh(a\sqrt{s}/2)$, the network functions assume a simpler, non-transcendental form, noted in Corollaries II and III.

In Section 2.3, a similar treatment is given to a new class of distributed networks, the $\overline{URCR}$ segments. A second transformation, in addition to the one above, permits straightforward characterization of the $\overline{URCR}$ parameters by non-hyperbolic expressions.

The most desirable physical realization employing $\overline{URC}$O two-ports is the cascade configuration (Fig. 2-1(a)). This configuration is preferable for available microelectronic fabrication techniques, since it minimizes the number of fabrication steps, and eliminates most elemental interconnections which otherwise would be required. A general $\overline{RC}$ synthesis technique which always results in a cascade embodiment is achieved in Chapter Four.

Other possible connections are illustrated in Fig. 2-1. All possess at least one of the following serious disadvantages, compared to the cascade structure:

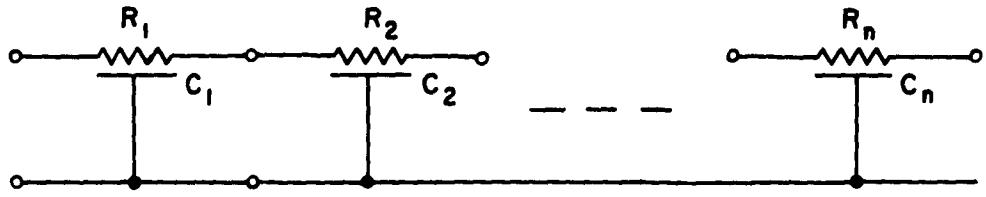

(a)

CASCADE CONFIGURATION OF $\overline{RC}$ TWO PORTS

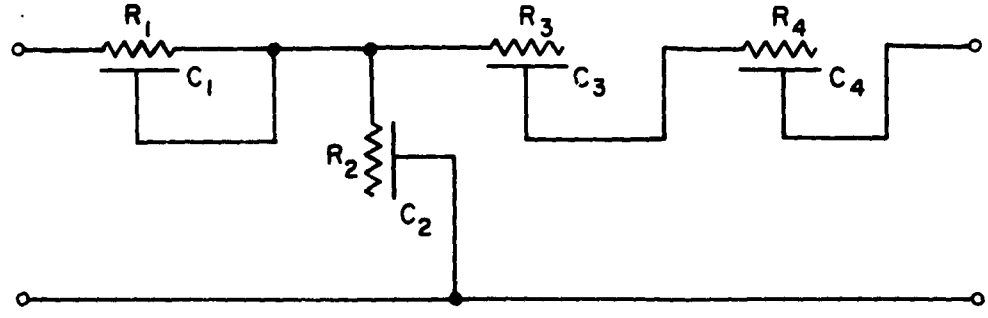

(b)

LADDER CONNECTION OF $\overline{RC}$ TWO PORTS

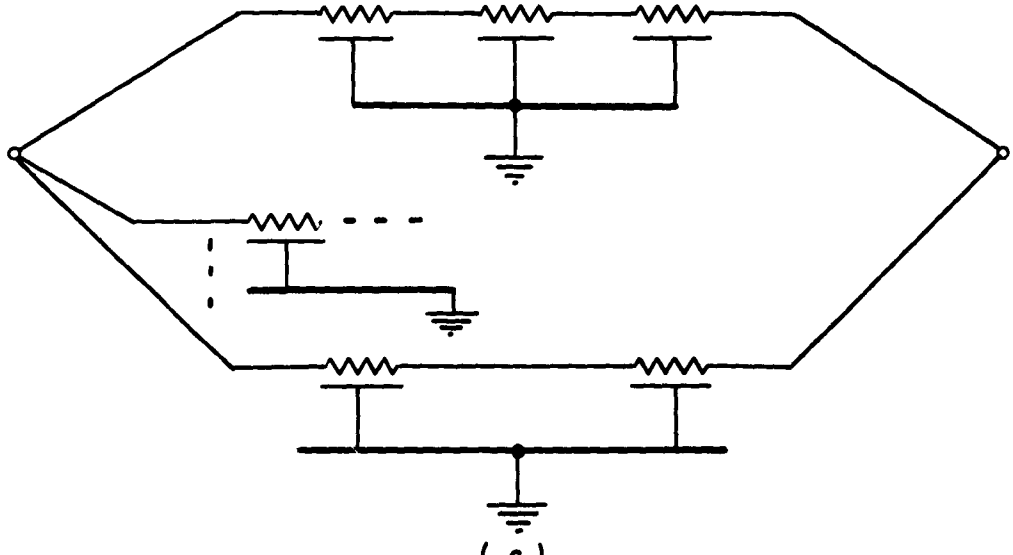

(c)

PARALLEL CASCADES OF $\overline{RC}$ TWO PORTS

FIG. 2-1

POSSIBLE INTERCONNECTIONS OF $\overline{RC}$ NETWORKS

1) The use of but one port of each elemental two-port,

2) The possibility of ungrounded one-port multilayered structures,

3) A large number of (possibly unreliable) interconnections,

4) Excessive network area.

2.1 $\overline{\text{URC}}$ Segments

Prior to the synthesis of cascaded $\overline{\text{RC}}$ networks, it is necessary to investigate the individual segments and the classes of driving point immittances which may be synthesized with them, and outline the fundamental mathematical ideas used in the development. Later, when $\overline{\text{RC}}$ immittances realized with cascaded sections are developed, the cascade realizability conditions are found to be identical with those developed in Theorems IV, V and VI.

The network of Fig. 2-2(c), with the output open circuited, has the impedance matrix,

$$Z = \begin{bmatrix} \dfrac{R_o \coth L\sqrt{sR_oC_o}}{\sqrt{sR_oC_o}} & \dfrac{R_o \operatorname{csch} L\sqrt{sR_oC_o}}{\sqrt{sR_oC_o}} \\ \dfrac{R_o \operatorname{csch} L\sqrt{sR_oC_o}}{\sqrt{sR_oC_o}} & \dfrac{R_o \coth L\sqrt{sR_oC_o}}{\sqrt{sR_oC_o}} \end{bmatrix} \tag{1}$$

If the network is terminated in an arbitrary Z_L, as in Fig. 2-2(a), its driving point impedance is

$$Z_{in} = \frac{\left(\dfrac{R_o \coth L\sqrt{sR_oC_o}}{\sqrt{sR_oC_o}}\right)\left(Z_L + \dfrac{R_o \coth L\sqrt{sR_oC_o}}{\sqrt{sR_oC_o}}\right) - \left(\dfrac{R_o}{\sqrt{sR_oC_o}\sinh L\sqrt{sR_oC_o}}\right)^2}{\left(Z_L + \dfrac{R_o \coth L\sqrt{sR_oC_o}}{\sqrt{sR_oC_o}}\right)} \tag{2}$$

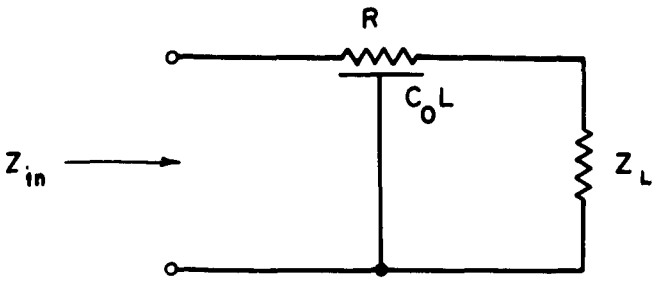

(a)

$\overline{URC}$ NETWORK TERMINAL IN ARBITRARY LOAD

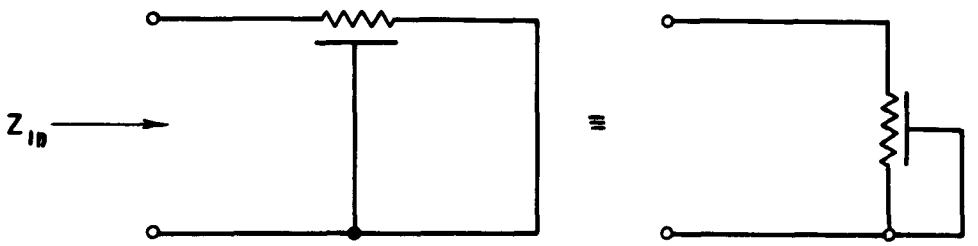

(b)

$\overline{URCS}$ ONE PORT

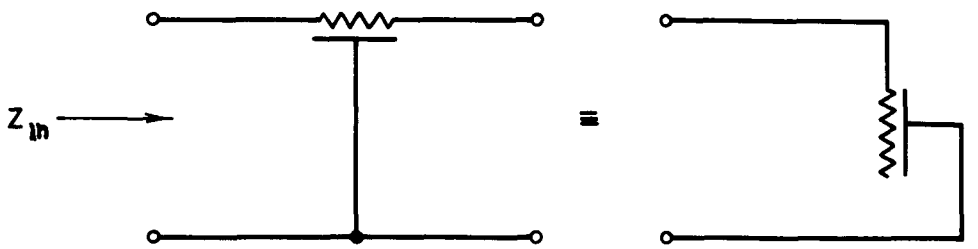

(c)

$\overline{URCO}$ ONE PORT

FIG. 2-2

$\overline{URC}$ ONE – PORTS

R_o and C_o are constant impedance density functions in ohms per unit length and farads per unit length respectively. If $Z_L \equiv 0$, the $\overline{URC}$ output port is short circuited and effectively a $\overline{URCS}$ one port is left for which (Fig. 2-2(b))

$$Z_{in_s}(s) = \frac{1}{Y_{11}} = \frac{R_o \tanh L\sqrt{sR_oC_o}}{\sqrt{sR_oC_o}} \tag{3}$$

If $Z_L = \infty$, an $\overline{URCO}$ one-port is obtained which is characterized by

$$Z_{in_o} = Z_{11} = \frac{R_o \coth L\sqrt{sR_oC_o}}{\sqrt{sR_oC_o}} \tag{4}$$

Note at this point that an $\overline{LC}$ impedance in the $\sqrt{s}$ plane is obtained from an $\overline{RC}$ impedance in the s plane by multiplying the RC impedance by $\sqrt{s}$. The resulting impedance, considered in the $\sqrt{s}$ plane, represents that of a uniform $\overline{LC}$ network. Mathematically,[22]

Theorem I. If $Z_{RC}(s)$ is the driving point (DP) impedance of an $\overline{RC}$ network, $Z_{LC}(\sqrt{s}) = \sqrt{s}\, Z_{RC}(s)$ is the driving point impedance of a reactive network in the $\sqrt{s}$ plane.

Corollary I. If $Y_{RC}(s)$ is the DP admittance of an $\overline{RC}$ network, $Y_{LC}(\sqrt{s}) = \frac{1}{\sqrt{s}}\, Y_{RC}(s)$ is the driving point admittance of an LC network in the $\sqrt{s}$ plane.

Thus (3) and (4) become respectively

$$Z_{in_s}(\sqrt{s}) = \frac{\sqrt{s}\, R_o \tanh L\sqrt{sR_oC_o}}{\sqrt{sR_oC_o}} = \sqrt{\frac{R_o}{C_o}} \tanh\left(\sqrt{s}\,\sqrt{R_oC_oL^2}\right) \tag{5a}$$

$$Z_{1no}(\sqrt{s}) = \frac{\sqrt{s}\, R_o \coth L\sqrt{sR_oC_o}}{\sqrt{sR_oC_o}} = \sqrt{\frac{R_o}{C_o}} \coth\left(\sqrt{s}\sqrt{R_oC_oL^2}\right) \quad (5b)$$

These are recognized as driving point impedances of $\overline{LC}$ lines in the $\sqrt{s}$ plane.

2.2 The S → s Transformations: Applications to $\overline{RC}$ Functions

Consider the positive real mapping*

$$S(\sqrt{s}) = \frac{c \sinh^2\left(\frac{a\sqrt{s}}{2}\right) + d}{\cosh\frac{a\sqrt{s}}{2} \sinh\frac{a\sqrt{s}}{2}} \quad (6)$$

$$c \text{ and } d \text{ real}, \; 0 > c \geq d.$$

This transformation is the sum of two transformations which may form the basis for the reduction of distributed system functions to lumped system functions. For d = 0 and c = 1, (6) reduces to

$$S_1(\sqrt{s}) = \tanh(a\sqrt{s}/2) = \frac{e^{a\sqrt{s}} - 1}{e^{a\sqrt{s}} + 1} \quad (7)$$

and for d = c = 1, (6) reduces to

$$S_2(\sqrt{s}) = \coth(a\sqrt{s}/2) = \frac{e^{a\sqrt{s}} + 1}{e^{a\sqrt{s}} - 1} \; . \quad (8)$$

*F(s) is a positive real mapping of s if with $s = \sigma + j\omega$
a) F(s) is analytic for $\sigma > 0$.
b) F(σ) is real.
c) $\sigma \geq 0$ maps into Re F(s) ≥ 0.
See pages 357 ff. of reference 22.

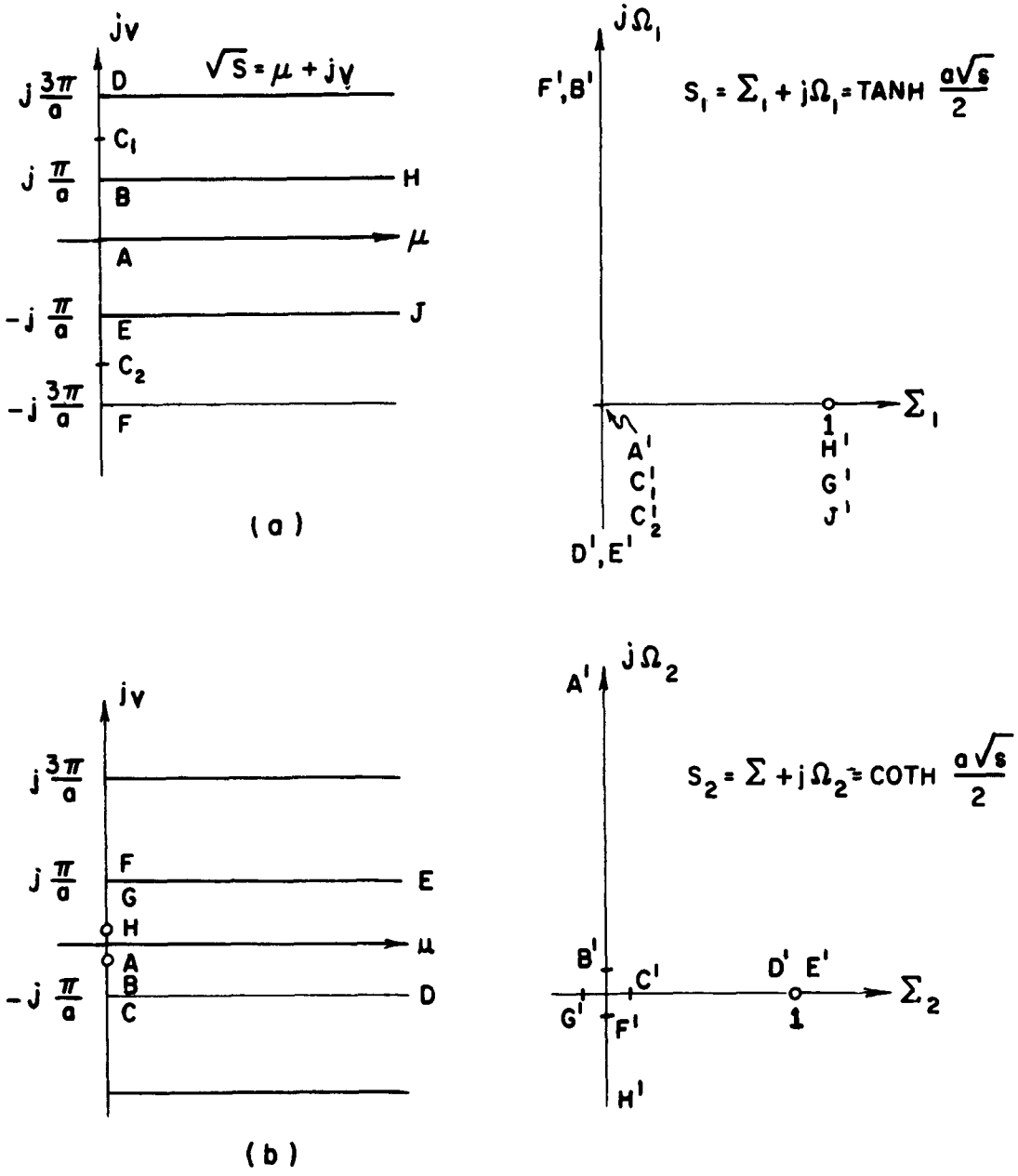

FIG. 2-3

TRANSFORMATIONS (7) AND (8)

It is sufficient to consider either of the two transformations. $S_1(\sqrt{s})$ will be examined here. Recalling that (5) represents lossless ($\overline{LC}$) functions, with an infinite array of poles and zeros alternating on the $j\omega$ axis in the $\sqrt{s}$ plane, positive real transformations (7) and (8) must again result in LC functions, in the S_1 plane. In fact, (7) and (8) possess the ability to transform distributed impedances (5) into lumped impedances. Using (7),

$$Z_{in_S}(\sqrt{s}) = \sqrt{\frac{R_o}{C_o}}\, S_1 \tag{9}$$

and

$$Z_{in_O}(\sqrt{s}) = \sqrt{\frac{R_o}{C_o}}\ \frac{1}{S_1}\ . \tag{10}$$

Eqs. (9) and (10) reveal the power of the synthesis procedure described in Fig. (1-5). The elegance of this technique is that the mathematics of the synthesis procedure is executed in the (lumped LC) S plane, after the $s \rightarrow S$ transformation, and employs only finite polynomials, as opposed to the infinite polynomials which characterize the $\overline{URC}$ functions. Fig. 2-3 presents transformations (7) and (8), which are clearly positive real.

A correlation is thus obtained between lumped L's and C's in the S_1 plane and $\overline{URCS}$ and $\overline{URCO}$ networks in the s plane. Certainly this is not a one-to-one transformation, as evidenced by the multiple strip equivalency of the $\sqrt{s}$ plane to the S plane. In fact, precisely the absence of the one-to-one property allows a distributed network with its infinite constellation of poles and zeros, to be transformed conformally into a lumped equivalent.[16] It is clear from Fig. 2-3 that any point in the

S plane has an infinity of images in the $\sqrt{s}$ plane. The correlation for (7) and (8) is given by Theorems II and III:

Theorem II.* If $Z_{\overline{RC}}(s)$ is the driving point impedance of a $\overline{URC}$ network composed of segments with RC product equal to $(a/2)^2$, $Z_{LC}(S_1) = \sqrt{s}\, Z_{\overline{RC}}(s)$ is a lumped LC driving point impedance with $S_1 = \tanh(a\sqrt{s}/2)$.

Corollary II. If transformation (7) is employed, each

a) C in the lumped LC network in the S_1 plane may be realized as a $\overline{URCO}$ network in the s plane.

b) L in the lumped LC network in the S_1 plane may be realized as a $\overline{URCS}$ network in the s plane.

Theorem III.* If $Z_{\overline{RC}}(s)$ is the driving point impedance in the s plane of a $\overline{URC}$ network composed of segments with RC product = $(a/2)^2$, $Z_{LC}(S_2) = \sqrt{s}\, Z_{RC}(s)$, with $S_2 = \coth(a\sqrt{s}/2)$, is a lumped LC driving point impedance in the S_2 plane.

Corollary III. If the transformation (8) is employed, each

a) C in the LC network in the S_2 plane may be realized as a $\overline{URCS}$ network in the s plane.

b) L in the LC network in the S_2 plane may be realized as a $\overline{URCO}$ network in the s plane.

The philosophy of the distributed synthesis procedure is suggested by the preceding development. An original analytical specification

*For proof, see Appendix.

of the driving point immittance function to be realized by a $\overline{URC}$ network is stated. The function must be tested, as will be described by Theorem VI, to determine its potential to be realized by a $\overline{URC}$ network. If Z(s) is a suitable candidate, it is transformed into a lumped LC function by

$$S_1 = \tanh \frac{a\sqrt{s}}{2} = \frac{e^{a\sqrt{s}} - 1}{e^{a\sqrt{s}} + 1} \qquad \text{(a)}$$

$$e^{a\sqrt{s}} = \frac{(1 + S_1)}{(1 - S_1)} \qquad \text{(b)} \qquad (11)$$

or

$$S_2 = \coth \frac{a\sqrt{s}}{2} = \frac{e^{a\sqrt{s}} + 1}{e^{a\sqrt{s}} - 1} \qquad \text{(a)}$$

$$e^{a\sqrt{s}} = \frac{(1 - S_2)}{(1 + S_2)} \qquad \text{(b)} \qquad (12)$$

Proceeding from Z(S), the problem is now reduced to finding a suitable LC network to realize Z(S). Each L and C may be replaced by $\overline{URC}$S and $\overline{URC}$O one-ports, and the desired $\overline{RC}$ network may be constructed. Although ladder interconnections of L's and C's would solve the mathematical problem, the corresponding $\overline{RC}$ embodiment would be a clumsy interconnection of $\overline{URC}$S and $\overline{URC}$O one-ports illustrated in Fig. 2-1(b). An improved technique employing cascaded $\overline{URC}$O two-ports is described in Section 4.4.

Since the two-port properties of $\overline{URC}$O networks are to be exploited, the $\overline{URC}$O transmission term z_{12} (Eq. (1)), is recalled to be:

$$z_{21}(s) = z_{12}(s) = \frac{R_o}{\sqrt{sR_oC_o} \sinh L \sqrt{sR_oC_o}} \qquad (13)$$

Under (7) this becomes

$$z_{21}(S) = z_{12}(S) = \frac{R_o \sqrt{1 - S^2}}{\sqrt{R_o C_o}\, S} \tag{14}$$

More must be said in Chapter Five concerning the factor $\sqrt{1 - S^2}$. At this time note (Fig. 2-3) that $S = \pm 1$ corresponds to $s = \infty$. Thus all of the transmission zeros of the $\overline{URCO}$ two-port lie at infinity, physically arising from the shunt capacitance of the model presented in Fig. 2-1. This may cause serious limitations in the realization of $\overline{RC}$ transmission properties, and suggests the use of $\overline{RCR}$ networks, described in the next section.

2.3 $\overline{URCR}$ Networks

As indicated in Section 2.2, it is not possible to achieve finite zeros of transmission with in-line $\overline{RC}$ structures. Consequently, another structure designed to assure negative real transmission zeros is suggested. This $\overline{RCR}$ network, illustrated in Fig. 2-4, consists of a dielectric layer interposed between a conducting strip and a resistive layer. The impedance matrix for the network is given by

$$z(p) = \begin{bmatrix} R_A \dfrac{\coth nL}{n} & R_A \dfrac{1}{n \sinh nL} \\ R_A \dfrac{1}{n \sinh nL} & R_A \dfrac{\coth nL}{n} \end{bmatrix} \tag{15}$$

where $$n = \sqrt{\frac{pR_AC}{1+p\ C/G_B}} = \sqrt{R_AG_B}\sqrt{\frac{p\ C/G_B}{1+p\ C/G_B}} = k\sqrt{\frac{p'}{1+p'}}\ ;$$

$$k = \sqrt{R_AG_B}\ ;\quad p' = p\ C/G_B$$

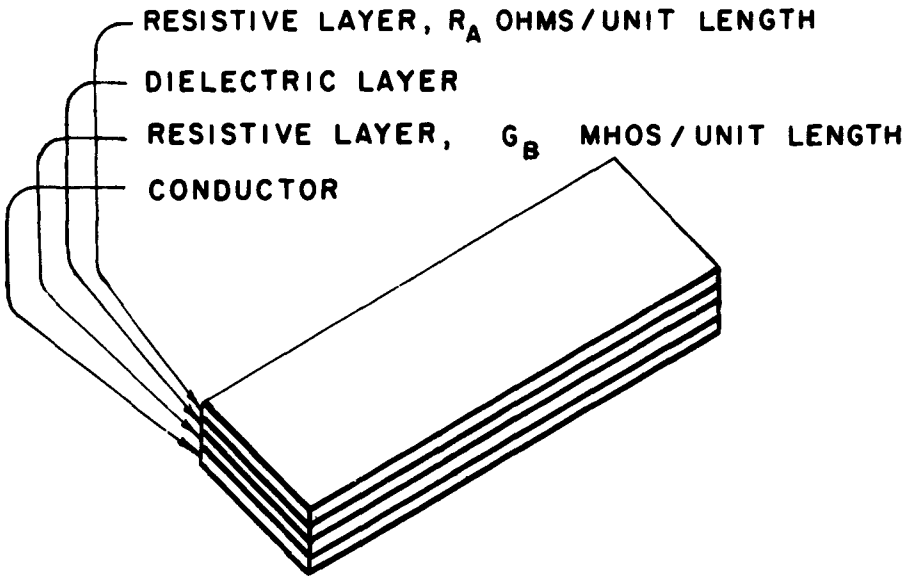

PHYSICAL MODEL

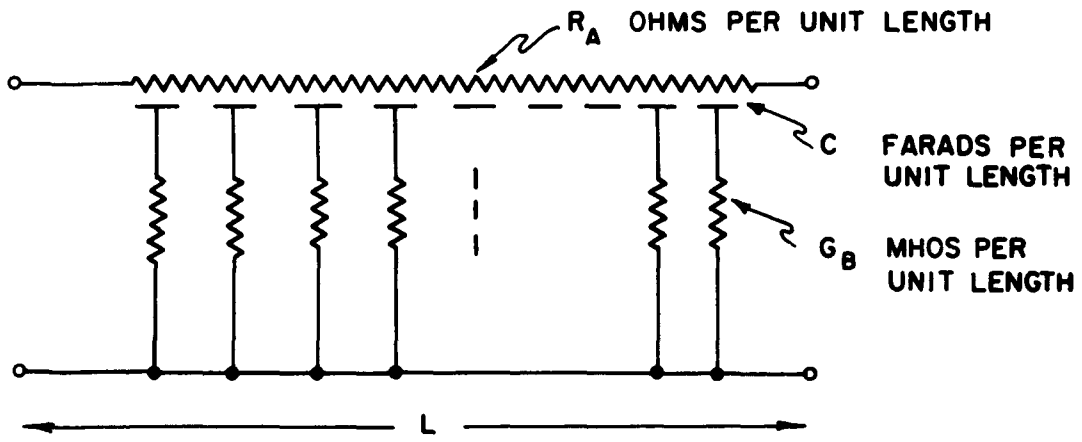

ELECTRICAL MODEL

FIG. 2-4

$\overline{RCR}$ LINE SEGMENT

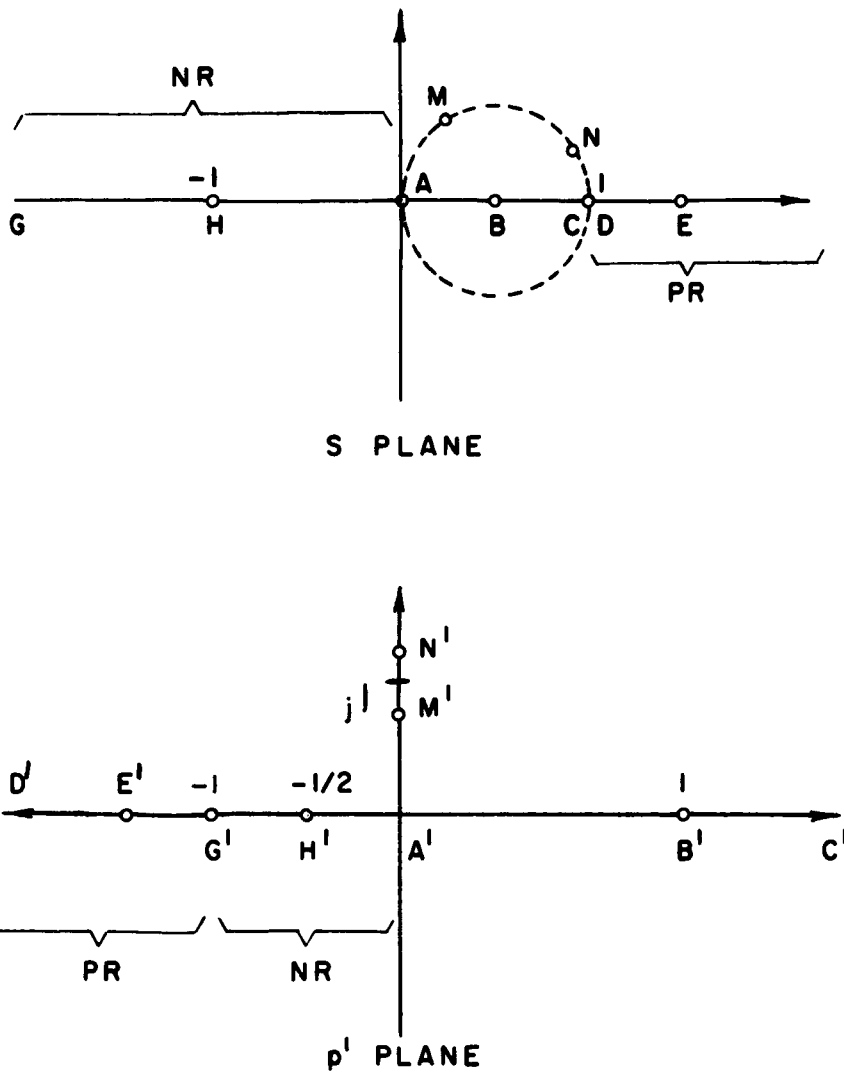

FIG. 2-5

p' ⟶ s MAPPING

Now if a new complex variable, s, is defined by $s = p'/(1+p')$, s is clearly a positive real function of p', and maps the right half of the p' plane into the right half of the s plane, as in Fig. 2-5.

The first important conclusion is that the entire negative real axis in the s plane has as its image the finite segment of the negative real p' axis from the origin to -1. Thus a function with a denumerably infinite set of negative real zeros in the s plane possesses an uncountably infinite number of zeros on the segment $-1 \leq p' \leq 0$ in the p' plane. In this case, -1 would be a limit point.*

Consider the Z parameters for the $R_A C R_B$ network:

$$z_{11}(p') = z_{22}(p') = \frac{R_A}{k\sqrt{\frac{p'}{1+p'}}} \coth kL\sqrt{\frac{p'}{1+p'}} \tag{16}$$

$$z_{21}(p') = z_{12}(p') = \frac{R_A}{k\sqrt{\frac{p'}{1+p'}}} \frac{1}{\sinh kL\sqrt{\frac{p'}{1+p'}}} \tag{17}$$

Letting $s = p'/(1+p')$, Z(s) must represent a realizable (and $\overline{RC}$) network. Indeed,

$$z_{11}(s) = \frac{R_A}{k\sqrt{s}} \coth kL\sqrt{s} \tag{18}$$

$$z_{12}(s) = \frac{R_A}{k\sqrt{s}} \frac{1}{\sinh kL\sqrt{s}} \tag{19}$$

*Gross and Braga (see reference 25) refer to such a limit point as a finite accumulation point.

Comparing Eq. (18) and (19) with the $\overline{URC}$ Z-parameters of Eq. (1), a remarkable coincidence is noted. Under the frequency transformation $s = p'/(1+p')$, the $\overline{RCR}$ two port has an impedance matrix identical with the original $\overline{URC}$O network, all of whose transmission zeros are at infinity! The poles and zeros of z_{11} for the original network alternated and were denumerably infinite. In light of the foregoing discussion of this transformation, the poles and zeros of $z_{11}(p')$ must be in the finite plane with a limit point at -1. In fact, by the Mittag-Leffler Theorem,[33] $z_{11}(p')$ may be expressed as

$$z_{11}(p') = \frac{R_A(p'+1)}{k^2Lp'} \prod_{M=1}^{\infty} \left(\frac{M}{M-\frac{1}{2}} \right)^2 \left[\frac{\{(kL)^2 + (M-\frac{1}{2})^2\pi^2\}}{\{(kL)^2 + (M\pi)^2\}} \right] \frac{p' + \frac{(M-\frac{1}{2})^2\pi^2}{(kL)^2 + (M-\frac{1}{2})^2\pi^2}}{p' + \frac{(M\pi)^2}{(kL)^2 + (M\pi)^2}} \qquad (20)$$

The poles and zeros of this expression are depicted in Fig. 2-6. $\overline{RCR}$ networks, significantly, allow the synthesis of a wider class of driving point impedances than was possible with $\overline{URC}$O networks alone. It is further noted that, unlike its $\overline{URC}$O counterpart, the $\overline{URCR}$ network has a finite driving point admittance at infinite frequency, due to G_B.

The transfer impedance of the $\overline{R_ACR_B}$ network, likewise, has its $\overline{URC}$O counterpart. $z_{12}(p')$ may be expanded into

$$z_{12}(p') = \frac{R_A}{k\sqrt{\frac{p'}{1+p'}}} \frac{1}{\sinh kL\sqrt{\frac{p'}{1+p'}}} = \frac{R_A(p'+1) \prod_{M=1}^{\infty} (p'+1) \left(\frac{1}{1 + (kL/M\pi)^2} \right)}{k^2Lp' \prod_{M=1}^{\infty} p' + \frac{1}{1 + (kL/M\pi)^2}} \qquad (21)$$

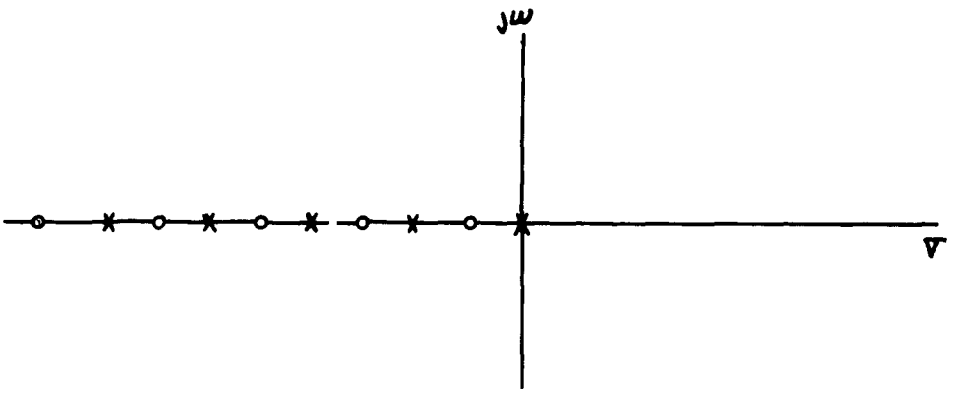

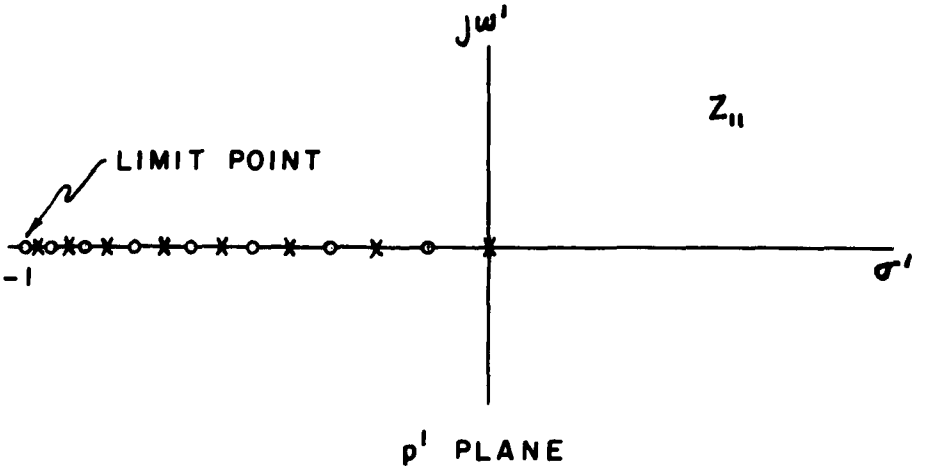

FIG. 2-6

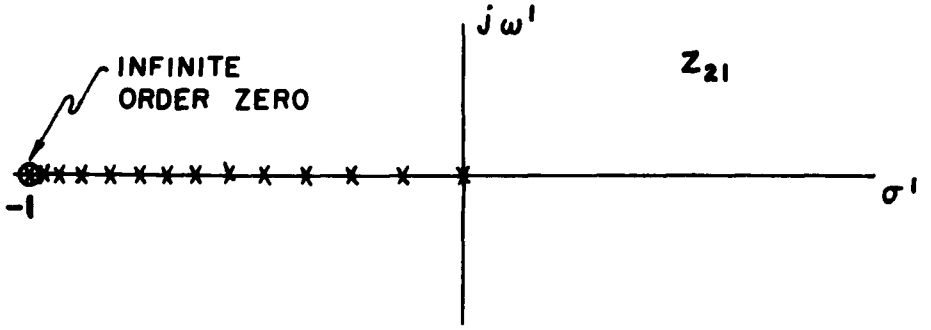

FIG. 2-7

$\overline{\text{RCR}}$ IMPEDANCE POLE ZERO PLOTS

The $\overline{RCR}$ network transfer impedance involves an infinite number of zeros at -1 in the p' plane, or at $-1/R_BC$ in the p plane, and an uncountably infinite sequence of poles between p' = 0 and p' = -1 on the negative real p' axis. Fig. 2-7 presents the configuration. Along the $j\omega'$ axis, the effect may be approximated by the pole at the origin, the next M poles, and a zero of order M+1 at p' = -1.

$\overline{RCR}$ network functions such as (18) and (19), expressed as functions of s under the mapping of Fig. 2-5, may now be operated on by transformation (11). The resultant network functions are then expressed as ratios of finite-order polynomials in S. Proceeding from Z(S), the distributed synthesis problem is again reduced to finding the proper LC network to realize Z(S).

2.4 Concluding Remarks

The characterization of distributed RC network functions has led to hyperbolic functions of frequency which would be rather difficult to work with in an orderly synthesis technique. Under the proper transformations, it has been shown that these functions may be materially reduced in complexity, and put into such a form that lumped LC synthesis techniques may be adapted to the $\overline{RC}$ problem.

CHAPTER THREE

THE APPROXIMATION PROBLEM

3.0 Introduction

$\overline{URC}$ immittance and gain functions were shown in Chapter Two to be given by hyperbolic functions of the argument, $\sqrt{s\tau}$. For the wide band synthesis problem, it is unfeasible to approximate the hyperbolic functions by either truncated infinite product expansions such as by the use of the Mittag-Leffler Theorem,[33] or by truncated infinite series. Nonetheless, such expansions do provide valuable insight into the real frequency behavior of $\overline{RC}$ network functions, since the infinite product or series expansions of any of the two-port parameters of finite $\overline{URC}$ networks involve only integral powers of s.

An example of a typical $\overline{RC}$ driving point impedance, expressed in infinite product and infinite series forms, was seen to be

$$z(s) = \frac{\tanh \sqrt{sRC}}{\sqrt{sRC}} = \frac{\sinh \sqrt{sRC}}{\sqrt{sRC}\cosh \sqrt{sRC}} \tag{1}$$

which may be written as[33]

$$z(s) = \frac{\sqrt{sRC}\prod_{k=1}^{\infty}\left(1+\frac{sRC}{k^2\pi^2}\right)}{\sqrt{sRC}\prod_{k=1}^{\infty}\left(1+\frac{sRC}{[(k-\frac{1}{2})\pi]^2}\right)} \tag{2}$$

or

$$z(s) = \frac{\left[\sqrt{sRC} + \frac{(sRC)^{3/2}}{3!} + \frac{(sRC)^{5/2}}{5!} + \cdots\right]}{\sqrt{sRC}\left[1 + \frac{sRC}{2!} + \frac{(sRC)^2}{4!} + \cdots\right]} \tag{3}$$

From the infinite product expansion, the driving point function is seen to possess an infinite number of alternating and countable negative real poles and zeros. This is characteristic of $\overline{URC}$ networks.

3.1 Importance of Approximation in the s Plane

As was noted in Fig. 1-5 of Chapter One, the $\overline{RC}$ synthesis technique of interest herein is based on conformal transformations which map the s plane into the S plane. It will be recalled that the actual synthesis will be undertaken in the S plane, where the distributed RC functions of s are characterized by ratios of finite polynomials in S. Driving point and transfer function realizability conditions are most readily derived in the S plane. Suppose, however, the network designer begins with a graphical impedance-magnitude function plotted against ω (i.e., $s = j\omega$), and applies the conformal $s \rightarrow S$ transformation to achieve a graphical magnitude characteristic in the S plane. The first analytical approximation of the function will be in the S plane. It would then be inconvenient to formulate an analytic impedance expression or analytical realizability conditions on the function in the original s plane.

It is thus important to begin with a graphical representation of the desired network behavior, and within the framework of a set of realizability conditions, translate the graphical specifications directly into hyperbolic functions of $\sqrt{s}$. The synthesis procedure from this point on becomes direct and mathematically exact. Because $\overline{URC}$ networks are not characterized by ratios of finite polynomials in s, it is profitless to approximate a graphical specification by such a ratio.

Consider now the general form of hyperbolic approximation for a given magnitude-frequency specification as detailed in Eq. (4). At this time, since no particular classes of functions (i.e., driving point, transfer or gain) have been discussed, a general network function will be formulated. It will be shown in Chapters Four and Five that realizable $\overline{RC}$ driving point and transfer immittance functions are subclasses of this general network function. The general function that is of considerable interest in approximating a specified graphical function of frequency is given by

$$H(s)=\frac{\alpha\left(1 \pm e^{a\sqrt{s}}\right)\prod_{1}^{\omega}\left(e^{2a\sqrt{s}} + B_i e^{a\sqrt{s}} + 1\right)}{F(s)\left(1 \mp e^{a\sqrt{s}}\right)\left(1 + e^{a\sqrt{s}}\right)^{p}}$$

$$\frac{\prod_{1}^{z}\left(e^{4a\sqrt{s}} + C_i e^{3a\sqrt{s}} + (2-C_i)\, e^{2a\sqrt{s}} + C_i e^{a\sqrt{s}} + 1\right)}{\prod_{1}^{m}\left(e^{2a\sqrt{s}} + A_i e^{a\sqrt{s}} + 1\right)\prod_{1}^{n}\left(e^{4a\sqrt{s}} + D_i e^{3a\sqrt{s}} + (2-D_i)\, e^{2a\sqrt{s}} + D_i e^{a\sqrt{s}} + 1\right)} \qquad (4)$$

where A_i, B_i, C_i, and D_i are real;

$|B_i| < 2$, $|A_i| < 2$, $\infty > C_i > 1$, $\infty > D > 1$,

p is a positive integer,

and $F(s) = 1$, $H(s)$ = a gain function

$\sqrt{s}$, $H(s)$ = an impedance function

$\frac{1}{\sqrt{s}}$, $H(s)$ = an admittance function

The "exponential polynomial" factors in Eq. (4) are shown in Chapters Four and Five to be sufficient to characterize $\overline{URC}$ impedance and gain functions. It will be necessary to understand the magnitude characteristics of the exponential polynomials thoroughly; hence they are introduced here. Presently, it will be shown that practical "straight-line" magnitude approximations exist for each of the polynomial factors described in Eq. (4). Accordingly, a procedure analogous to the straight-line "Bode Approximation" for lumped networks is developed. Exponential polynomials provide the vehicle for approximating graphical specifications of real frequency directly by analytic expressions in the original plane of definition.

3.2 Graphical Magnitude Characteristics

Figures 3-1 through 3-7 present the real frequency magnitudes of the exponential factors of interest. The abscissas represent the log 10 of the normalized frequency $\frac{\omega a^2}{2}$, which will be most useful in the general synthesis problem. Since the several immittance and gain functions to be realized involve products and quotients of such exponential polynomial factors, the logarithms of the factors need only be added together graphically to produce a desired $\overline{RC}$ specification.

Figure 3-1 is a plot of exponential polynomials of the form

$$\frac{1}{e^{2a\sqrt{s}} + B_1 e^{a\sqrt{s}} + 1} ,$$

for various values of B_1, with $s = j\omega$. A disadvantage of this plot is large db falloff encountered at high frequency. Practically this may

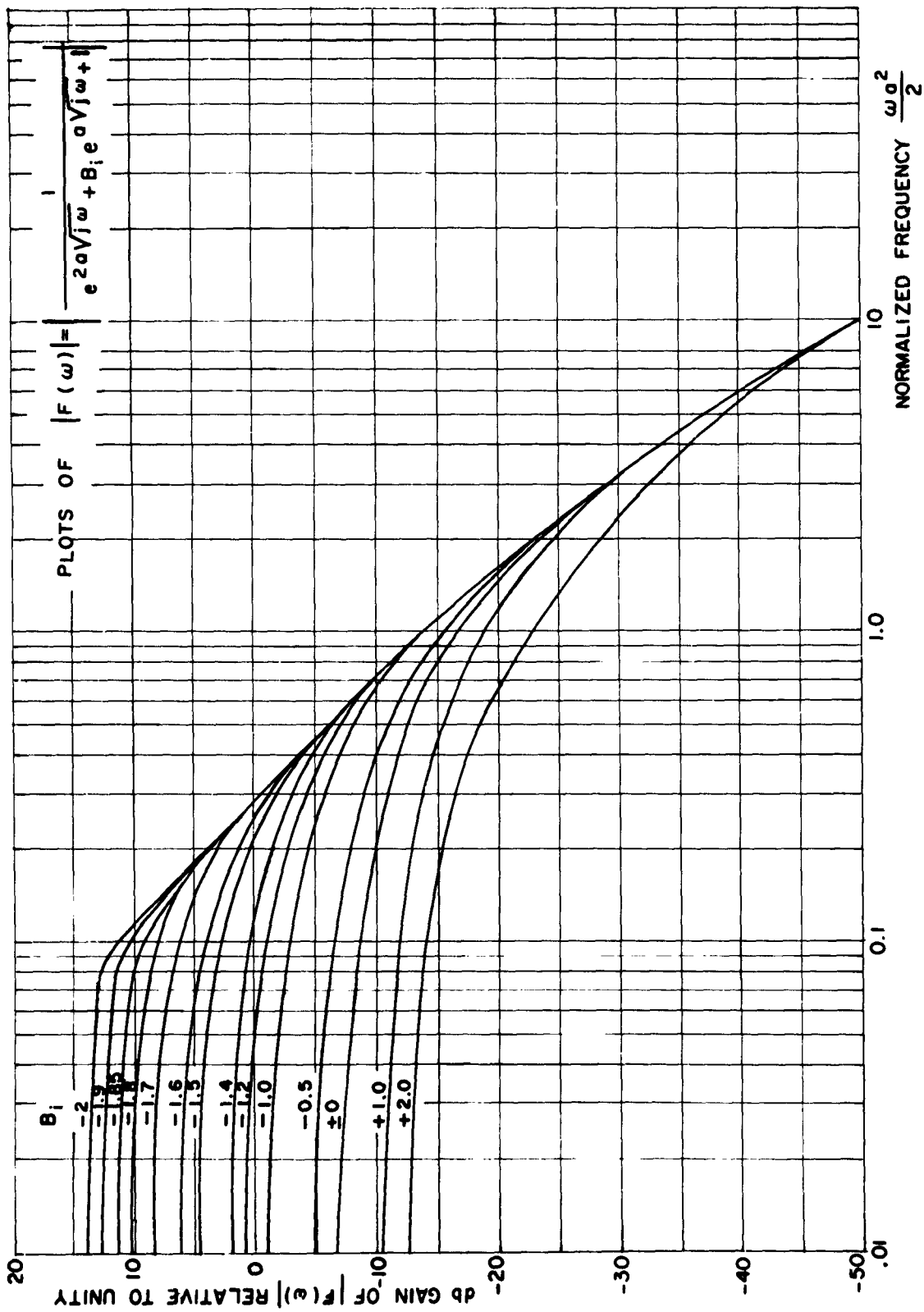
PLOTS OF $|F(\omega)| = \left| \frac{1}{e^{2a\sqrt{j\omega}} + B_i e^{a\sqrt{j\omega}} + 1} \right|$
B_i
-2
-1.9
-1.85
-1.8
-1.7
-1.6
-1.5
-1.4
-1.2
-1.0
-0.5
±0
+1.0
+2.0
db GAIN OF $|F(\omega)|$ RELATIVE TO UNITY
20
10
0
-10
-20
-30
-40
-50
.01
0.1
1.0
10
NORMALIZED FREQUENCY $\frac{\omega a^2}{2}$

FIG. 3-1

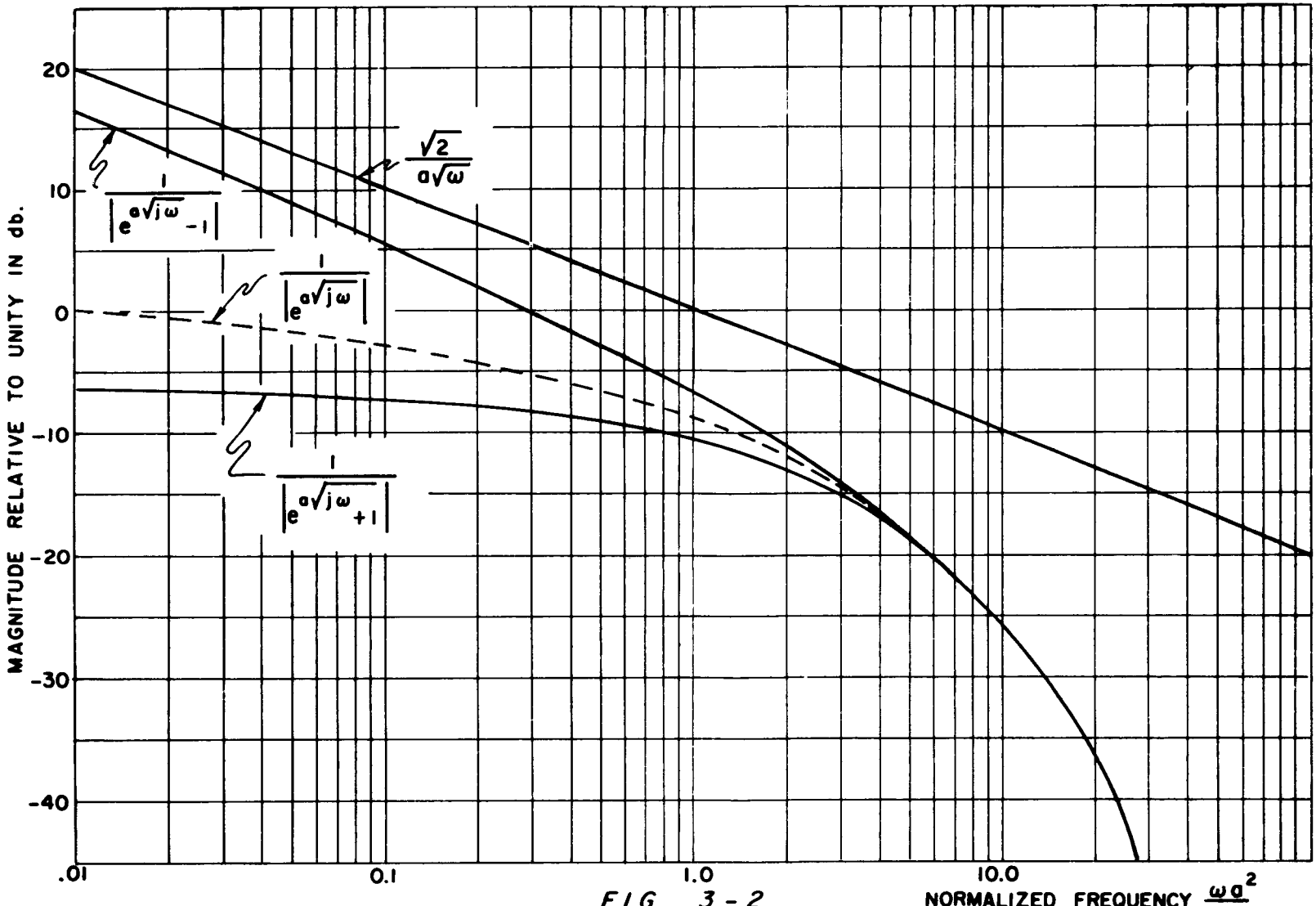

FIG. 3-2

MAGNITUDE FUNCTIONS FOR RC SYNTHESIS

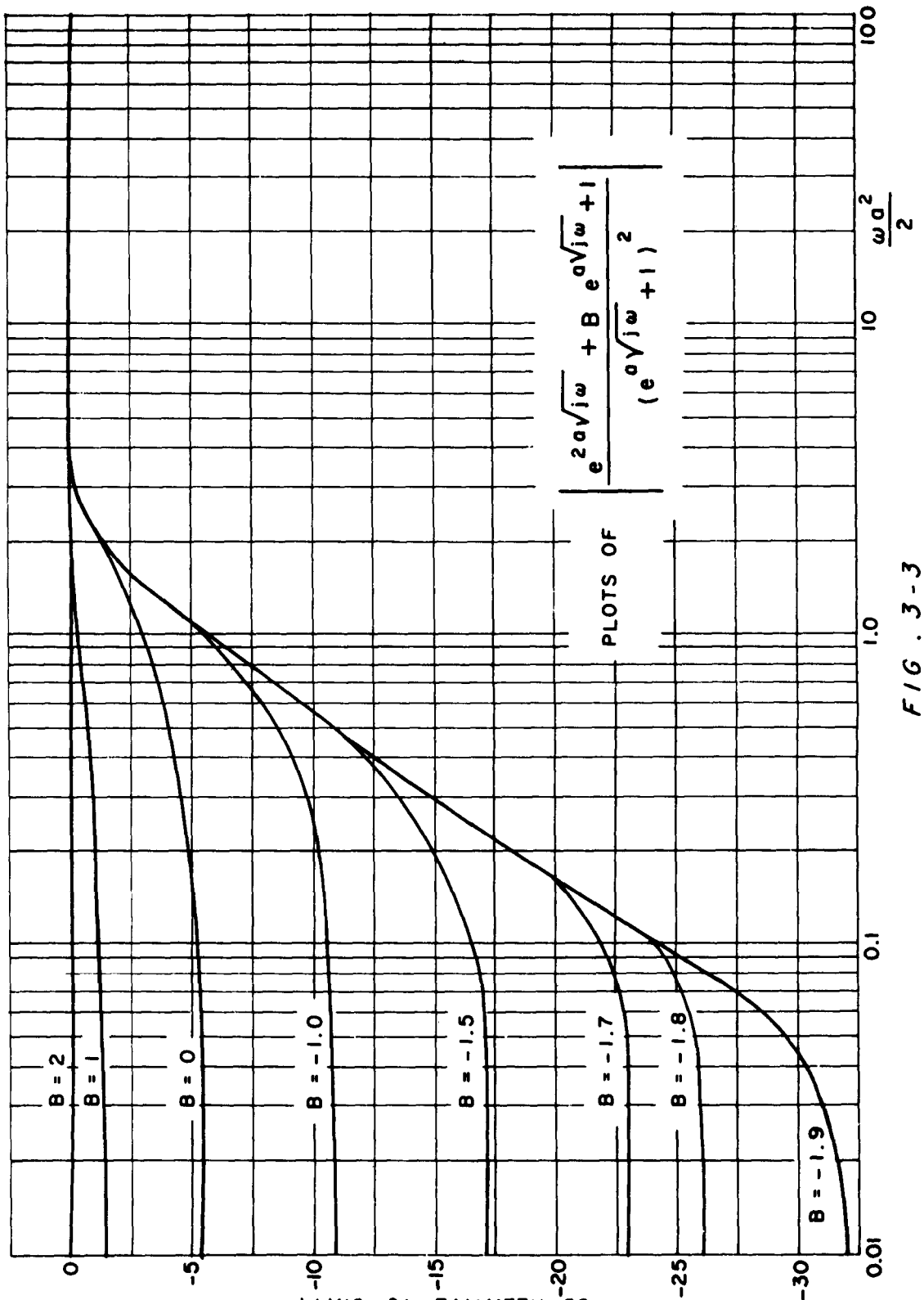
PLOTS OF
$\left| \frac{e^{2a\sqrt{j\omega}} + B\, e^{a\sqrt{j\omega}} + 1}{(e^{a\sqrt{j\omega}} + 1)^2} \right|$
db RELATIVE TO UNITY
0
-5
-10
-15
-20
-25
-30
0.01
0.1
1.0
10
100
$\frac{\omega a^2}{2}$
B = 2
B = 1
B = 0
B = -1.0
B = -1.5
B = -1.7
B = -1.8
B = -1.9

FIG. 3-3

result in error by the network designer taking the small difference of two large numbers to achieve a desired characteristic. Such difficulty may be circumvented by use of the exponential polynomial ratios of Fig. 3-3. Note that the expressions in Fig. 3-3 reach asymptotic values for zero and infinite frequencies. The curves are computed for $\sqrt{j\omega} = (j+1)\cdot\sqrt{\omega/2}$.

Figure 3-2 represents the magnitude of other terms found in the general network expression. Figs. 3-4, 5, 6 and 7 present the magnitude of the polynomial factors above, with the complex variable 's' replaced by $p'/(1+p')$, for $p' = j\omega$. Such plots are necessary in the synthesis of $\overline{RCR}$ networks, discussed in Chapter Four.

3.3 Example of Approximation Technique

Let the high pass characteristic of Fig. 3-8 be required within 3 db. for all normalized frequencies $\frac{\omega a^2}{2} > 0.1$, subject to the following conditions:

1) The function $A(e^{a\sqrt{s}})$ used to approximate the graphical characteristic must be identically zero for zero frequency, and asymptotically approach a constant as the frequency approaches infinity.

2) Below $\frac{\omega a^2}{2} = .1$, the magnitude of A must be at least 30 db. below its reference level at high frequencies.

It is to be noted at this point that since no realizability conditions for a particular physical embodiment of $A(e^{a\sqrt{s}})$ have been considered, $A(e^{a\sqrt{s}})$ will be constructed without regard to such conditions. In Chapters Four and Five, such restrictions will be introduced, and will detail the choice of exponential polynomials available to construct the magnitude function of interest.

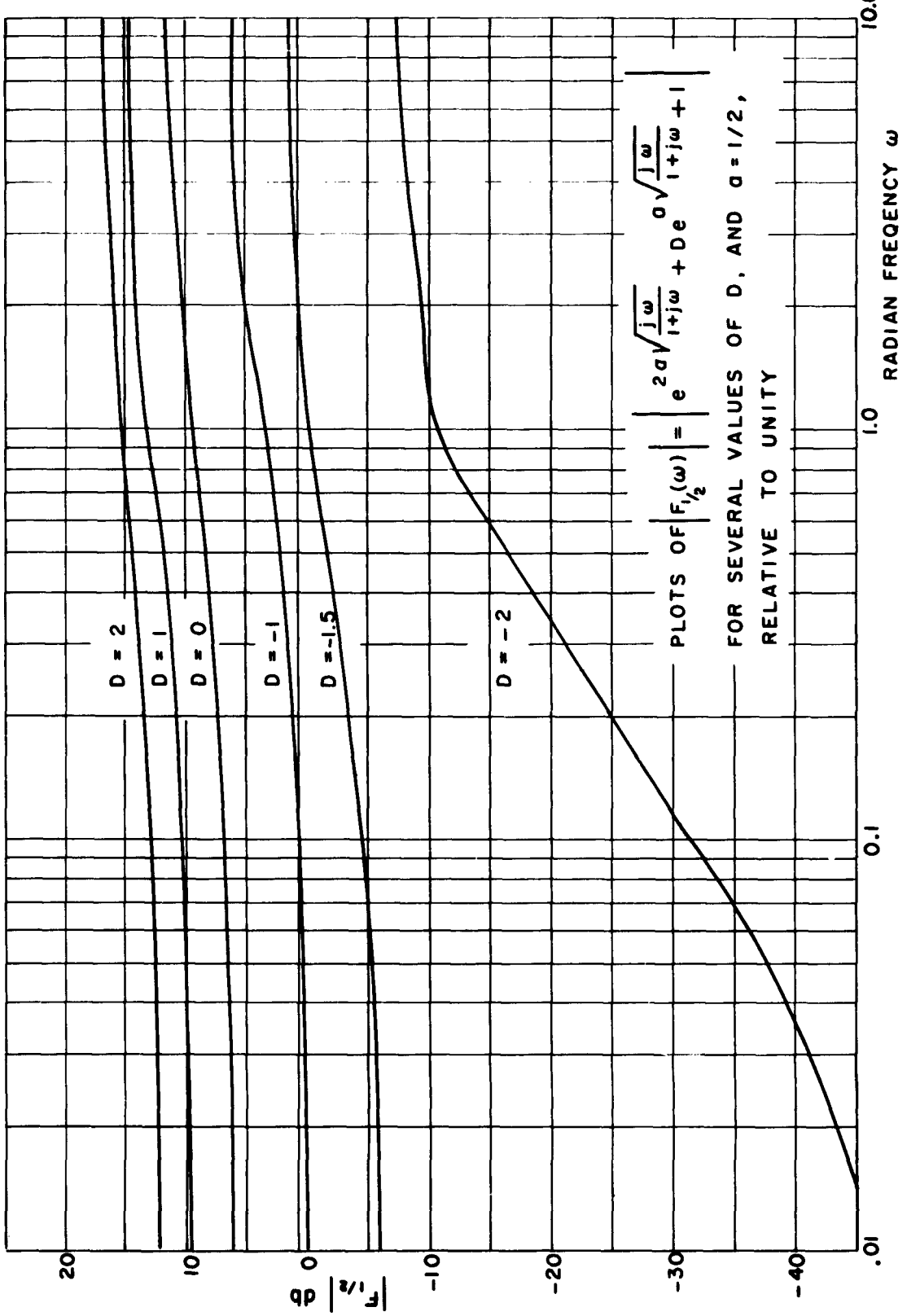
D = 2
D = 1
D = 0
D = -1
D = -1.5
D = -2
PLOTS OF $\left|F_{1/2}(\omega)\right| = \left| e^{2a\sqrt{\frac{j\omega}{1+j\omega}}} + De^{a\sqrt{\frac{j\omega}{1+j\omega}}+1} \right|$
FOR SEVERAL VALUES OF D, AND a = 1/2,
RELATIVE TO UNITY
$|F_{1/2}|$ db
20
10
0
-10
-20
-30
-40
.01
0.1
1.0
10.0
RADIAN FREQENCY ω

FIG. 3-4

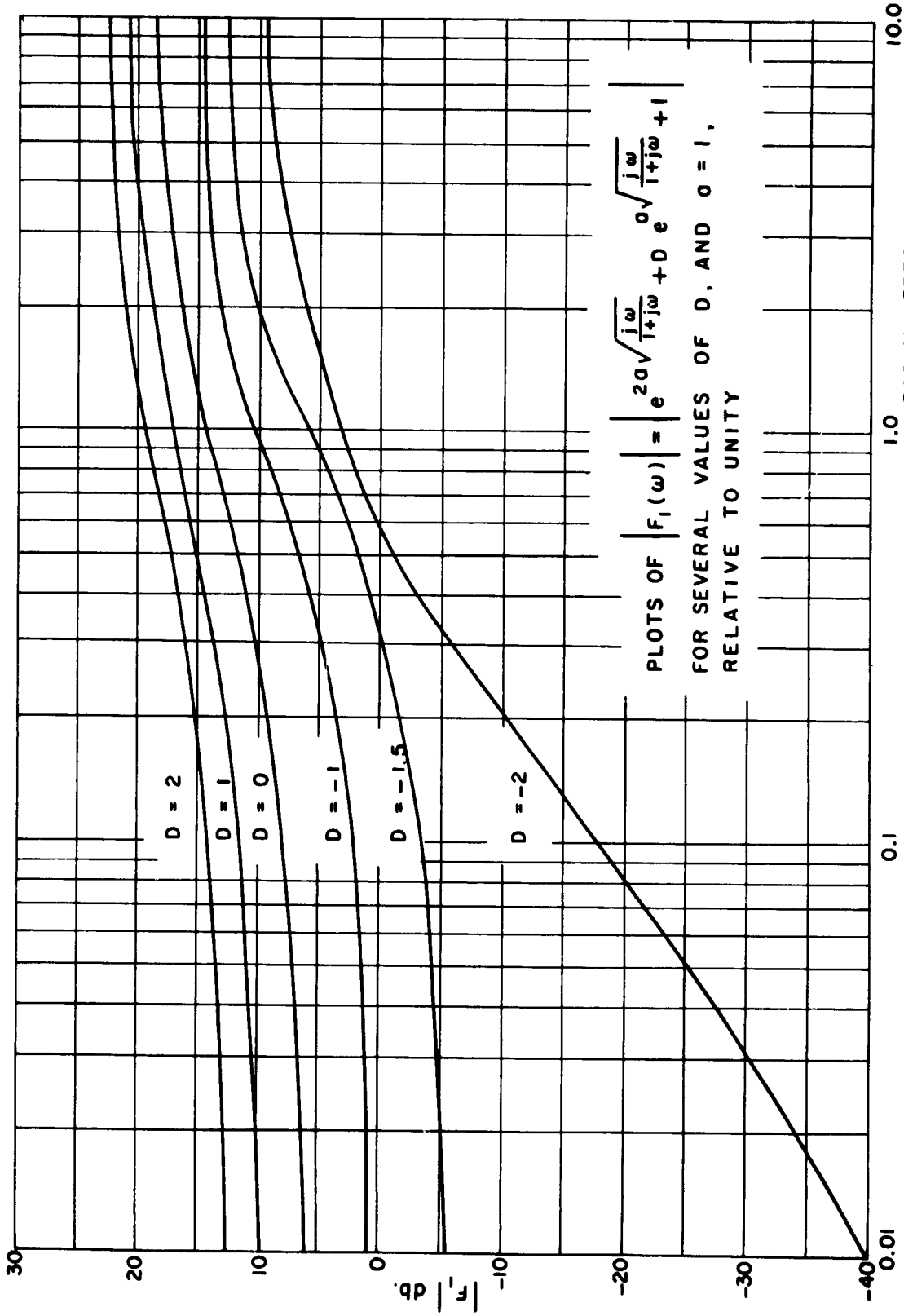
PLOTS OF $|F_1(\omega)| = \left| e^{2a\sqrt{\frac{j\omega}{1+j\omega}}} + D\, e^{a\sqrt{\frac{j\omega}{1+j\omega}}} + 1 \right|$
FOR SEVERAL VALUES OF D, AND a = 1,
RELATIVE TO UNITY
D = 2
D = 1
D = 0
D = -1
D = -1.5
D = -2
$|F_1|$ db.
30
20
10
0
-10
-20
-30
-40
0.01
0.1
1.0
10.0
RADIAN FREQUENCY ω

FIG. 3-5

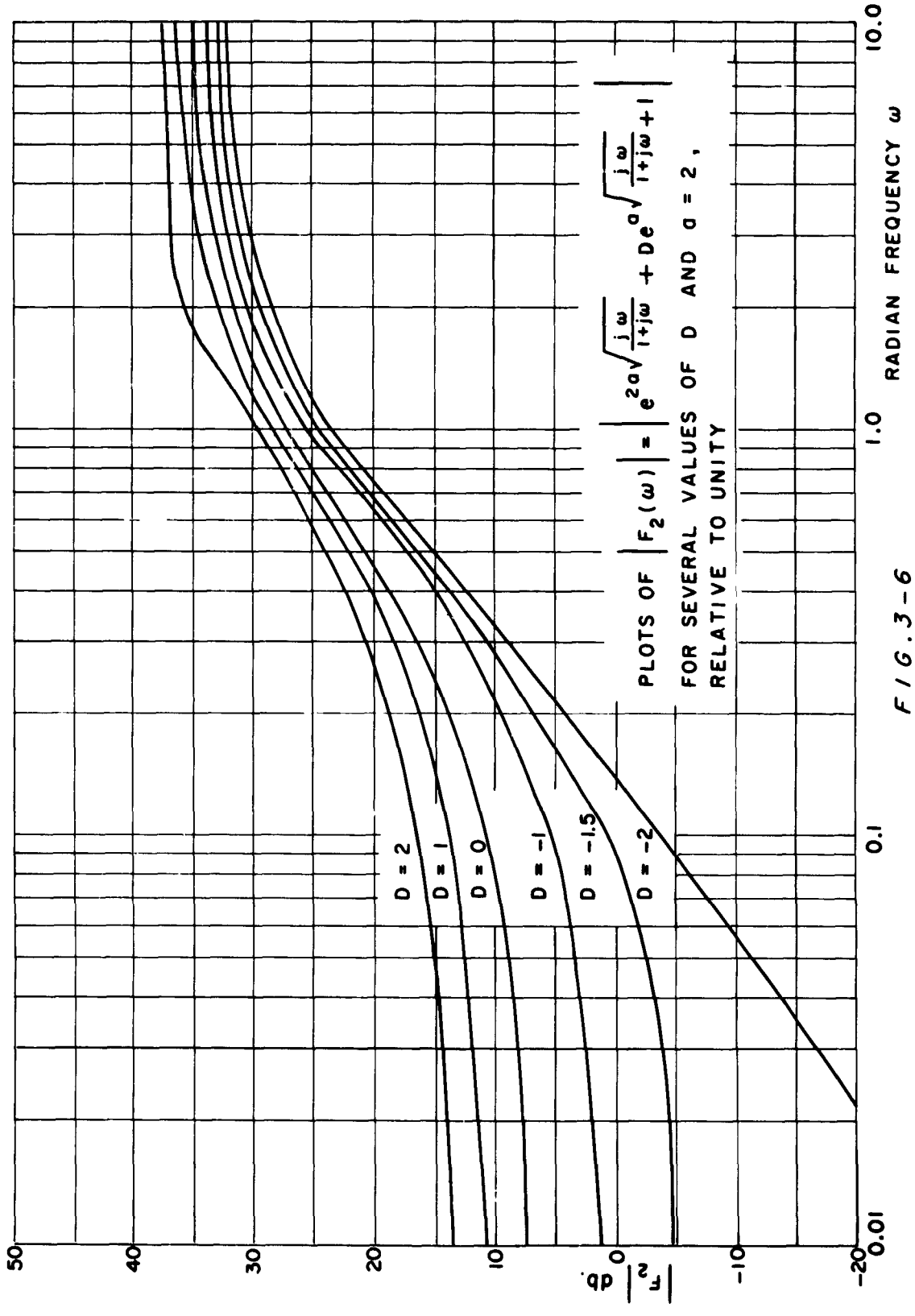
PLOTS OF $|F_2(\omega)| = \left| e^{2a\sqrt{\frac{j\omega}{1+j\omega}}} + De^{a\sqrt{\frac{j\omega}{1+j\omega}}+1} \right|$
FOR SEVERAL VALUES OF D AND a = 2,
RELATIVE TO UNITY
D = 2
D = 1
D = 0
D = -1
D = -1.5
D = -2
$|F_2|$ db.
50
40
30
20
10
0
-10
-20
0.01
0.1
1.0
10.0
RADIAN FREQUENCY ω

FIG. 3-6

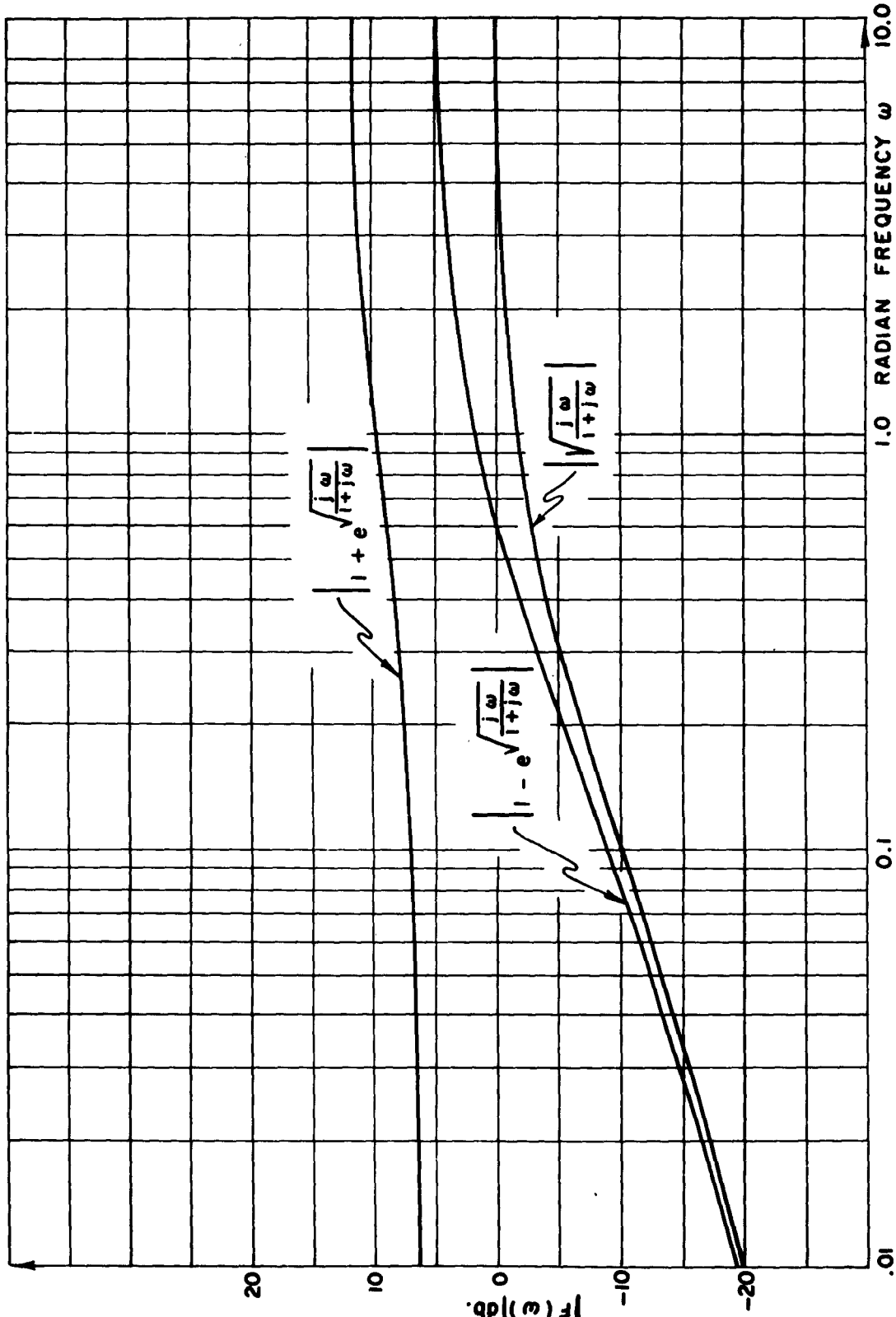

FIG. 3-7

MAGNITUDE FUNCTIONS FOR $\overline{RCR}$ SYNTHESIS

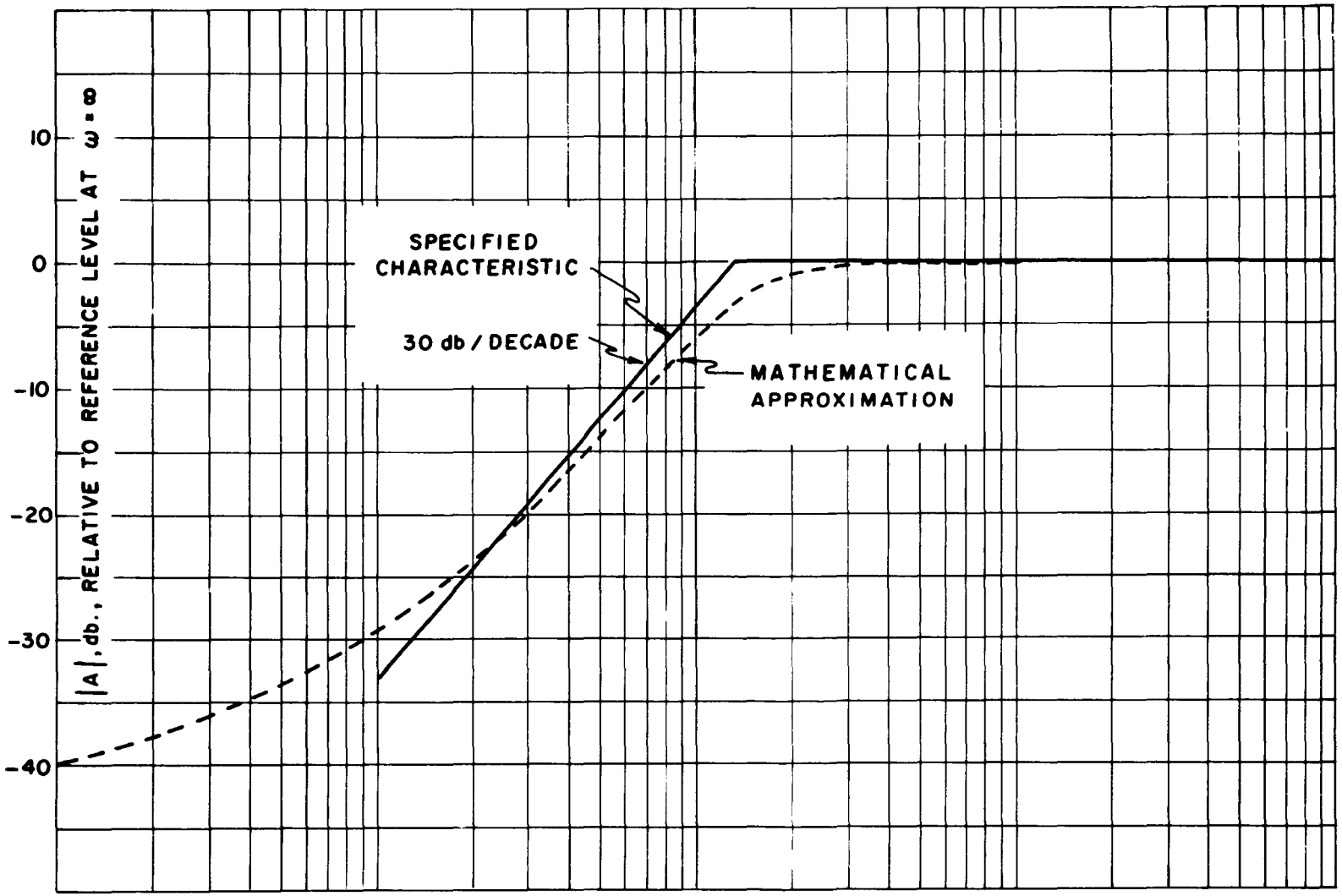

FIG. 3-8

APPROXIMATION OF A(s) BY EXPONENTIAL POLYNOMIALS

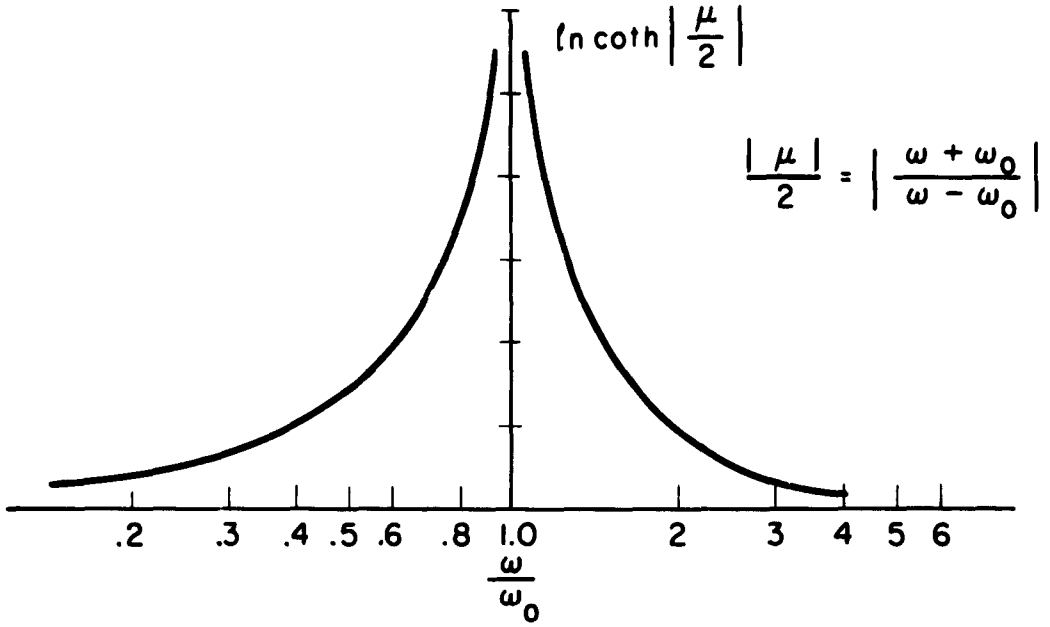

FIG. 3-9

PLOT OF WEIGHTING FACTOR $\ln \coth \frac{|\mu|}{2}$

Since $|A|$ is required to be identically zero at dc, a term of the form $(e^{a\sqrt{s}} - 1)$ is placed in the numerator. This term may have its magnitude cancelled out at high frequency by a denominator term of the form $(e^{a\sqrt{s}} + 1)$, noted in Fig. 3-2. The term $(e^{a\sqrt{s}} - 1)$ also helps meet the 30 db./decade requirement. From Fig. 3-2, and the specifications on $|A|$, a graphical characteristic may be rapidly plotted which will determine the require contribution of the other (as yet unknown) exponential polynomial factors to $|A|$. When this is done, an upward break frequency of about $\frac{\omega a^2}{2} = 0.15$ is clearly needed, requiring a second order polynomial with B_1 about -1.8. For a finite overall gain at high frequency, trial and error quickly shows that a denominator polynomial with A_1 equal to zero will permit all of the specifications to be met. The final mathematical expression is

$$A(s) = \frac{(e^{a\sqrt{s}} - 1)(e^{2a\sqrt{s}} - 1.8e^{a\sqrt{s}} + 1)}{(e^{a\sqrt{s}} + 1)(e^{2a\sqrt{s}} + 1)} \qquad (5)$$

The prescribed and approximating graphical characteristics are compared in Fig. 3-8.

3.4 Graphical Magnitude Specifications Derived From Phase Specifications

Appropriate relationships between magnitude and phase characteristics of minimum phase shift networks were first introduced by Bode.[31] Phase tables[32] may assist in the systematic computation of the phase function from a given magnitude function. In this dissertation, the converse problem is of interest. The $\overline{RC}$ synthesis procedure, limited to

minimum phase networks, begins with an analytic characterization of the magnitude characteristic. From the phase specification, it is necessary first to find the magnitude function.

Letting $A(\omega)$ represent the magnitude function, and $\theta(\omega)$ represent the phase function,

$$A_c - A_\infty = -\frac{1}{\pi\omega_c}\int_{-\infty}^{\infty}\frac{d(\omega\theta)}{du}\log\coth\left|\frac{u}{2}\right|du \qquad (a)$$

$$A_c - A_0 = -\frac{\omega_c}{\pi}\int_{-\infty}^{\infty}\frac{d(\theta/\omega)}{du}\log\coth\left|\frac{u}{2}\right|du \qquad (b) \qquad (6)$$

where

$$u = \log(\omega/\omega_c) \qquad (7)$$

The reference levels A_∞ and A_0 at $\omega = \infty$ and $\omega = 0$ respectively are used because the magnitude functions so derived are not unique. For minimum phase networks with specified magnitude functions, the associated phase is uniquely specified. However, since an arbitrary magnitude component such as a constant loss may be added without affecting the phase characteristic, (6(a)) and (6(b)) indicate that $A(\omega)$ may be determined only within an arbitrary constant.

Although (6(a)) and (6(b)) represent a considerable amount of evaluation effort, the weighting function $\log\coth|u/2|$ (see Fig. 3-9) simplifies the calculation. Outside of the vicinity of $u = 0$ (or $\omega = \omega_c$), $\log\coth|u/2|$ falls off rapidly. Most of the contribution to the integrand at ω_c comes from the slope of $\frac{\theta}{\omega}$ or $\omega\theta$ in the immediate vicinity

of ω_c. Evaluation of (6(a)) or (6(b)) at a sufficient number of values of ω will allow the graphical determination of $A(\omega)$. The graphical magnitude characteristic is the departure point for the $\overline{RC}$ synthesis. Conditions relating degree of approximation in the magnitude function and the phase function have not been derived. Thomas has stated that a $\pm \frac{1}{2}$ db. gain approximation results in 3° phase accuracy.[32] Examples of calculations of (6(a)) and (6(b)) have been carried out by Bode in Sections 14.8-9 of reference 31.

Bode (Section 13.10, reference 31) considers the extension of the above formulae to systems other than lumped networks. The particular restriction on the application of these integrals is the one which limits the behavior of Z(s) - (where $Z(j\omega) = A(j\omega)+jB(j\omega)$) at infinity. Z(s) may increase at most logarithmically, so that Z(s)/s vanishes for infinite frequency. Difficulty arises when an exact expression for Z(s) is not at hand, particularly since distributed functions often include essential singularities. Each distributed network function should be tested to ascertain that it meets the conditions that it have no right-half-plane or imaginary axis singularities, and that it approach infinity no faster than log s. The driving point impedances of $\overline{URCO}$ and $\overline{URCS}$ one-port networks given in Eq. (3) and (4) of Chapter 2 satisfy these conditions, as well as the networks which are realizable by Theorem IV. As Bode has pointed out in connection with the application of these integrals to the distributed functions, "It is evidently unwise to dogmatize about so general and vague a problem."

3.5 Concluding Remarks

The material in this chapter provides the foundation for specifying analytical $\overline{RC}$ immittance functions from which networks with prescribed magnitude characteristics may be constructed. In Chapters Four and Five, realizability conditions will be derived which require the exact expression of distributed network functions in terms of hyperbolic functions of $s^{\frac{1}{2}}$. Such magnitude characteristics as will be required in Chapters Four and Five have been plotted in this chapter in db. vs. $\log_{10} \omega$, and permit the approximation of prescribed magnitude plots by products of exponential polynomials.

CHAPTER FOUR

THE SYNTHESIS OF RC DRIVING POINT IMMITTANCES

4.0 Introduction and Objectives

From the viewpoint of mathematical development, it is desirable first to formulate a synthesis technique which realizes driving point immittance functions employing uniform $\overline{RC}$ networks. Such a development is to be carried on to conclusion in this chapter. In accordance with the discussion in Section 2.0, it is preferable to achieve an $\overline{RC}$ synthesis which is embodied in a cascade configuration, as opposed to the alternate ladder connections of $\overline{RC}$ one-ports depicted in Figure 2-2.

A general cascade synthesis is detailed in this chapter, with the help of Richard's Theorem. Using the mathematical groundwork presented here, the transfer function and gain function synthesis problem is considered in Chapter 5.

4.1 Realizability of Z(s) by $\overline{URC}$ Networks

The necessary and sufficient conditions that $Z_{\overline{RC}}(s)$ may be realized under transformations (7) and (8) of Chapter 2 by a finite number of $\overline{URCS}$ and $\overline{URCO}$ immittances are shown to be

Theorem IV.* Z(s) may be realized as a driving point impedance of a finite number of elemental $\overline{URCS}$ and $\overline{URCO}$ networks using (7) and (8) of Chapter 2 if and only if

*For proof, see Appendix.

a) $Z(s)$ may be expressed as

$$Z(s) = \frac{k_\infty}{\sqrt{s}} \tanh \frac{a\sqrt{s}}{2} + \frac{k_o}{\sqrt{s} \tanh \frac{a\sqrt{s}}{2}} + \sum_{i=1}^{n} \frac{2 k_i \tanh \frac{a\sqrt{s}}{2}}{\sqrt{s} \left[\tanh^2 \frac{a\sqrt{s}}{2} + \Omega^2_i\right]}$$

b) where k_∞, k_o, and $k_i \geq 0$

An equivalent theorem may be formulated, such that

Theorem V.* $Z(s)$ may be realized as a driving point impedance by a finite number of elemental $\overline{URCS}$ and $\overline{URCO}$ networks using (7) and (8) of Chapter 2 if and only if

a) $\sqrt{s}\, Z(s)$ is a rational function of $e^{a\sqrt{s}}$

b) Re $(\sqrt{s}\, Z(s)) = 0$ for $\sqrt{s} = jq$, q real

or $s = -q^2$, q real

c) Re $(\sqrt{s}\, Z(s)) \geq 0$, Re $\sqrt{s} > 0$

It is noted that Re $Z(s) = 0$, $s \to \infty$.

Returning to the inverse transformation of either (11) or (12) in Chapter 2, it is clear that the most useful analytic expression of the $\overline{RC}$ impedance, $Z_{\overline{RC}}(s)$, must be of the form

$$Z_{\overline{RC}}(s) = \frac{1}{\sqrt{s}} \frac{N(e^{a\sqrt{s}})}{D(e^{a\sqrt{s}})} \qquad (1)$$

*For proof, see Appendix.

where N and D are rational polynomials in $e^{a\sqrt{s}}$. The rational function Z(S) may then be arrived at by substituting

$$e^{a\sqrt{s}} = \frac{1 + S}{1 - S} \tag{2}$$

into (1), thus transforming Z into a rational function of S. It is important to be able to arrive at (1) in a direct fashion, if Z(s) is originally specified by, say, a graphical magnitude function.

Consider the construction of

$$\sqrt{s}\, Z_{RC}(s)\Big|_{s=j\omega} = \frac{N(e^{a\sqrt{s}})}{D(e^{a\sqrt{s}})}\Bigg|_{s=j\omega} \tag{3}$$

A plot of the magnitude of the left side of (3) in db., as a function of log ω, will be related to a similar plot of (1) by the simple difference of 10 db./decade, arising from the factor $\sqrt{\omega}$. Thus if (1) is specified graphically, (3) may be similarly represented.

Because Z(s) is an $\overline{RC}$ function, it is at once apparent that $|Z(s)|_{s=j\omega}$ must be a monotonically decreasing function of ω, and that $Z(\infty) = 0$. With these conditions satisfied, it may be possible to approximate Z(s) as will be described presently.

Theorem VI. Z(s) may be realized as a $\overline{URC}$ network under (7) of Chapter 2 if and only if $\sqrt{s}\, Z(s)$ may be expressed as

$$\sqrt{s}\,Z(s) = \frac{(e^{a\sqrt{s}}+1)^{2(m-n)+1}}{(e^{a\sqrt{s}}-1)} \frac{\prod_{1}^{n}(e^{2a\sqrt{s}}+B_k e^{a\sqrt{s}}+1)}{\prod_{1}^{m}(e^{2a\sqrt{s}}+A_k e^{a\sqrt{s}}+1)}$$

or its inverse, where $A_k > B_k$, $|A_k| < 2$, $|B_k| < 2$ and $m = n$ or $n-1$. Note that either one A_k or one B_k may be zero, but not both.

4.2 Realizability of Z(s) by $\overline{\text{URCR}}$ Networks

Under the relationship which has been carefully established between s and p/(1+p), it is clear that Theorems IV, V and VI hold for $\overline{\text{RCR}}$ networks with proper modification. In Theorem IV, (a), replace s by s/(1+s) in the right side of the equation. Make the same substitution in parts (a) through (c) of Theorem V, as made in Theorem IV. Again, make the substitution $\frac{p'}{\sqrt{1+p'}} = s$ in the right side of the equation of Theorem VI. The above statements refer to the fact that the theorems may be applied directly to $\overline{\text{URCR}}$ functions after transformation from $\frac{p'}{1+p'}$ to s. Note that $Z(p)\Big|_{p \to \infty}$ will be finite and non-zero.

The construction of $\overline{\text{RCR}}$ realizable functions follows from the form indicated in (3). In the case of the $\overline{\text{RCR}}$ networks the desired immittance function is first approximated as ratios of polynomials in $e^{a\sqrt{p'/1+p'}}$; the graphical approximation of such polynomials is indicated from Figs. 3-4 through 3-7. Additional design freedom is available from the constants 'a' and $R_A C$, compared to the $\overline{\text{RC}}$ synthesis.

4.3 Realization of Z(s) by Cascade Synthesis: Introduction

Consider the properties of a cascade configuration of several $\overline{URCO}$ lines. Each line is assumed to have the same $R_oC_oL^2$ product, but different R_oL terms. This restriction is implied by the use of the transformation $S = \tanh a\sqrt{s}/2$ in which 'a' is kept constant for the entire synthesis.* It is convenient to consider the ABCD cascade matrices for each of the $\overline{RC}$ line segments. Letting $\tau = R_oC_oL^2 = (a/2)^2$, and the total segment resistance $R_i = R_oL$, the cascade matrix for the i^{th} segment is given by

$$\begin{bmatrix} A_i & B_i \\ C_i & D_i \end{bmatrix} = \begin{bmatrix} \left(\cosh\sqrt{s\tau}\right)\left(\dfrac{R_i \sinh\sqrt{s\tau}}{\sqrt{s\tau}}\right) \\ \dfrac{\sqrt{s\tau}\sinh\sqrt{s\tau}}{R_i} \qquad \cosh\sqrt{s\tau} \end{bmatrix} = \cosh\sqrt{s\tau}\begin{bmatrix} 1 & \dfrac{R_i\tanh\sqrt{s\tau}}{\sqrt{s\tau}} \\ \dfrac{\sqrt{s\tau}\tanh\sqrt{s\tau}}{R_i} & 1 \end{bmatrix} \tag{4}$$

The overall ABCD matrix for n different sections in cascade is

$$\begin{bmatrix} A & B \\ C & D \end{bmatrix}_o = (\cosh\sqrt{s\tau})^n \prod_{i=1}^{n} \begin{bmatrix} 1 & \dfrac{R_i\tanh\sqrt{s\tau}}{\sqrt{s\tau}} \\ \dfrac{\sqrt{s\tau}\tanh\sqrt{s\tau}}{R_i} & 1 \end{bmatrix} \tag{5}$$

B_i has the units of an RC impedance, while C_i has the units of an RC admittance. Thus it is possible to discuss an equivalent $\overline{LC}$ network, by Theorem I, for which A_i and D_i are unchanged and

$$B_{i\overline{LC}} = \sqrt{s}\, B_{i\overline{RC}} \; ; \quad C_{i\overline{LC}} = \frac{1}{\sqrt{s}}\, C_{i\overline{RC}} \tag{6}$$

*This practically restricts the entire network being synthesized to be made up of RC segments of the same length. In Section 4.7 the decomposition of the network frunction being synthesized into several networks with separate L's is considered.

The overall matrix (5) is transformed to that of the associated uniform $\overline{LC}$ structure:

$$\begin{bmatrix} A & B \\ C & D \end{bmatrix}_o = (\cosh \sqrt{s\tau})^n \prod_{i=1}^{n} \begin{bmatrix} 1 & \frac{R_i \tanh \sqrt{s\tau}}{\sqrt{\tau}} \\ \frac{\sqrt{\tau} \tanh \sqrt{s\tau}}{R_i} & 1 \end{bmatrix} \tag{7}$$

Application of the transformation

$$S_1(\sqrt{s}) = \tanh \frac{a\sqrt{s}}{2} \tag{8}$$

to (7) results in a matrix which is again LC in the S plane; for driving point immittances, the resulting functions will be realizable as lumped immittances in the S plane. Note that under (8) the resulting transfer immittances, as opposed to the driving point terms, cycle every 'a/2' units instead of every 'a' units. This arises from the fact that for $\overline{URC}$ networks, the transfer quantities involve the factors

$$\cosh \frac{a\sqrt{s}}{2} = \frac{e^{\frac{a\sqrt{s}}{2}} + e^{\frac{-a\sqrt{s}}{2}}}{2} = \frac{1}{\sqrt{1 - S^2}} \tag{9}$$

and

$$\sinh \frac{a\sqrt{s}}{2} = \frac{e^{\frac{a\sqrt{s}}{2}} - e^{\frac{-a\sqrt{s}}{2}}}{2} = \frac{S}{\sqrt{1 - S^2}} \tag{10}$$

while the driving point impedances involve only

$$\tanh \frac{a\sqrt{s}}{2} = \frac{e^{a\sqrt{s}} - 1}{e^{a\sqrt{s}} + 1} \equiv S \tag{11}$$

Thus, for the general i^{th} RC segment, (4) becomes

$$\begin{bmatrix} A & B \\ C & D \end{bmatrix}_I = \frac{1}{\sqrt{1 - S^2}} \begin{bmatrix} 1 & \frac{R_i S}{\sqrt{\tau}} \\ \frac{\sqrt{\tau} S}{R_i} & 1 \end{bmatrix} \qquad \text{(a)}$$

For two such identical segments in cascade, (12)

$$\begin{bmatrix} A & B \\ C & D \end{bmatrix}_{II} = \frac{1}{1 - S^2} \begin{bmatrix} 1 + S^2 & \frac{2R_i S}{\sqrt{\tau}} \\ \frac{2\sqrt{\tau} S}{R_i} & 1 + S^2 \end{bmatrix} \qquad \text{(b)}$$

Likewise, for n units in cascade, with n an even integer, the resulting networks will all involve only integral powers of S. Similarly, the respective [Y] matrices may be calculated to be

$$[Y]_I = \begin{bmatrix} \frac{\sqrt{\tau}}{R_i S} & \frac{-\sqrt{\tau}(1-S^2)^{\frac{1}{2}}}{R_i S} \\ \frac{-\sqrt{\tau}\,(1-S^2)^{\frac{1}{2}}}{R_i S} & \frac{\sqrt{\tau}}{R_i S} \end{bmatrix} \qquad \text{(a)}$$

and (13)

$$[Y]_{II} = \begin{bmatrix} \frac{\sqrt{\tau}\,(1+S^2)}{2R_i S} & \frac{-(1-S^2)\sqrt{\tau}}{2R_i S} \\ \frac{-(1-S^2)\sqrt{\tau}}{2R_i S} & \frac{\sqrt{\tau}\,(1+S^2)}{2R_i S} \end{bmatrix} \qquad \text{(b)}$$

4.4 Cascade Synthesis by Richard's Theorem

A straightforward $\overline{RC}$ driving point immittance synthesis procedure applies Richard's Theorem[16,21] to the $\overline{RC}$ network representations in the S plane. Richard's Theorem was first exploited by Bott and Duffin in their lumped transformerless synthesis procedure and has also been used in the design of UHF and microwave lossless filters.[26,27] It may be stated as follows:[28]

> If Y(S) is a positive real function, and
>
> $$Y_L(S) = Y(1)\,\frac{Y(S) - S\,Y(1)}{Y(1) - S\,Y(S)}$$
>
> is constructed, $Y_L(S)$ is again a positive real function. Additionally, if Y(S) is LC, $Y_L(S)$ must be LC.

In light of Richard's Theorem, consider the cascade admittance Y_1 of n sections of $\overline{RC}$ line, in Fig. 4-1. It may be shown that

$$Y_i(s) = \frac{1}{R_i}\,\frac{R_i\,Y_{i+1} + \sqrt{s\tau}\,\tanh\sqrt{s\tau}}{1 + R_i\,Y_{i+1}\,\dfrac{\tanh\sqrt{s\tau}}{\sqrt{s\tau}}} \tag{14}$$

Solving for $Y_{i+1}(s)$,

$$Y_{i+1}(s) = \frac{1}{R_i}\,\frac{R_i\,Y_i(s) - \sqrt{s\tau}\,\tanh\sqrt{s\tau}}{1 - R_i\,Y_i(s)\,\dfrac{\tanh\sqrt{s\tau}}{\sqrt{s\tau}}} \tag{15}$$

where it is assumed that $Y_i(s)$ is a given and realizable $\overline{RC}$ function. Thus $Y_i(s)/\sqrt{s}$ must be a realizable $\overline{LC}$ function in the $\sqrt{s}$ plane. In particular,

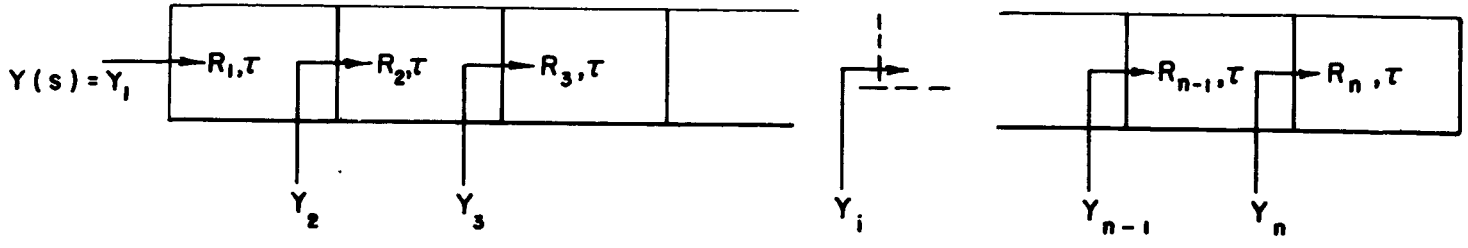

FIG. 4-1

CASCADED $\overline{RC}$ LINE SEGMENTS

$$\frac{Y_i(s)}{\sqrt{s}} \equiv Y_{i\overline{LC}}(\sqrt{s}) = \frac{1}{R_i} \frac{R_i \frac{Y_{i+1}}{\sqrt{s}} + \sqrt{\tau} \tanh \sqrt{s\tau}}{1 + R_i Y_{i+1} \frac{\tanh \sqrt{s\tau}}{\sqrt{s\tau}}} \tag{16}$$

Similarly,

$$Y_{i+1}(\sqrt{s}) = \frac{1}{R_i} \frac{R_i \frac{Y_i(s)}{\sqrt{s}} - \sqrt{\tau} \tanh \sqrt{s\tau}}{1 - R_i Y_i(s) \frac{\tanh \sqrt{s\tau}}{\sqrt{s\tau}}} \tag{17}$$

is an $\overline{LC}$ driving point admittance in the $\sqrt{s}$ plane, and under (8) may be transformed into $Y_i(S)$, a PR and LC function in the S plane. In a like manner, if (8) is again applied,

$$\begin{aligned} Y_{i+1\ LC}(S) &= \frac{1}{R_i} \frac{R_i Y_i(S) - \sqrt{\tau}\, S}{1 - \frac{R_i}{\sqrt{\tau}} S\, Y(S)} \\ &= \frac{\sqrt{\tau}}{R_i} \frac{Y_i(S) - S \frac{\sqrt{\tau}}{R_i}}{\frac{\sqrt{\tau}}{R_i} - S\ \ Y(S)} \end{aligned} \tag{18}$$

Observe that the final expression in (18) is identical with that of Richard's Theorem if $\sqrt{\tau}$ and R_i are positive and thus R_i is <u>uniquely</u> specified for each line segment. The process is repeated until $Y_n(S) = 1/S$ or S remains. The process will always so converge,[16] as is noted in the next section. The significance of the theorem in the present application is that an $\overline{RC}$ line may always be 'extracted' from a desired function, and the resulting simpler driving point admittance may always be realized as a cascade of a finite number of $\overline{RC}$ lines through a repetition of the

process. Thus any driving point immittance which fulfills the conditions of Theorems IV, V or VI may be realized as a cascade configuration of $\overline{RC}$ lines. By application of Sections 2.3 and 4.2 $\overline{RCR}$ functions may similarly be constructed.

4.5 Example of RC Cascade Driving Point Synthesis

In order to illustrate the application of Richard's Theorem, consider the realization of Z(s) corresponding to $Z(S) = \frac{(S^2+9)(S^2+25)}{(S)\ (S^2+16)}$. Four ladder connected $\overline{URC}$ segments (one ports) would realize the driving point impedance alone. This is an undesirable configuration. Four $\overline{RC}$ cascaded two-port segments are required, but allow a desirable fabrication technique. To begin the synthesis, suppose that the original specifications require $\sqrt{\tau} = 1$.

$$Y_1(S) = Y(S) = 1/Z(S) = \frac{S(S^2+16)}{(S^2+9)(S^2+25)} \tag{19}$$

$$Y_1(1) \equiv \frac{1}{R_1} = \frac{(1)(17)}{(10)(26)} = .0654$$

$$Y_2(S) = \frac{1}{R_1} \quad \frac{Y(S) - \frac{S}{R_1}}{\frac{1}{R_1} - S\ Y(S)}$$

$$= .0654 \quad \frac{\frac{S(S^2+16)}{(S^2+9)(S^2+25)} - .0654\ S}{.0654 - \frac{S^2(S^2+16)}{(S^2+9)(S^2+25)}}$$

$$= .00454\ S \quad \frac{(S^2+24.8)\cancel{(S^2-1)}}{(S^2+15.75)\cancel{(S^2-1)}}$$

Now, let $Y_2(S)$ be fabricated. By Richard's Theorem, $Y_2(S)$ is PR and LC.

$$Y_2(1) = \frac{.00454\ (25.8)}{16.75} = .00700 = \frac{1}{R_2}$$

$$\therefore Y_3(S) = .007\ \frac{Y_2(S) - .00700\ S}{.00700 - S\ Y_2(S)}$$

$$= .007\ \frac{\dfrac{.00454\ S(S^2+24.8)}{S^2+15.75} - .007\ S}{.007 - \dfrac{.00454\ S^2(S^2+24.8)}{S^2+15.75}}$$

$$= \frac{.00381\ S(S^2-1)}{(S^2+24.4)(S^2-1)}$$

Finally,

$Y_3(S)$ is PR and

$$Y_3(1) = \frac{.00381}{25.4} = .000150$$

$$\therefore Y_4(S) = .00015\ \frac{Y_3(S) - .00015\ S}{.00015 - S\ Y_2(S)}$$

$$= (.00015)\ \frac{\dfrac{3.81\ S}{S^2+24.4} - .15\ S}{.15 - \dfrac{S^2(3.8)}{S^2+24.4}} = .00015\ \frac{.15(S^2-1)}{3.65(S^2-1)}$$

$$= 6.18 \times 10^{-6}\ S$$

The network corresponding to the previous calculations is found in Fig. 4-2(a). The physical embodiment of this network is pictured in Fig. 4-2(b).

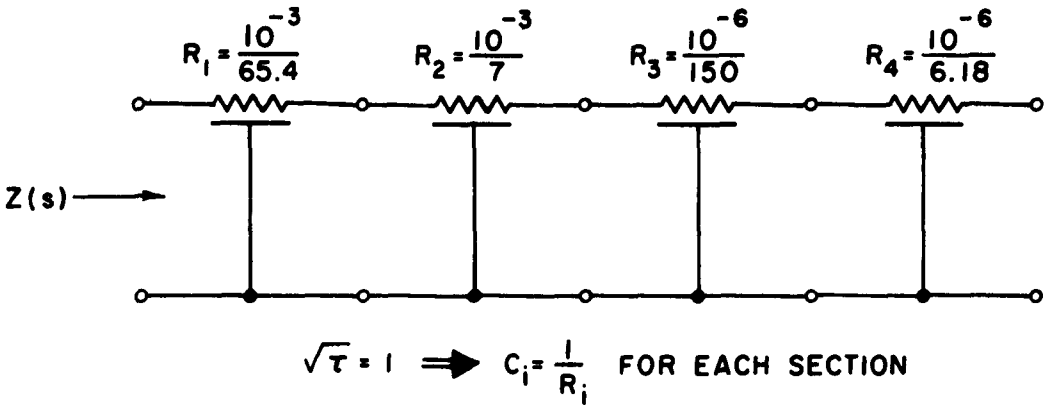

FIG. 4-2(a)

$\overline{RC}$ SYMBOLIC REALIZATION

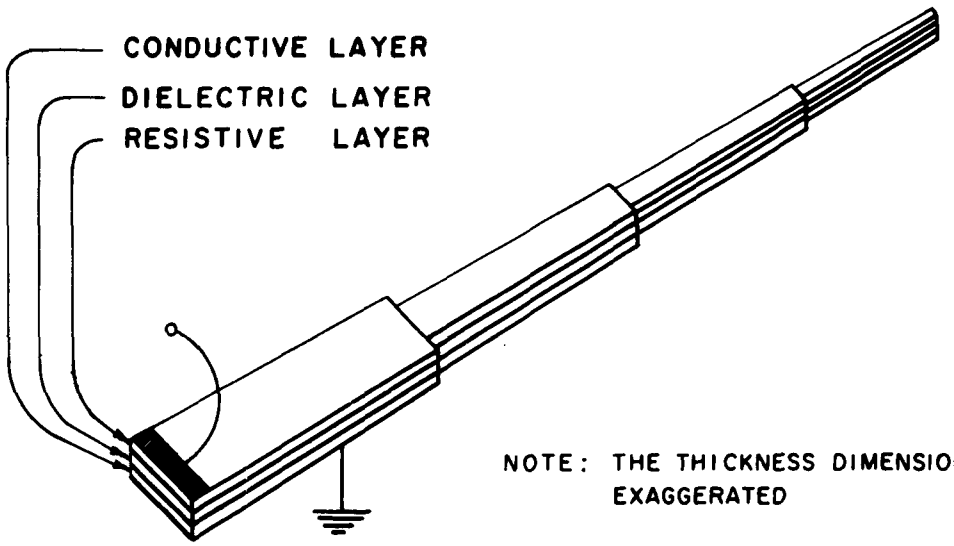

FIG. 4-2(b)

$\overline{RC}$ NETWORK REALIZATION

4.6 Example of $\overline{RC}$ Driving Point Synthesis From Graphical Magnitude Specification

As a typical problem, consider synthesizing the function depicted in Fig. 4-3. The first step is to normalize the graph with respect to frequency and it will be assumed in Fig. 4-3 that this has been done. Application of the magnitude curves of Chapter Three within the framework of Theorem VI suggests that the graphical data of Fig. 4-3 may be approximated by

$$Z(s) = \frac{1}{\sqrt{s}} \quad \frac{e^{a\sqrt{s}} + 1}{e^{a\sqrt{s}} - 1} \quad \frac{e^{2a\sqrt{s}} - 1.9\, e^{a\sqrt{s}} + 1}{e^{2a\sqrt{s}} + e^{a\sqrt{s}} + 1} \tag{20}$$

Referring to Fig. 3-1, $B_1 = -1.9$ is used because of the wide frequency spread (almost two decades) between break points. Eq. (20), plotted in Fig. 4-3, is compared with the magnitude-normalized original specification. Note that the magnitude normalization (by 120 db.) simply involves multiplication of resistive values by 10^6 and division of all capacitance values by the same number.

Using the transformation (2), (20) becomes

$$Z(S) = \frac{1}{S}\left[\frac{3.9\,S^2 + 0.1}{S^2 + 3}\right]$$

$$= \frac{3.9}{S}\left[\frac{S^2 + .0256}{S^2 + 3}\right] \tag{21}$$

In order to apply Richard's Theorem, the associated admittance function is found to be

$$Y(S) = \frac{S}{3.9}\left[\frac{S^2 + 3}{S^2 + .0256}\right] \tag{22}$$

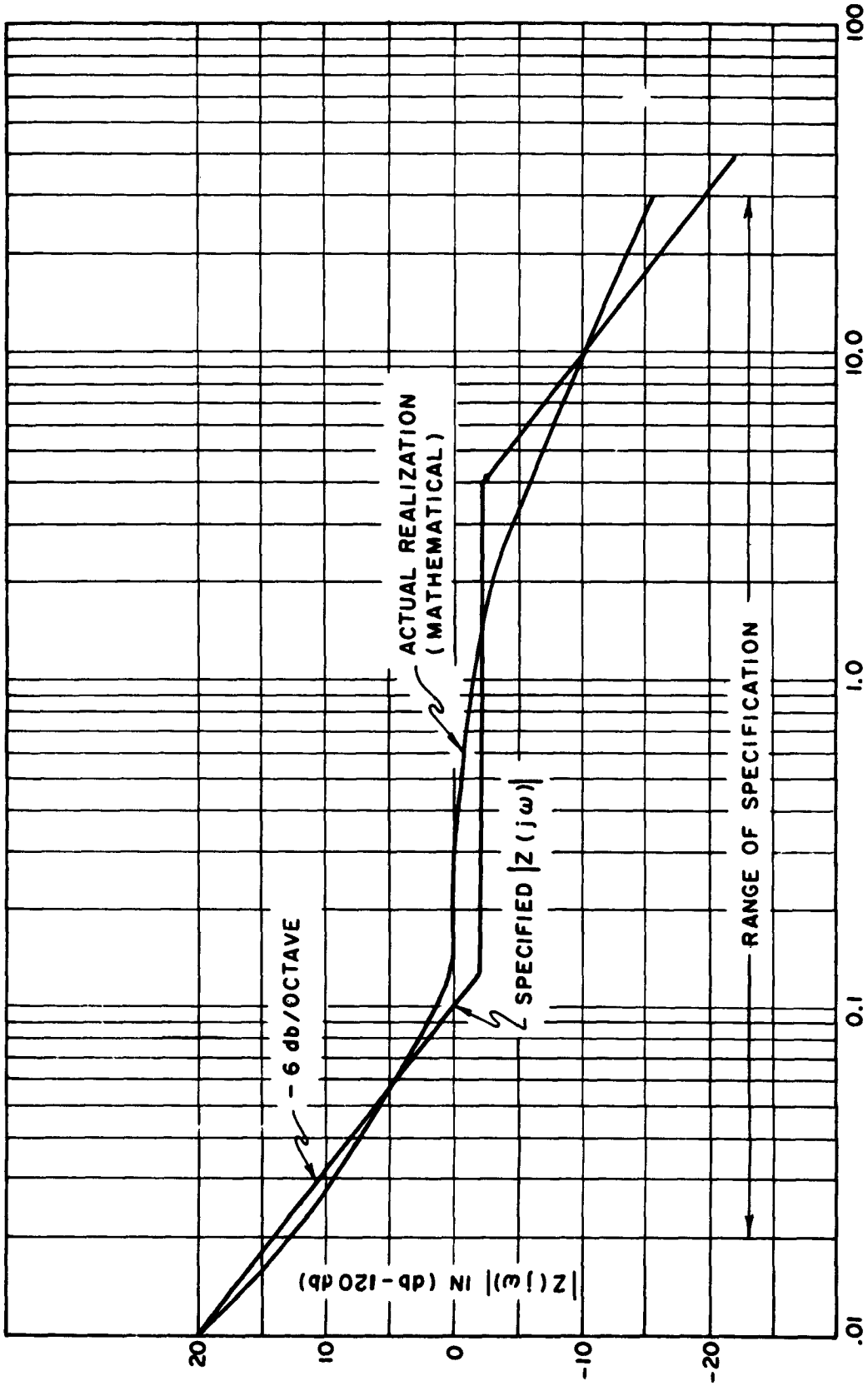

FIG. 4-3

ILLUSTRATION OF EXAMPLE OF SECTION 4.6

from which

$$Y(1) = 1 \tag{23}$$

Since Y(1) is known, $Y_1(S)$ may be computed to be

$$Y_1(S) = Y(1)\ \frac{Y(S) - S\,Y(1)}{Y(1) - S\,Y(S)} \tag{24}$$

$$= \frac{\frac{S}{3.9}\left[\frac{S^2+3}{S^2+.0256}\right] - S}{1 - \frac{S^2}{3.9}\left[\frac{S^2+3}{S^2+.0256}\right]}$$

$$= \frac{2.9\,S(S^2-1)}{(S^2+.1)(S^2-1)} = \frac{2.9\,S}{S^2+.1} \tag{25}$$

Then

$$Y_1(1) = 2.64 \tag{26}$$

$$Y_2(S) = Y_1(1)\ \frac{Y_1(S) - S\,Y_1(1)}{Y_1(1) - S\,Y_1(S)}$$

$$= 2.64\,S\left[\frac{2.64 - 2.64\,S^2}{-.26\,S^2+.26}\right]$$

$$= 26.9\,S \equiv \frac{\sqrt{\tau}}{R_2}\,S \tag{27}$$

The individual segment parameters are found to be

$$\frac{1}{Y(1)} = \frac{R_0}{\sqrt{\tau}} = 1 \qquad \frac{1}{Y_1(1)} = \frac{R_1}{\sqrt{\tau}} = \frac{1}{2.64} = .378 \qquad \frac{1}{Y_2(1)} = \frac{R_2}{\sqrt{\tau}} = \frac{1}{26.9} = .0372 \tag{28}$$

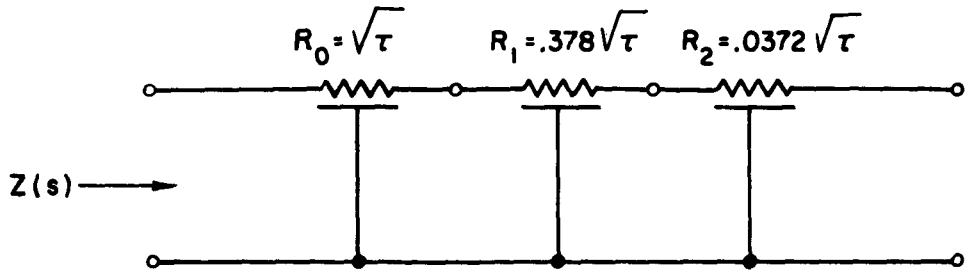

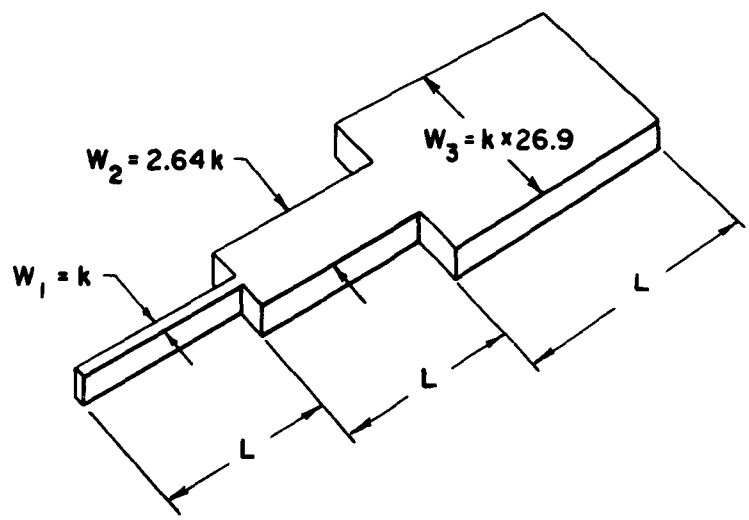

FIG. 4-4

$\overline{RC}$ NETWORK TO REALIZE FIG. 4-3

The physical embodiment of the normalized network appears in Fig. 4-4. $\sqrt{\tau} = RC$ may be chosen for the proper frequency scaling. If $RC = 10^{-6}$, $\sqrt{\tau} = 10^{-3}$ and

$$R_0 = 10^{-3}\ \Omega \qquad R_1 = .378 \times 10^{-3}\ \Omega \qquad R_2 = .0372 \times 10^{-3}\ \Omega$$
$$C_0 = \frac{\tau}{R_0} = 10^{-3}\ f \qquad C_1 = 2.64 \times 10^{-3}\ f \qquad C_2 = 27 \times 10^{-3}\ f \tag{29}$$

To raise the impedance level by 10^6 (or 120 db.), the previous values are changed to $10^6 \times R_1$ and $10^{-6} \times C_1$, or

$$R_0' = 10^3\ \Omega \qquad R_1' = 378\ \Omega \qquad R_2' = 37.2\ \Omega$$
$$C_0' = 10^{-9}\ f \qquad C_1' = 2640\ pf. \qquad C_2' = 27000\ pf. = .027\ uf.$$

As a check on the validity of the technique, Z(s) for the network of Fig. 4-4 may be computed (without recourse to the S plane) to be

$$Z(s) = \frac{R_0}{\sqrt{s\tau}\tanh\sqrt{s\tau}}\left[1 - \frac{(R_1 + R_2)R_0}{(R_0 + R_1)(R_1 + R_2)\cosh^2\sqrt{s\tau} - R_1^2}\right] \tag{30}$$

and with the normalized RC parameters, this is seen to be

$$\frac{R_0}{\sqrt{s\tau}\tanh\sqrt{s\tau}}\left[\frac{e^{2a\sqrt{s}} - 1.9\,e^{a\sqrt{s}} + 1}{e^{2a\sqrt{s}} + e^{a\sqrt{s}} + 1}\right] \tag{31}$$

which checks with the original specifications.

The preceding network was experimentally built using Teledeltos

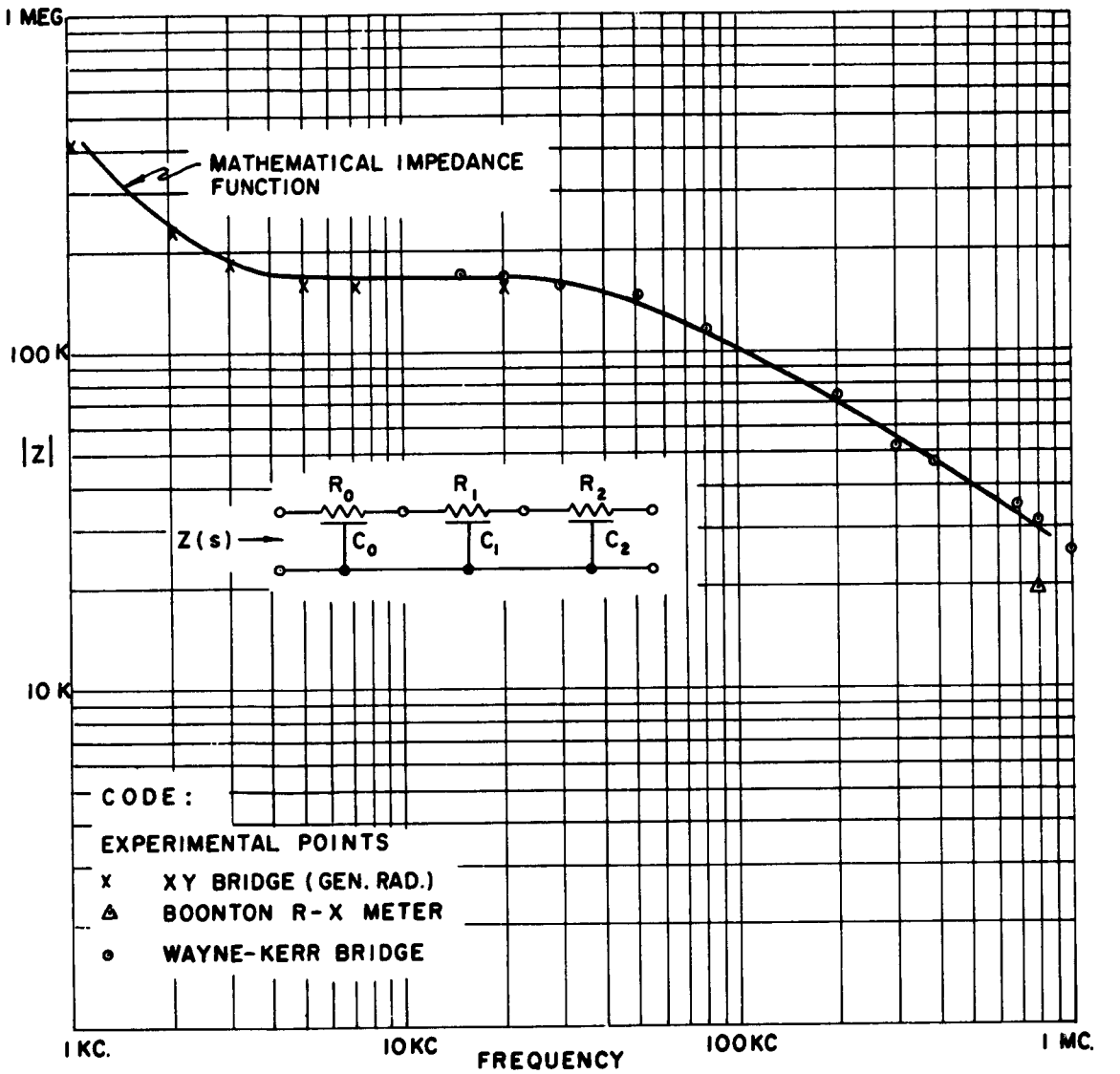

FIG. 4–5

EXPERIMENTAL VERIFICATION OF EXAMPLE OF SECTION 4-6

Resistance Paper* firmly pressed against copper conductor, geometrically formed as indicated in Fig. 4-4. The resistance of each segment was measured precisely. The capacitance per square inch for such a layout is known from previous experience to be 310 picofarads per square inch. For this experiment, R_0 was 115 kilohms, R_1 was 43.6 kilohms and R_2 was 4.26 kilohms. The RC product was 7.95×10^{-6} for each segment. The experimental and mathematical realizations are considered in Fig. 4-5, where excellent agreement is to be noted.

4.7 Concluding Remarks

In this chapter, a straightforward distributed RC synthesis technique has been evolved which significantly does not require recourse to a digital computer for implementation. The broad class of monotonically decreasing functions of real frequency which may be synthesized by these techniques has been detailed in Theorem VI. The eventual realization of the driving point functions by cascade $\overline{RC}$ structures was shown to be of practical significance, and theoretical examples and experimental results were shown to compare closely. Additionally, $\overline{URCR}$ networks were introduced. These networks allow a broader class of impedances to be achieved, and permit non-zero driving point impedances to be realized at high frequencies.

Certain limitations are inherent in the classes of functions which may readily be synthesized by the previous techniques. Further research directed toward relaxing these restrictions is indicated.

---

*Available from Western Union Co., New York City.

Some information is available in the literature which indicates that non-uniform lines[9] are superior in certain performance aspects to uniform lines. Their use in the previous driving point synthesis without recourse to computers would be possible, if for the variously tapered lines, conformal transformations were found so that the synthesis might be carried out in the S plane.

A more immediate limitation of the present method arises from the use of a constant RC product for each $\overline{URCO}$ segment. As seen from Figs. 3-1 and 3-3, breakpoints in the magnitude function may be achieved over about two decades. If a network function is to be achieved for which breakpoints exist over more than two decades some kind of network decomposition into subnetworks must be employed; each subnetwork will be characterized by a different RC product and will be used to realize breakpoints in different frequency bands. In the normalized plots of Figs. 3-1, 2 and 3, it is noted that the frequency is normalized to $a/2 = (RC)^{\frac{1}{2}}$, so that the plots may be applied universally.

CHAPTER FIVE

SYNTHESIS OF $\overline{RC}$ TRANSFER FUNCTIONS

5.0 Introduction

The transfer function synthesis problem in lumped networks is often phrased as follows: "Design a network N with a specified voltage (current) gain, working from a source into a given load." Since either gain function may be written in terms of a driving point immittance, a transfer immittance, and the given load immittance, the above requirement is identical to asking the designer to find a network with a prescribed driving point immittance and prescribed transmission zeros. The transmission and driving point functions are intimately related, however, as evidenced by the Fialkow-Gerst conditions. Assuming that the two functions have the same denominator, the specification of y_{11} and the zeros of y_{12} describes y_{12} within an arbitrary constant. Often this is the best that can be achieved, although in the case of gain functions it may be preferable to attempt to keep the constant as large as possible in order to avoid unnecessary inband loss.

A similar synthesis problem for $\overline{RC}$ networks will now be undertaken. Although the synthesis may be based on either the S plane or the s plane, it is usually advantageous to design in the former. The specific problem under consideration is the realization of a network having a prescribed gain function, fed by an ideal current or voltage source and working into a load which is nominally resistive. It is convenient to assume

that the load is coupled through a distributed capacitance, as is typically done in current microelectronic amplifier design[12] (see Fig. 5-9). If the load is directly connected to the network, it is realistic to assume that some stray capacitance exists across it. The effective load is thus a lumped parallel RC network, whose driving point impedance is rational in s, but not rational in S. This poses a distinct problem, since the power of the synthesis techniques under consideration lies in the fact that driving point impedances which are realized are rational in S. This situation may be handled with no difficulty, however, as shall be seen presently.

It is useful to make some preliminary observations at this point concerning the origin of the lumped RC load which has been mentioned. First, the load may be exactly what is postulated: a resistor, with some lumped capacitance across it. Second, the parallel RC circuit may itself be an approximation, valid within a certain degree of accuracy and over a certain frequency range, of a more general RC network such as the input of a thin-film transistor.[19,20] In the latter case, a distributed RC network approximation might have been more appropriate to begin with, and should have been formulated. In the former case, it is necessary to approximate the driving point characteristic of the lumped RC load by a distributed $\overline{RC}$ load which is then used in the actual synthesis procedure. This approximation is particularly simple at low frequencies (below $\omega RC = 2$), where a single $\overline{URCS}$ network approximates the lumped case quite well.[29] Over the range indicated, both the postulated lumped network and its distributed counterpart are primarily resistive. At higher frequencies, it

may be necessary to employ a more complicated distributed load to approximate the lumped load characteristic, in accordance with the methods of Chapter Three.

5.1 Transmission Zeros in the S and the s Planes

Consider the mathematical forms which the gain or immittance functions may assume to be realized by S plane techniques. In the S plane, transmission zeros may generally be realized anywhere except on the region of the positive real axis between the origin and unity. This segment corresponds to the entire positive real axis in the s plane. Generally, then, zeros may exist with quadrantal symmetry in the S plane, or in conjugate symmetry on the $j\Omega$ axis. In the S plane they will be finite in number. By reference to Fig. 2-3, quadrantal symmetry of poles or zeros in the S plane corresponds to left half-plane conjugate symmetry of a family of poles or zeros in the s plane. Conjugate imaginary zeros in the S plane map into negative purely real zeros in the s plane. These equivalences should be borne in mind, so that one may freely work in either plane.

If the transmission zeros in the S plane occur with quadrantal symmetry, terms of the form

$$P(s) = (e^{4a\sqrt{s}} + Be^{3a\sqrt{s}} + (2-B)\, e^{2a\sqrt{s}} + Be^{a\sqrt{s}} + 1) \qquad (1)$$

with

$$\infty > B > 1 \qquad (2)$$

will occur in $y_{12}(s)$. Such a form is obtained by application of the

transformation (2) of Chapter 4 to the S plane polynomial, $(S^4 + a^4)$. By similar application, conjugate imaginary S plane zeros are reflected in $y_{12}(s)$ by terms having the form

$$Q(s) = (e^{2a\sqrt{s}} + Be^{a\sqrt{s}} + 1) \tag{3}$$

where $|B| < 2$. It was shown in Section 2.2 that each $\overline{URC}O$ cascaded two-port which is employed contributes a numerator factor in the S plane

$$R(s) = (1 - S^2)^{\frac{1}{2}} \tag{4}$$

These factors represent zeros at $S = \pm 1$ or $s = \infty$, which are physically caused by the shunt capacitance of the $\overline{RC}$ elements, in cascade.

Thus finite transmission zeros on the imaginary S axis (or negative real axis of the s plane) must be realized by other than cascaded $\overline{RC}$ elements. When such transmission zeros are realized, it may be possible to realize transmission zeros with quadrantal symmetry in the S plane. One of the objectives of the present chapter is to achieve finite negative real transmission zeros which assist in meeting prescribed characteristics in the s plane.

In order to realize finite transmission zeros, stubs (which are really shunt elements) can be employed to modify the cascade type synthesis of Chapter Four. Fig. 5-1 illustrates the new configuration.

A 'resonant stub' in the S plane represents a shunt element which realizes one pair of conjugate imaginary S plane zeros of transmission by effecting a "short circuit" at the frequency of interest. This entails

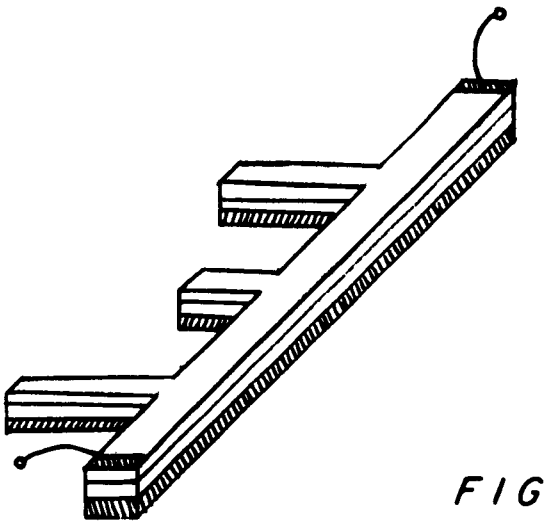

FIG. 5-1

A CASCADE-STUB REALIZATION

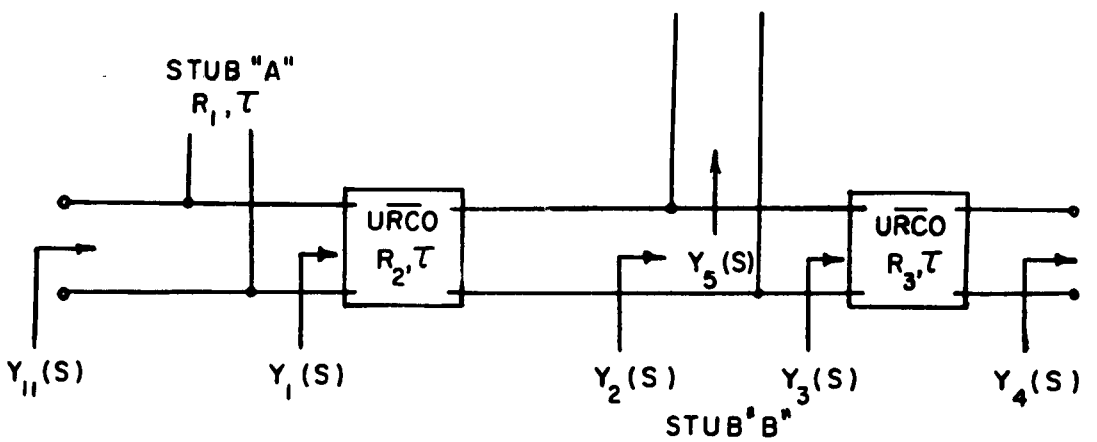

FIG. 5-2

CASCADE-STUB EXTRACTION CYCLE

the removal of one term of the form $(e^{2a\sqrt{s}} + Be^{a\sqrt{s}} + 1)$ from the corresponding s plane expression. Other RC elements will then be extracted to complete the cycle associated with the desired transmission zeros, following the approach of the work of Ikeno[27] in his lossless coaxial filter designs.

5.2 Qualitative Discussion of Permissible Transfer Functions

Using S plane synthesis procedures to be detailed in this section and Section 5.3, it is shown that the class of transfer admittances in the S plane described by

$$-y_{21}(S) = M_{21} \frac{\left[\prod_{1}^{n} (S^2 + D_j^2)\right]\left[1 - S^2\right]^{q/2}}{S \prod_{1}^{m} \left[S^2 + C_k^2\right]} \qquad (5)$$

where

m, n, q are positive integers

$q/2 \geq n$

$m \geq n + q/2 - 1$

M_{21} = real positive number,

may be realized within an arbitrary constant. Under the technique, the zeros of transmission, along with the exact driving point admittance, are achieved.

In the s plane, which is the plane of definition of the $\overline{RC}$ network function, application of the transformation $e^{a\sqrt{s}} = \frac{1 + S}{1 - S}$ leads to the following transfer admittance.

$$-y_{21}(s) = \frac{M'_{21}\sqrt{s}\,(e^{qa\sqrt{s}/2})^{(2(m-n)-q+1)}\quad(e^{a\sqrt{s}}+1)\prod_{1}^{n}(e^{2a\sqrt{s}}+B_j e^{a\sqrt{s}}+1)}{(e^{a\sqrt{s}}-1)\prod_{1}^{m}(e^{2a\sqrt{s}}+A_k e^{a\sqrt{s}}+1)} \tag{6}$$

where

$$|A_k| < 2 \tag{7}$$

$$|B_j| < 2 \tag{8}$$

It is of considerable interest at this point to gain some insight into the real frequency magnitude properties of this function, before proceeding to stipulate realizability conditions on (6). Qualitatively, the terms of principal interest in (6) are the second order exponential polynomials. If comparison is made between the driving point expression of Theorem VI, and the expression in (6), it is noted that the condition $A_k > B_k$ does not apply to (6). This is true because pole-zero alternation in the S plane is no longer required for a transfer impedance. The second order exponential polynomials in the numerator of Eq. (6) have magnitude functions which increase monotonically with frequency. They are to be chosen in accordance with the graphical representations of Chapter Three, and the realizability conditions to follow. The second order polynomials in the denominator of (6) cause $y_{21}(s)$ to decrease in magnitude with increasing frequency. From the known properties of the expressions in (6) it is anticipated that there will be little difficulty in accomplishing low pass characteristics of rather arbitrary graphical specifications. The second order polynomial factors allow the shaping of such characteristics.

Because of the basically low-pass nature of $\overline{RC}$ networks, including those with stubs, there will be difficulty in realizing bandpass characteristics. A method of overcoming this obstacle is suggested in Section 5.6. Without the stubs, however, it would be impossible to realize the second-order exponential polynomials in the numerator of (6), or, for that matter, any finite transmission zeros to assist in shaping the transmission magnitude characteristics.

The 'cascade and stub' network introduced in Fig. 5-1 requires the stubs to extract the second order transmission numerator terms. The cascade elements will contribute zeros at infinity in the s plane which is to say that $y_{21}(S)$ will contain factors of the form $(1-S^2)$. At least one such factor must exist for each transmission zero pair removed in the S plane, which is why the condition $q/2 \geq n$ appears.

5.3 Transfer Function Extraction Cycle for Finite Zeros

The motivation and the technique for the 'cascade and stub' transfer synthesis procedure is evident if the following extraction cycle is postulated. With reference to Fig. 5-2, for synthesis in the S plane, the finite product of second order (B_i) exponential polynomials of Eq. (6) corresponds to the $(S^2 + D_j^2)$ term of Eq. (5). The latter terms represent $j\Omega$ transmission zeros in the S plane, and it is these zeros which the stubs of Fig. 5-2 will be called upon to supply.

In order that y_{21} possess a zero at $S = jQ$, let $Y_2(jQ) = \infty$. This pole will be directly attributed to stub B. Since

$$Y_2(jQ) = \infty \tag{9}$$

and by Richard's Theorem,

$$Y_2(S) = Y_1(1) \frac{Y_1(S) - S\,Y_1(1)}{Y_1(1) - S\,Y_1(S)} , \tag{10}$$

$Y_2(S)$ must have a pole at jQ implying

$$Y_1(1) = S\,Y_1(S)\Big|_{S = jQ} . \tag{11}$$

Thus

$$Y_1(1) = jQ\,Y_1(jQ) . \tag{12}$$

Since

$$Y(S) = Y_1(S) + S\sqrt{\tau}/R_1 , \tag{13}$$

$S\sqrt{\tau}/R_1$ must be chosen so that both (12) and (13) are satisfied. With $S = 1$, (13) implies that

$$Y(1) = Y_1(1) + \sqrt{\tau}/R_1 . \tag{14}$$

Also, with $S = jQ$, (13) becomes

$$Y(jQ) = Y_1(jQ) + jQ\sqrt{\tau}/R_1 . \tag{15}$$

Solving (14) and (15) for $jQY_1(jQ)$, and substituting in (12),

$$\sqrt{\tau}/R_1 = (Y(1) - jQY(jQ))/(1 + Q^2) \tag{16}$$

or

$$R_1 = \sqrt{\tau}\,(1 + Q^2)/(Y(1) - jQY(jQ)) \tag{17}$$

The specific procedure to synthesize $y_{11}(S) = Y(S)$ and $y_{12}(S)$ simultaneously, follows. $y_{11}(S) = Y(S)$ is such that either

$$Y(\infty) = 0 \quad \text{or} \quad Y(\infty) = \infty \quad . \tag{18}$$

If the former is true, a cascade section may always be extracted, using Richard's Theorem, so that

$$Y(\infty) = \infty \quad . \tag{19}$$

When (19) is satisfied, an $\overline{\text{URCO}}$ element always may be removed whose minimum total resistance is given by

$$R_o = \sqrt{\tau}\, S/Y(S)\Big|_{S \to \infty} \tag{20a}$$

and whose total capacitance is given by

$$C_o = Y(S)\, \sqrt{\tau}/S\Big|_{S \to \infty} \tag{20b}$$

At a finite transmission zero jQ_i in the S plane, $Y(jQ_i)$ is purely imaginary. For each zero of transmission, compute

$$R_{o_i} = \sqrt{\tau}\, (1 + Q^2)/(Y(1) - jQY(jQ)) \quad . \tag{21}$$

Of the set $\langle R_{o_i}, R_o \rangle$, some elements may be negative, some will be positive. Remove the largest positive member, R_1, as a shunt $\overline{\text{URCO}}$ stub, of admittance $S\sqrt{\tau}/R_1$. The remaining admittance is seen to be

$$Y_1(S) = Y(S) - S\sqrt{\tau}/R_1 \quad . \tag{22}$$

Since, $\sqrt{\tau}/R_1 < \sqrt{\tau}/R_0$,

$$Y_1(\infty) = \infty \tag{23}$$

Remove a cascade element, $Y_1(1)$, from $Y_1(S)$, and by Richard's Theorem the remaining admittance is given by

$$Y_2(S) = Y_1(1) \frac{Y_1(S) - SY_1(1)}{Y_1(1) - SY_1(S)} \tag{24}$$

Now it is seen that $Y_2(S)$ has a pole wherever $Y_1(1) = SY_1(S)$. But by (12), at a transmission zero, $Y_1(1) = jQY_1(jQ)$. Hence $Y_2(S)$ must have a pole at the required transmission zero. This pole may be removed by a stub whose admittance is given by

$$Y_s(S) = \frac{S\left[Y_2(S) \frac{S^2 + Q^2}{S} \right]_{S \to jQ}}{S^2 + Q^2} \tag{25}$$

which may itself be realized by two successive applications of Richard's Theorem, as a cascade of two $\overline{\text{URCO}}$ two ports. The remaining admittance $Y_3(S)$ is

$$Y_3(S) = Y_2(S) - Y_s(S) \tag{26}$$

Thus $Y_3(\infty) = 0$. A cascade element may again be removed and $Y_4(\infty) = \infty$. The cycle is complete.

5.4 Simultaneous Realizability of y_{11} and ky_{12} by the Cascade and Stub Method

The transmission matrix of the desired network in the S plane may be specified as

$$K = \frac{1}{(\sqrt{1 - S^2})^q f(S)} \begin{bmatrix} v_1(S) & u_1(S) \\ u_2(S) & v_2(S) \end{bmatrix} \tag{27}$$

where the passivity of the network requires that

$$v_1(S)\, v_2(S) - u_1(S)\, u_2(S) = (1 - S^2)^q\, (f(S))^2 \tag{28}$$

In terms of this matrix,

$$y_{11} = D/B,\ y_{21} = y_{12} = -1/B \text{ and } y_{22} = A/B \tag{29}$$

may be translated into

$$y_{11}(S) = \frac{v_2(S)}{u_1(S)} \tag{30}$$

$$y_{12}(S) = y_{21}(S) = -\frac{(\sqrt{1 - S^2})^q f(S)}{u_1(S)} \tag{31}$$

$$y_{22}(S) = \frac{v_1(S)}{u_1(S)} \tag{32}$$

The zeros of f(S) will yield the finite transmission zeros.

The following theorem concerns the realizability of transmission zeros, in the S plane, and is due to Kasahara and Fujisawa, as reported by Ikeno.[27] Ikeno's work has been concerned with the design of lossless filters made of coaxial cables.

Theorem VII. The zeros of f(S) (which are the transmission zeros) will be realizable together with a driving point impedance with no negative elements if

a) $S = \infty$ is a transmission zero of y_{21}/S^2 .

b) All finite $j\Omega$ transmission zeros are greater than the greatest root of $v_1(S)$ or $u_1(S)$, where $S = \Sigma + j\Omega$.

c) At least one finite $j\Omega$ transmission zero is greater than the greatest root of $v_2(S)$ or $u_2(S)$.

If only one driving point admittance is specified, the conditions of Theorem VII are relaxed to those of Corollary III.

Corollary III. The zeros of transmission of y_{21} are realizable simultaneously with a given driving point admittance y_{11} using no negative elements if

a) $S = \infty$ is a transmission zero of $\frac{y_{21}(S)}{S^2}$.

b) All finite $j\Omega$ ($S = j\Omega + \Sigma$) transmission zeros of y_{12} are greater than or equal to the largest $j\Omega$ pole of $y_{12}(S)$.

c) At least one finite $j\Omega$ transmission zero is greater than or equal to the greatest finite zero of $y_{11}(S)$.

The following theorem, derived from one by Ikeno, as translated by Matsumato[27] relaxes the conditions for transmission zero realizability, and considers the inclusion of some negative elements.

Theorem VIII. A 'Brune' $\overline{RC}$ cycle, with a negative $\overline{URCS}$ one-port, as shown in Fig. 5-3(a), may be transformed into an equivalent unit loop, shown in Fig. 5-3(b), where $b = c + d$, $a \leq b$ and

$$e = \frac{abc(1 + \sigma^2)}{p}$$

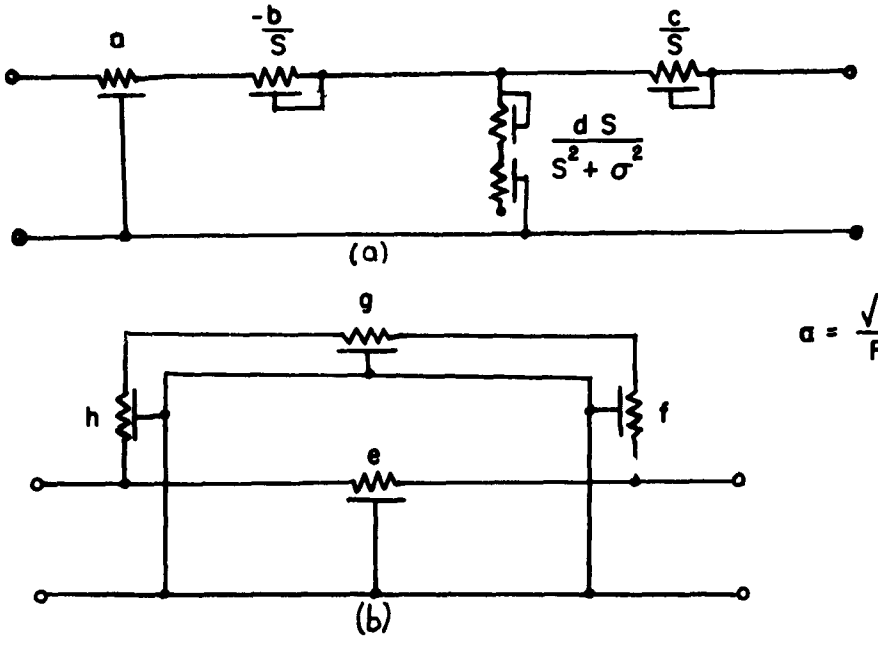

FIG. 5-3

A BRUNE $\overline{RC}$ CYCLE EQUIVALENCE

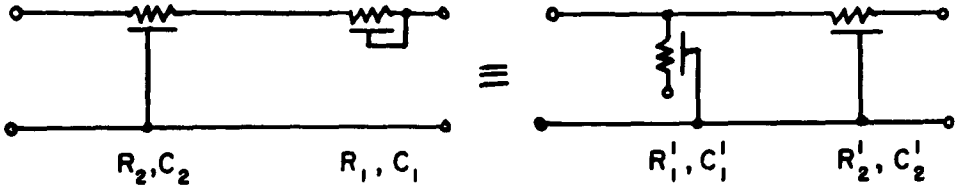

FIG. 5-4

EQUIVALENT $\overline{RC}$ NETWORKS

$$f = \frac{cd(b - a)}{p}$$

$$g = \frac{bd(b + a\sigma^2)}{\sigma^2 p}$$

$$h = \frac{ad(b + a\sigma^2)}{p}$$

and $$p = b^2 + \sigma^2(ad + bc)$$

The network of Fig. 5-3 may also be redrawn, due to a theorem which may be derived from Kuroda's Identity,[26] and was derived independently by the author.

Theorem IX. The two networks of Fig. 5-4 are equivalent, if

$$R_1' = R_2 + \frac{R_2^2}{R_1}$$

$$R_2' = R_1 + R_2$$

$$C_1' = \frac{\tau}{R_1'}$$

$$C_2' = \frac{\tau}{R_2'}$$

and both networks may be turned end for end.

The significance of Theorem IX is that it permits a (possibly negative) series $\overline{RC}$ segment to be replaced by a similar shunt segment, which may be realized by a stub, and widens the applicability of the Brune $\overline{RC}$ Cycle of Fig. 5-3.

If the network of Fig. 5-3 is followed by an $\overline{\text{URC}}0$ two-port, the $\overline{\text{URC}}$S series element of admittance C/S may be replaced by an $\overline{\text{URC}}0$ shunt one-port following the added $\overline{\text{URC}}0$ two-port. This is illustrated in Fig. 5-5. Furthermore, the two networks of Fig. 5-6 are equivalent.

Now return to the realizability conditions for the transmission zeros. If 'unit loops' are permitted, the conditions of Theorem VII may be relaxed to those of Theorem X.[27] Essentially the unit loops with positive elements permit the limited replacement of stubs with negative parameters.

Theorem X.* Let the finite $j\Omega$ transmission zeros of $y_{12}(S)$ be $0 \leq \sigma_1 \leq \sigma_2 \ldots < \sigma_k \ldots \leq \sigma_n \leq \infty$. These zeros are realizable if there exist $n + k - 1$ or more real frequency poles of $y_{12}(S)$ that are not greater than σ_k.

Note that under Theorem X, S = 0 may not be a transmission zero (and thus s = 0 may not be either), since there must be (at least) one pole less than zero on the positive $j\Omega$ axis, which is impossible.

The poles of $y_{12}(S)$ and $y_{11}(S)$ are chosen by the network designer if only the overall gain function is specified, since the gain function involves the ratios of the zeros of $y_{ii}(S)$ to those of $y_{ij}(S)$, and the immittance poles are not specified. This allows more freedom in meeting the previous realizability conditions.

*The statement of this theorem, originally proven in Japanese by Fujisawa, was translated in reference 27 by Akio Matsumato.

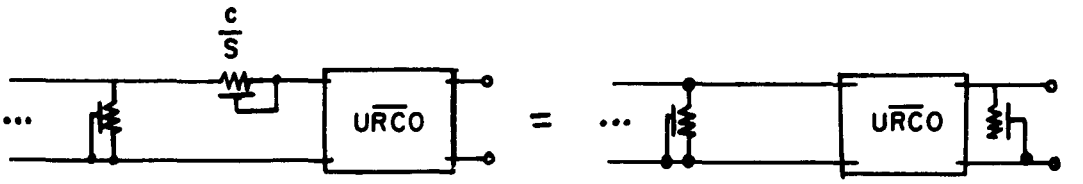

FIG. 5-5

APPLICATION OF THEOREM IX

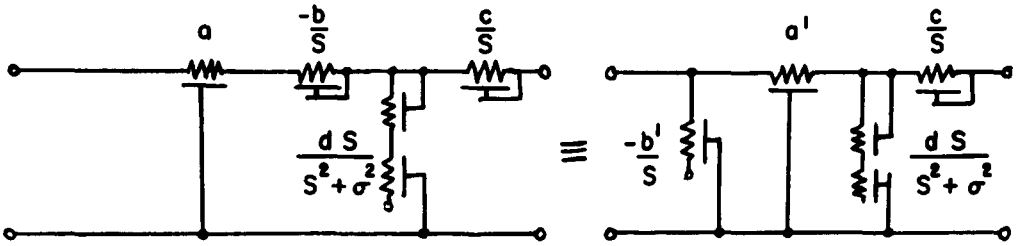

FIG. 5-6

EQUIVALENT $\overline{RC}$ NETWORKS

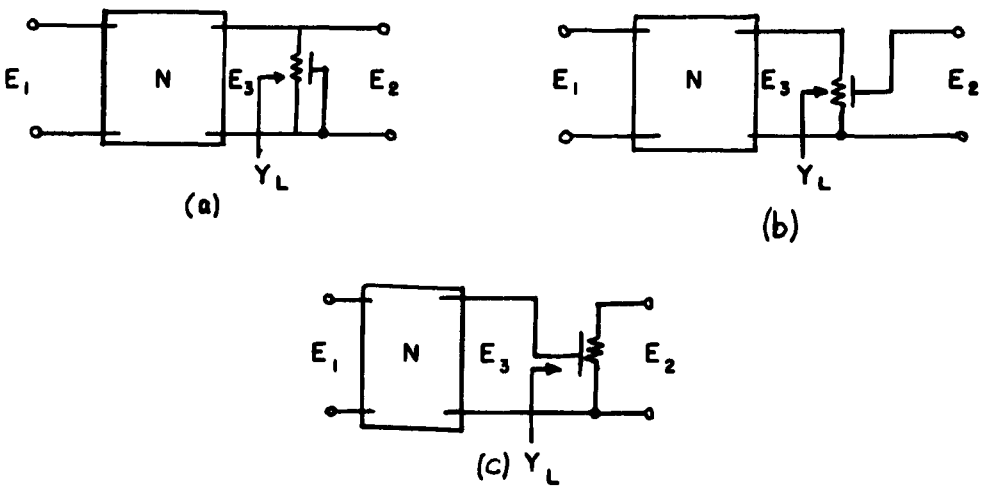

FIG. 5-7

THREE $\overline{RC}$ CONFIGURATIONS

The conditions of Corollary III may be considered in the s plane:

Theorem XI.* Using a cascade and stub $\overline{RC}$ network $y_{12}(s)$ may be realized simultaneously within a constant with $y_{11}(s)$ if

a) $y_{11}(s)$ fulfills the conditions of Theorem VI and possesses the same A_i polynomials as $y_{12}(s)$.

b) $-y_{12}(s)$ may be expressed as

$$-y_{12}(s) = \frac{\sqrt{s}\, e^{qa\sqrt{s}/2}}{e^{a\sqrt{s}} - 1} \cdot \frac{\prod_{1}^{w} e^{2a\sqrt{s}} + B_i e^{a\sqrt{s}} + 1}{(e^{a\sqrt{s}} + 1)^{2(w-m)+q-1} \prod_{1}^{m} (e^{2a\sqrt{s}} + A_i e^{a\sqrt{s}} + 1)}$$

where

1) $|B_i|, |A_i| < 2$, $A_{i+1} > A_i$, $B_{i+1} > B_i$.

2) $B_i > A_m$, $i = 1, 2, 3, \ldots w$.

3) $B_w > C_w$ where C_w is largest C_j of y_{11} numerator polynomials.

4) $m \geq w + q/2 - 1$.

5) $q/2 \geq w$

Theorem X may be written in terms of the variable s, as Theorem XII. This represents a relaxation of the conditions of Theorem XI.

Theorem XII.* Using a cascade and stub $\overline{RC}$ network, including unit loops if necessary, $y_{12}(s)$ may be realized simultaneously with $y_{11}(s)$ if

a) $y_{11}(s)$ fulfills the conditions of Theorem VI, and

b) $y_{12}(s)$ may be written as in Theorem XI, where the following conditions replace those of Theorem XI:

*The proof of this Theorem is in Appendix I.

$|B_1| < 2$, $|A_1| < 2$, $A_{i+1} > A_i$, $B_{i+1} > B_i$, and there exist (w+k-1) 'A_i' terms such that $A_i < B_k$, i = 1, 2, ... w+k-1. Also, $m \geq 2w-1$.

5.5 Synthesis of $\overline{RC}$ Gain Functions

The synthesis of $\overline{RC}$ voltage and current gain functions follows directly from the simultaneous synthesis of the driving point and transfer immittances. Three particular cases will be considered here. Referring to Fig. 5-7, N represents the $\overline{RC}$ network which is to be synthesized. It will be assumed that the overall voltage gain function, including the presence of a specified load, is to be achieved, i.e.

$$A_V = E_2/E_1 \Big|_{I_2 = 0} \tag{33}$$

Each of the three network configurations and terminations chosen represent a typical application in microelectronic distributed network design.[2,12] Following a discussion of each case, the synthesis procedure will be outlined by examples.

Fig. 5-7(a) requires that a voltage gain specification E_2/E_1 be met, when the resistive load has some known, distributed shunt capacitance across it. As discussed in Section 5.0, this includes the practical case of a lumped resistive load, with some shunt capacitance across it. The voltage gain is given simply by

$$A_V = y_{21}/(y_{22} + Y_L) \tag{34}$$

Since Y_L and A_V are specified, the problem reduces to one of realizing y_{21} and y_{22} for the network N. It will be seen later that there is considerable freedom in the choice of y_{21} and y_{22}, and this freedom may be exploited profitably.

The use of a practical coupling network at the output, as in Fig. 5-7(b) presents more of a challenge to the network designer. Since the overall configuration involves two cascaded two-ports, (34) may not be applied directly. In fact,

$$E_3/E_1 = y_{21}/(y_{22} + Y_L) \tag{35}$$

instead of E_2/E_1. The Z matrix of the coupling network in Fig. 5-7(c) (or Fig. 5-7(b) , with z_{11} and z_{22} interchanged) is given by[2]

$$Z = \begin{bmatrix} \dfrac{R}{\sqrt{sRC}\,\tanh\sqrt{sRC}} & \dfrac{R}{\sqrt{sRC}}\tanh\dfrac{\sqrt{sRC}}{2} \\ \dfrac{R}{\sqrt{sRC}}\tanh\dfrac{\sqrt{sRC}}{2} & \dfrac{2R}{\sqrt{sRC}}\tanh\dfrac{\sqrt{sRC}}{2} \end{bmatrix} \tag{36}$$

Thus for the coupling networks of (b) and (c), the open circuit voltage gains are given by

$$A_{V2b} = \frac{z_{21}}{z_{22}} = \frac{\dfrac{R}{\sqrt{sRC}}\tanh\dfrac{\sqrt{sRC}}{2}}{\dfrac{2R}{\sqrt{sRC}}\tanh\dfrac{\sqrt{sRC}}{2}} = \frac{1}{2} \tag{37}$$

$$A_{V2c} \quad \frac{z_{21}}{z_{11}} = \frac{\dfrac{R}{\sqrt{sRC}}\tanh\dfrac{\sqrt{sRC}}{2}}{\dfrac{R}{\sqrt{sRC}}\dfrac{1}{\tanh\sqrt{sRC}}} = \tanh\sqrt{sRC}\tanh\frac{\sqrt{sRC}}{2} \tag{38}$$

By rewriting the voltage transfer function for Fig. 5-7(b) as

$$A_V = \left.\frac{E_2}{E_3}\right|_{I_2 = 0} \times \left.\frac{E_3}{E_1}\right|_{Y_L \text{ in place}} \tag{39}$$

the problem of working with cascade parameters of N and the coupling network is avoided. Noting that E_2/E_3 has the db. gain characteristic given in Fig. 5-8, the necessary graphical characteristic for N, E_3/E_1, may be drawn. The problem is then reduced to that of part (a) above. In particular, if A_V is given by a magnitude plot, in db., the difference function E_3/E_1 <u>with</u> Y_L in place may be graphically computed in a straightforward fashion , since

$$\left.\frac{E_3}{E_1}\right|_{Y_L \text{ in place}} = A_V|_{db} - \left.\frac{E_2}{E_3}\right|_{I_2 = 0_{db}} \tag{40}$$

Realization of a network N which possesses such a characteristic when loaded by Y_L completes the problem.

A very similar solution is possible in the case of the configuration of Fig. 5-7(c). The only difference is that the coupling network function,

$$A_{V2} = \left.\frac{E_2}{E_3}\right|_{I_2 = 0} \tag{41}$$

is given in Fig. 5-8, and is of the high pass type. Given $A_V = E_2/E_1$, and knowing A_{V2}, it is rather simple to find E_3/E_1 with Y_L fixed in place, and thus the problem is again reduced to that of synthesizing a stipulated y_{11} and y_{21} pair.

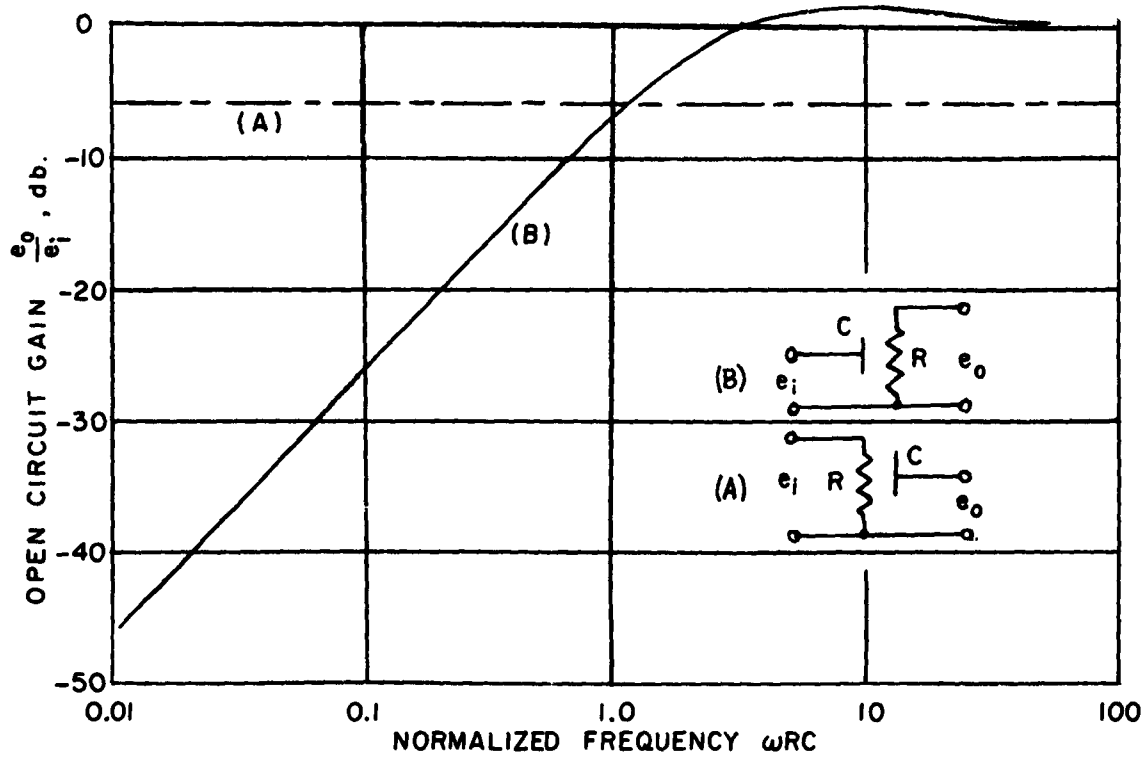

FIG. 5-8

$\overline{RC}$ NETWORK GAIN CHARACTERISTICS

5.6 Gain Function Synthesis Example

Suppose that it is desired to build a network, working into a load as shown in Fig. (5-10), having the gain characteristic of Fig. (5-11). At first it will be assumed that the RC product of the $\overline{URC}$ segments comprising network N will be the same as the R_LC_L product. The characteristic of the load network, E_2/E_3, is known and presented in Fig. 5-8(a). To find the voltage gain characteristic E_3/E_1 for the network N, loaded by the output network, the characteristic of Fig. 5-8(a) may be subtracted from that of Fig. 5-11. The resulting gain function for N is plotted in Fig. 5-12(a). The specifications of Fig. 5-11 are satisfied to the left of the bandpass region by the high pass network characteristics. Network N will now be designed to meet the graphical specification of Fig. 5-12(a), within an arbitrary constant.

The RC product is chosen by noting in Fig. 5-11 that the desired lower 3_{db} frequency ω_L must meet the condition

$$\omega_L = .25 \tag{42}$$

Applying the techniques of Chapter Three, the characteristic for the network N may be approximated closely by

$$A_V = \frac{e^{a\sqrt{s}}\,(e^{2a\sqrt{s}} + 1.9\,e^{a\sqrt{s}} + 1)}{(e^{2a\sqrt{s}} - 1.2\,e^{a\sqrt{s}} + 1)\,(e^{2a\sqrt{s}} + 1.2\,e^{a\sqrt{s}} + 1)} \tag{43}$$

Letting

$$S = \frac{e^{a\sqrt{s}} - 1}{e^{a\sqrt{s}} + 1}\,,\quad e^{a\sqrt{s}} = \frac{1 + S}{1 - S}\,,\quad e^{2a\sqrt{s}} = \frac{1 + 2S + S^2}{(1 - S)^2}$$

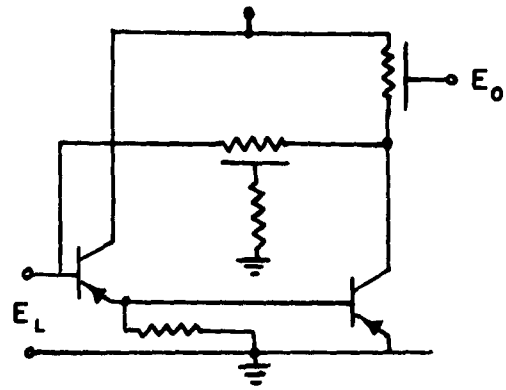

(a)

MICROSYSTEMS BAND PASS AMPLIFIER

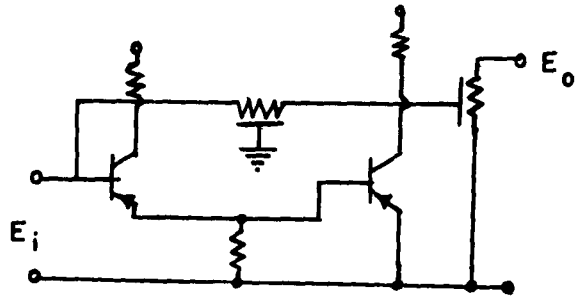

(b)

MICROSYSTEMS HIGH PASS AMPLIFIER

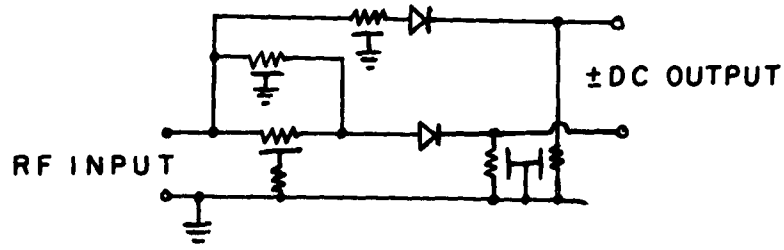

(c)

RC FREQUENCY DISCRIMINATOR

FIG. 5-9

TYPICAL $\overline{RC}$ MICROELECTRONIC CIRCUITRY

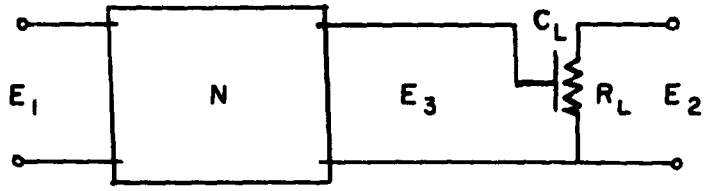

FIG. 5-10

REQUIRED CONFIGURATION

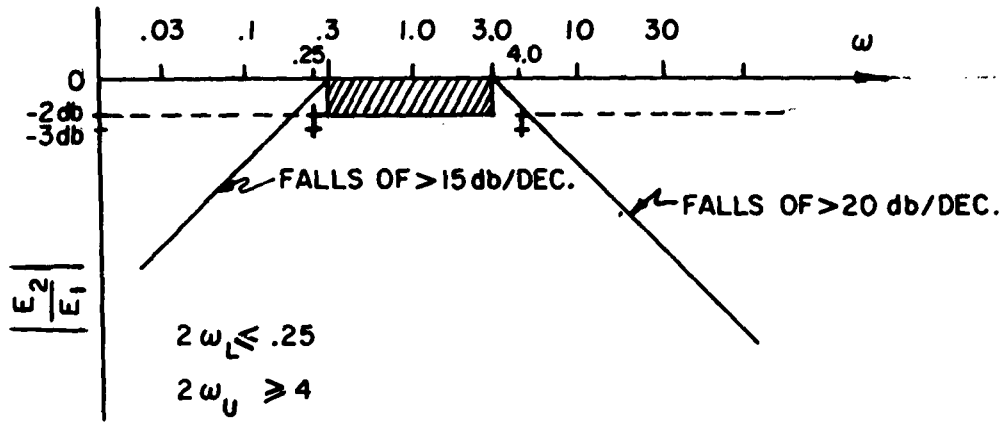

FIG. 5-11

REQUIRED GAIN CHARACTERISTIC

$$A_v(S) = \frac{(1 - S^2)\ (S^2 + 39)}{(S^2 + .25)\ (S^2 + 4)} \tag{44}$$

within an arbitrary constant.

Since

$$A_v = \frac{-\ y_{12}}{y_{22} + S\ k} \tag{45}$$

$y_{12}(S)$ and $y_{22}(S)$ must be chosen so that the realizability conditions of Corollary III or Theorem X are met.

If the admittances are chosen so as to meet the requirements of Corollary III, and to provide for driving point pole-zero alternation,

$$-y_{12}(S) = \frac{(1 - S^2)\ (S^2 + 39)}{S\ (S^2 + 1)} \tag{46}$$

and

$$y_{22} + k\ S = \frac{(S^2 + 4)\ (S^2 + .25)}{S\ (S^2 + 1)} \tag{47}$$

$$k = .1$$

then the driving point admittance of N is

$$y_{22}(S) = \frac{.9\ (S^2 + .255)\ (S^2 + 4.355)}{S\ (S^2 + 1)} \tag{48}$$

The conditions of Corollary III are met. The zeros of y_{21} contributed by $(S^2 + 39)$ and the $(1 - S^2)$ term may be achieved in one extraction cycle. The minimum resistance of a single segment shunt stub which may be extracted at first is given by (20(a)) to be

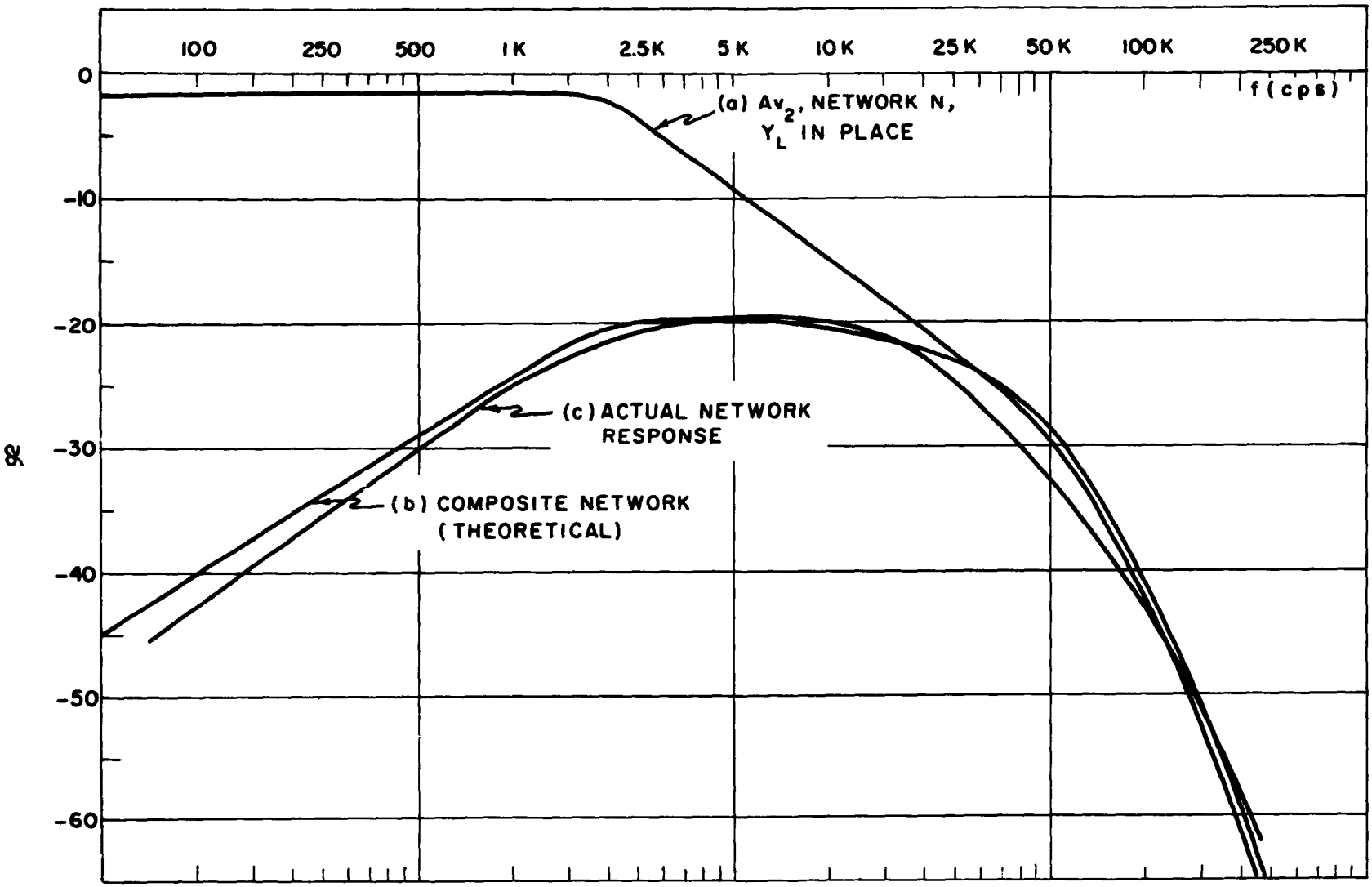
100
250
500
1K
2.5K
5K
10K
25K
50K
100K
250K
f (cps)
0
-10
-20
-30
-40
-50
-60
db
(a) Av_2, NETWORK N, Y_L IN PLACE
(c) ACTUAL NETWORK RESPONSE
(b) COMPOSITE NETWORK (THEORETICAL)

FIG. 5 - 12

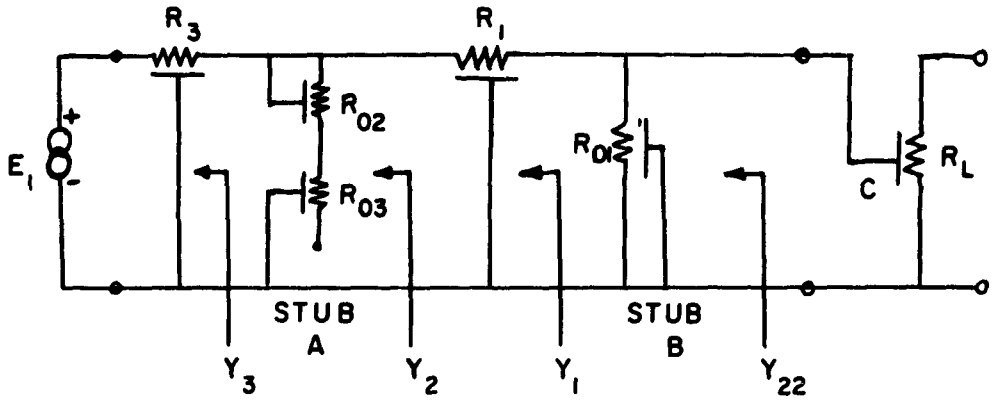

FIG. 5-13

FINAL $\overline{RC}$ NETWORK

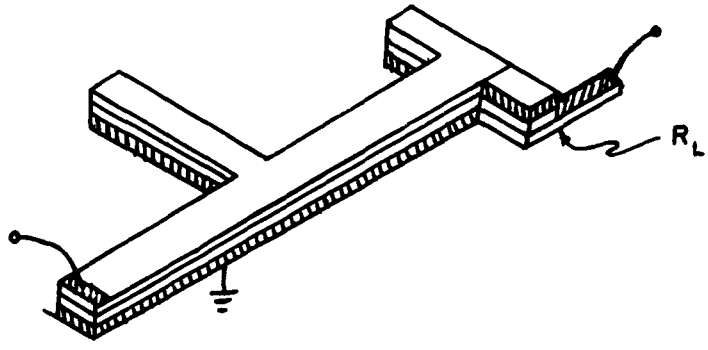

FIG. 5-14

PHYSICAL EMBODIMENT

$$\frac{\sqrt{\tau}}{R_o} = \frac{1}{S} Y(S) \Big|_{S \to \infty} \equiv 1 \tag{49}$$

Applying (21) at the transmission zero, $S = j\sqrt{39}$,

$$\frac{\sqrt{\tau}}{R_{o_1}} = \frac{Y(1) - \gamma_Q Y(j_Q)}{1 + Q^2} = \frac{3.36 + 35.32}{40} = .967 \tag{50}$$

may be extracted. Doing so,

$$Y_1(S) = Y_{22}(S) - .967\ S$$

$$= \frac{S^4 + 4.52\ S^2 + 1.028 - .967\ (S^2 + 1)}{S\ (S^2 + 1)}$$

$$= \frac{.033\ (S^4 + 107.7\ S^2 + 31.15)}{S\ (S^2 + 1)} \tag{51}$$

and $$Y_1(1) = 2.3075 = \frac{\sqrt{\tau}}{R_1} \tag{52}$$

Then, using Richard's Theorem, a cascade section is extracted:

$$Y_2(S) = Y_1(1)\ \frac{Y_1(S) - S\ Y_1(1)}{Y_1(1) - S\ Y_1(S)}$$

$$= \frac{2.3075\ [-2.2745\ S^4 + 1.246\ S^2 + 1.028]}{+ S\ [-.0331\ S^4 - 1.2455\ S^2 + 1.2795]}$$

$$= \frac{159.2\ (1 - S^2)\ (S^2 + .4519)}{(1 - S^2)\ (S)\ (S^2 + 39)}$$

$$= \frac{159.2\ (S^2 + .452)}{S\ (S^2 + 39)} \tag{53}$$

In accordance with (25), a two-segment stub is used to remove the transmission zeros due to the $(S^2 + 39)$ factor, and the resulting remaining admittance is

$$Y_3(S) = Y_2(S) - \frac{\alpha S}{S^2 + 39} \tag{54}$$

where

$$\alpha = \frac{159.2}{S^2}(S^2 + .452)\Big|_{S^2 \to -39} = 157.36$$

Finally,

$$Y_3(S) = \frac{159.2\,(S^2 + .452)}{S\,(S^2 + 39)} - \frac{157.36\,S^2}{S\,(S^2 + 39)}$$

$$= \frac{1.84\,(S^2 + 39)}{S\,(S^2 + 39)} = \frac{1.84}{S}$$

$$\therefore \frac{\sqrt{\tau}}{R_3} = 1.84$$

$$R_3 = \frac{\sqrt{\tau}}{1.84} \tag{55}$$

and the design is completed. The final network is shown in Fig. 5-13. Theoretical results were verified by experimental data, and the results which show good correlation; are given in Fig. 5-12(b).

5.7 Limitations of Transfer Synthesis Technique

One important limitation in the final design of the previous example is clear: a 20 db. in-band loss occurs. This loss need not be encountered if the restriction that the RC product of network N be the same as the $R_L C_L$ product is dropped.

If RC is different from R_LC_L, one of two cases obtains. First, the R_LC_L product may be an integral multiple of RC, by the proper choice of RC, in which case the load admittance Y_L will be more complicated than previously, but will be a rational function of S. Second, the loading effect of the R_LC_L combination may be so small compared to y_{22} of network N that it may be neglected.

The latter case will be considered here, to illustrate the possibility of reducing the in-band loss. Consider the result if the R_LC_L product is increased by a factor of 100, relative to the RC product of network N. In Fig. 5-15, it is seen that the output network gain characteristic moves to the left by two decades. The load possesses a driving point admittance which is rational in S, but which is the ratio of two higher ordered polynomials, due to the fact that the transformation constant is still 'RC' = $(a/2)^2$. Very little inband loss need be tolerated in this case, as seen in the composite characteristic of Fig. 5-15. Below the normalized radian frequency $wa^2/a = 1$, the load impedance level may be kept at least ten times that of $1/y_{22}$, permitting the designer to neglect the load driving point impedance in the gain expression for N.

Another procedure which requires further study is to decompose the network function for N into two or more functions, each of which is realized with their own RC products. This additional freedom might be useful in maximizing the gain constant.

In March 1960, Kuh and Paige[34] investigated and found the maximum gain constant for an RC ladder network explicitly in terms of the poles and zeros of the given transfer function. Rather straightforward

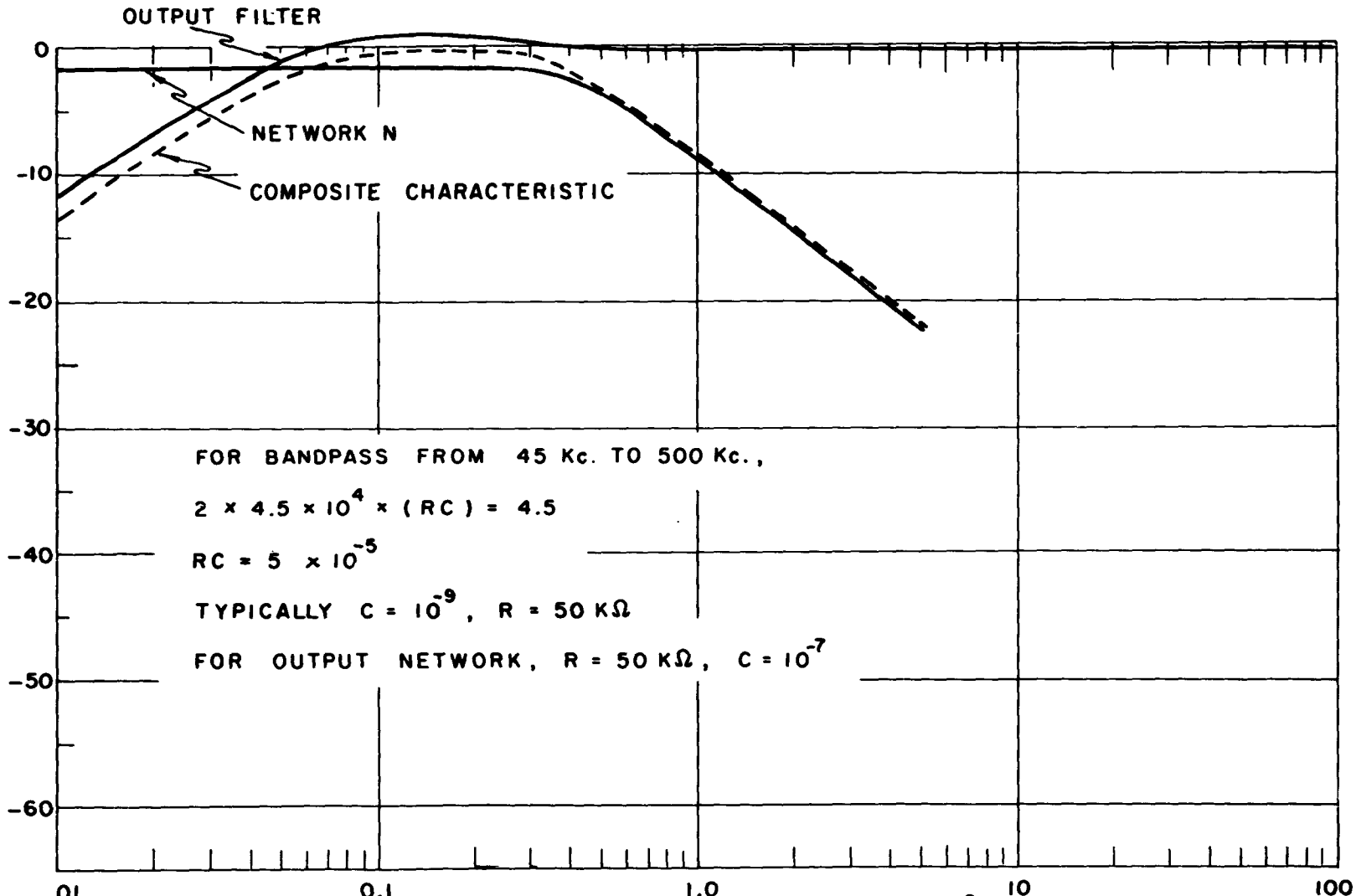
OUTPUT FILTER
NETWORK N
COMPOSITE CHARACTERISTIC
0
-10
-20
-30
-40
-50
-60
FOR BANDPASS FROM 45 Kc. TO 500 Kc.,
2 x 4.5 x 10^4 x (RC) = 4.5
RC = 5 x 10^-5
TYPICALLY C = 10^-9, R = 50 KΩ
FOR OUTPUT NETWORK, R = 50 KΩ, C = 10^-7
.01
0.1
1.0
10
100
ωa²/2 = 2ω(RC)n

FIG. 5-15

techniques were outlined to realize the maximum gain constant, by zero shifting and removal. Extension of these techniques directly from the lumped finite case to the distributed network formulation does not appear immediately feasible, and provides a topic for further study.

5.8 Concluding Remarks

A rather detailed synthesis technique has been described in this chapter which permits the realization of finite transmission zeros on the negative real axis in the s plane. Distributed RC elements are arranged in a practical cascade and stub configuration. An extraction cycle has been developed, explicitly outlining the method by which the negative real clusters of transmission zeros may be realized. As a vehicle for realizing these transmission zeros, exponential polynomials have been related to transmission zeros, finite in number, in the S plane, where the extraction cycle is explicitly undertaken. The realizability of such zeros by the cascade and stub method has been considered in Section 5.5, and 'unit loops' have been introduced to widen the class of transmission functions which may be so obtained. Finally, the synthesis of gain functions between a voltage or current source and a specified load has been discussed, several methods have been suggested, and a detailed example has been included.

CHAPTER SIX

THE DESIGN OF EXPERIMENTAL $\overline{RC}$ NETWORKS

6.0 Introduction

In this chapter, a review of the restrictions imposed by the previous design techniques on the final physical $\overline{RC}$ network embodiment will be made. These restrictions will be illustrated by the detailed design of a low pass filter. General expressions for the open circuit voltage gain and the transfer admittance of sharp-cutoff q section filters will be obtained, and the frequency characteristics of such networks will be compared with other well known filter characteristics.

6.1 Teledeltos Models Used for Experimental Verification

The experimental $\overline{RC}$ networks which were built to verify the theoretical results of this paper were modelled with Teledeltos Paper,* Mylar and Aluminum Foil or Copper as shown in Fig. 6-1. When the Mylar was used, and the layers were tightly compressed, a capacitance of about 200 pf. per square inch was attained. If the Mylar is omitted, and the paper backing of the resistance paper is used as the dielectric alone, about 310 pf. per square inch may be obtained. Experimental results indicate that $\overline{URC}$ segments do not behave as predicted by their mathematical models in Chapter Two, unless a conducting boundary is placed across the

*The Teledeltos Paper, nominally having a resistance of 2000 ohms per square, was supplied through the courtesy of Mr. Joseph Gagliardi, Western Union Co., Broadway at Worth Street, New York City. It is available in large rolls.

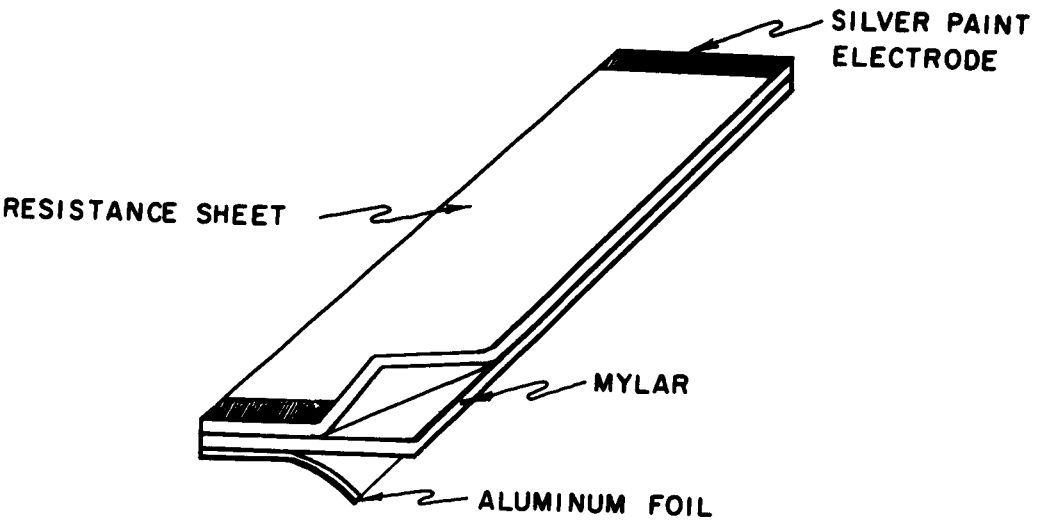

FIG. 6-1
TELEDELTOS $\overline{RC}$ MODEL

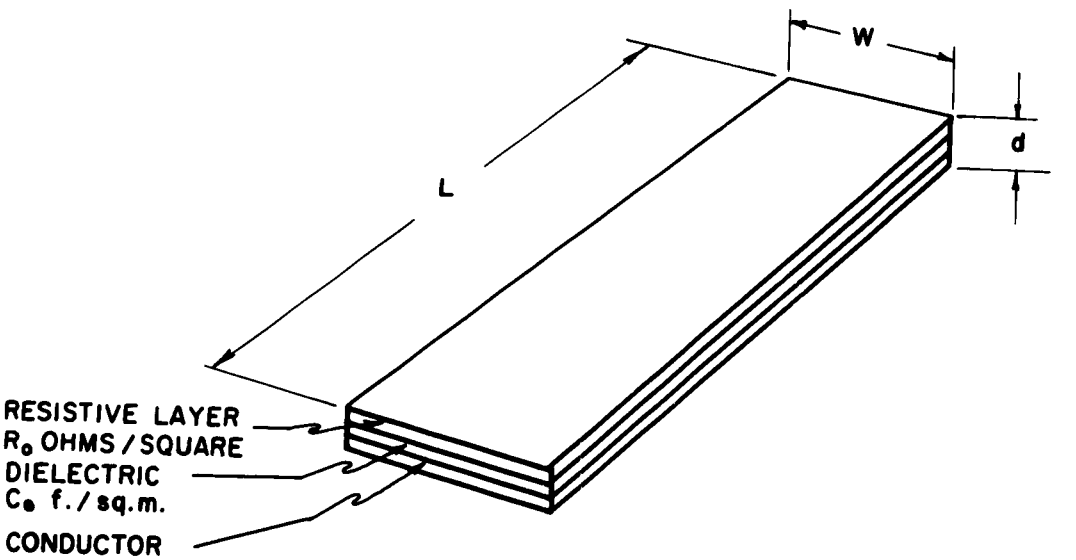

FIG. 6-2
$\overline{URC}$ LINE SEGMENT

end edges of each segment (as in Appendix II), or the segment length is considerably greater than their width. In the frequency ranges used for experimental data, from audio to a hundred kilocycles, a length to width ratio of at least five was maintained.

Difficulties in achieving practical $\overline{RC}$ structures often arise from several considerations. A network of several segments is to be deposited by three individual depositions. The resistive layer, for example, is to be deposited for all of the segments at once. Thus the resistive layer for all the segments will be of uniform thickness, and nominally be characterized by a uniform number of ohms per square. Each segment, however, must have a different total resistance. Further, since the RC products for each segment are equal, it follows that the lengths of each segment must be the same:

$$R = R_o L/W \tag{1}$$

$$C = C_o LW \tag{2}$$

$$RC = R_o C_o L^2 \tag{3}$$

The total resistance of each segment may only be controlled independently by changing the width of each segment. If the length of each segment is governed by the overall network size, and the maximum W_i of the i^{th} segment is chosen to be much less than L, then the W_i corresponding to the smallest R_i is the maximum W_i required. The value of R_o for all segments is determined from

$$R_o = W_{max}\, R_{min}/L \tag{4}$$

Having made this calculation, the minimum segment width may be calculated from

$$W_{min} = R_o L / R_{max} \tag{5}$$

For thin film networks built in keeping with the current state of the art, R_o should be kept below 5000 ohms per square, and W_{min} should be greater than 5 mils. If these requirements are not met concurrently, the length L of each segment will have to be increased. Resistive materials of nichrome and various oxides fall into the above ranges. Dielectrics such as aluminum dioxide or silicon monoxide may be used to obtain the proper capacitance. The total capacitance of each segment is obtained from

$$C_i = \frac{(RC)}{R_i} \tag{6}$$

6.2 The Design of Low Pass Filters: Preliminary Considerations

In Chapter Three, the exponential polynomial factors necessary to construct an $\overline{RC}$ network function were considered, and their magnitudes (in db.) were plotted as a function of $\log_{10} \omega$. Prior to designing low pass filters it is profitable to investigate these polynomial factors further to determine where the maximum rate of change of slope for each of the terms occurs. This information is necessary in designing low pass filters to have the sharpest cutoff characteristics possible for a given number of cascaded segments.

The polynomial terms and the derivatives of their magnitudes are given in Eqs. (7) through (11), and are graphically represented for rapid

interpretation in Fig. 6-3 and 6-4. Factors with large derivatives at low frequencies will be useful in sharp-cutoff low pass filter design. These functions, which are extracted from Eq. (6) of Chapter 5, and the derivatives of their magnitudes are:

$$f_1(s) = \sqrt{s}\, a$$
$$|f_1(j\omega)| = |\sqrt{\omega}|\, a \tag{7}$$
$$\frac{d\,|f_1(j\omega)|}{d\,\log_{10} \omega a^2} = 10 \text{ db/decade}$$

$$f_2(s) = e^{\frac{qa\sqrt{s}}{2}}$$

$$|f_2(j\omega)| = \left| e^{\frac{qa\sqrt{j\omega}}{2}} \right| \tag{8}$$

$$\frac{d\,|f(j\omega)|_{db}}{d\,\log_{10} \omega a^2} = \frac{5\, qa\sqrt{\omega}}{\sqrt{2}} \quad \frac{db}{decade}$$

$$f_3(s) = e^{a\sqrt{s}} + 1$$

$$|f_3(j\omega)| = |e^{a\sqrt{j\omega}} + 1| \tag{9}$$

$$\frac{d\,|f_3(j\omega)|_{db}}{d\,\log_{10} \omega a^2} = \frac{10\sqrt{\omega}\, e^{a\sqrt{\omega/2}}\,(e^{a\sqrt{\omega/2}} - \sin a\sqrt{\omega/2} + \cos a\sqrt{\omega/2})}{\sqrt{2}\,|e^{a\sqrt{j\omega}} + 1|^2}$$

$$f_4(s) = e^{a\sqrt{s}} - 1$$

$$|f_4(j\omega)| = |e^{a\sqrt{j\omega}} - 1| \tag{10}$$

$$\frac{d\ |f_4(j\omega)|_{db}}{d\ \log_{10} \omega a^2} = \frac{10\sqrt{\omega}\, e^{a\sqrt{\omega/2}}\,(e^{a\sqrt{\omega/2}} + \sin a\sqrt{\omega/2} - \cos a\sqrt{\omega/2})}{\sqrt{2}\ |e^{a\sqrt{j\omega}} - 1|^2}$$

$$f_5(s) = e^{2a\sqrt{s}} + B_1 e^{a\sqrt{s}} + 1$$

$$|f_5(j\omega)| = |e^{2a\sqrt{j\omega}} + B_1 e^{a\sqrt{j\omega}} + 1| \equiv \gamma$$

$$\frac{d\ |f_5(j\omega)|_{db}}{d\ \log_{10} \omega a^2} = \frac{1}{\gamma^2}\Big\{\Big(e^{a\sqrt{2\omega}} \cos a\sqrt{2\omega} + B_1 e^{a\sqrt{\omega/2}} \cos a\sqrt{\omega/2} + 1\Big)$$

$$\Big(\sqrt{2}\, e^{a\sqrt{2\omega}}\,(\cos a\sqrt{2\omega} - \sin a\sqrt{2\omega}) + B_1/\sqrt{2}\, e^{a\sqrt{\omega/2}}\,(\cos a\sqrt{\omega/2} - \sin a\sqrt{\omega/2})\Big)$$

$$+\Big(e^{a\sqrt{2\omega}} \sin a\sqrt{2\omega} + B_1 e^{a\sqrt{\omega/2}} \sin a\sqrt{\omega/2}\Big)$$

$$\Big(\sqrt{2}\, e^{a\sqrt{2\omega}}\,(\sin a\sqrt{2\omega} + \cos a\sqrt{2\omega}) + B_1/\sqrt{2}\, e^{a\sqrt{\omega/2}}\,(\sin a\sqrt{\omega/2} + \cos a\sqrt{\omega/2})\Big)\Big\} \tag{11}$$

Certain important features are to be noted in Figs. 6-3 and 6-4. In particular, the most rapid changes in slope occur in the second order polynomials for which B_1 approaches -2. For a filter design with sharp cutoff these polynomials should be placed only in the denominator of the filter transfer function; it will be necessary to verify that the function meets

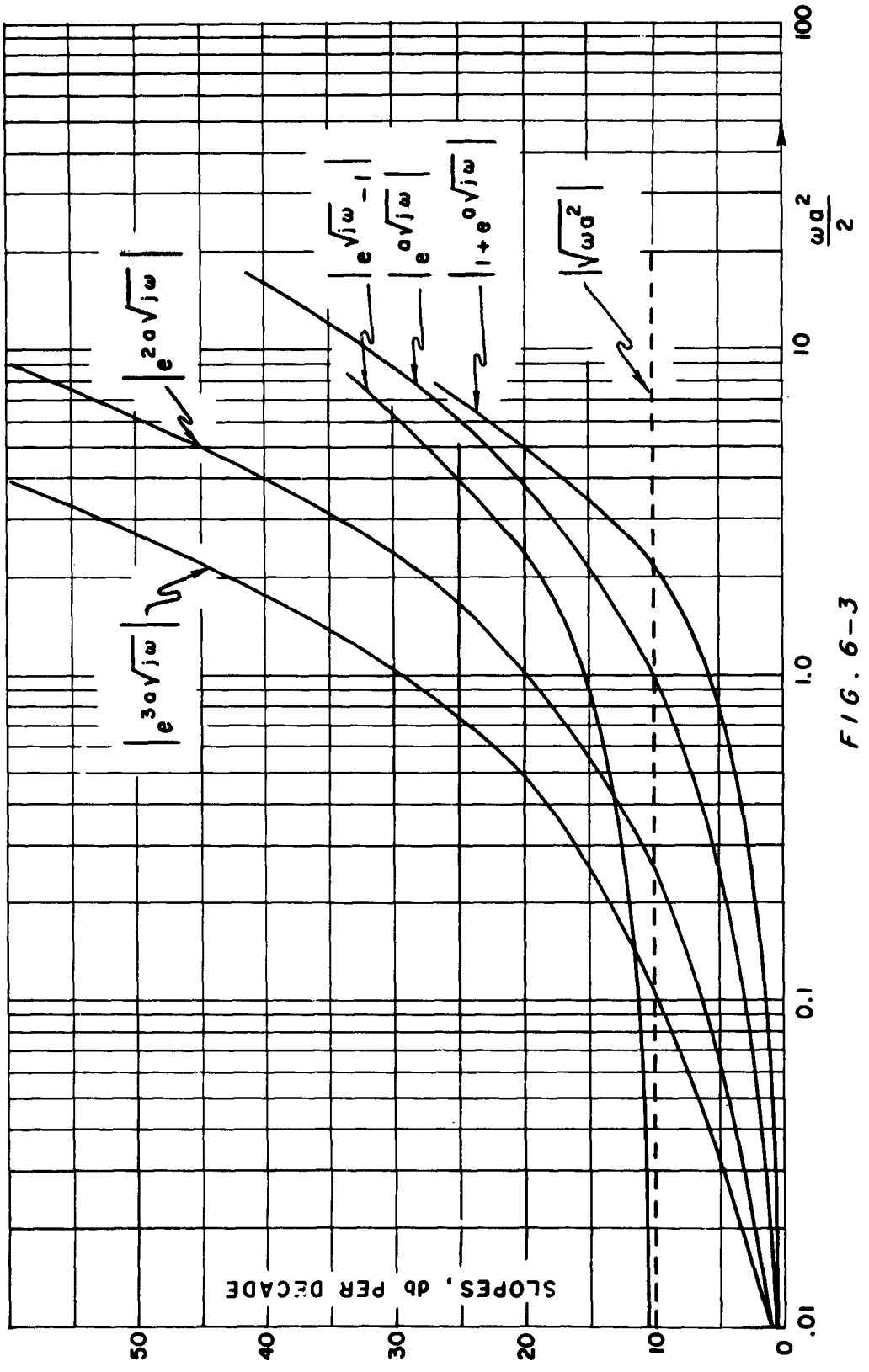

FIG. 6-3

SLOPES OF EXPONENTIAL FACTORS

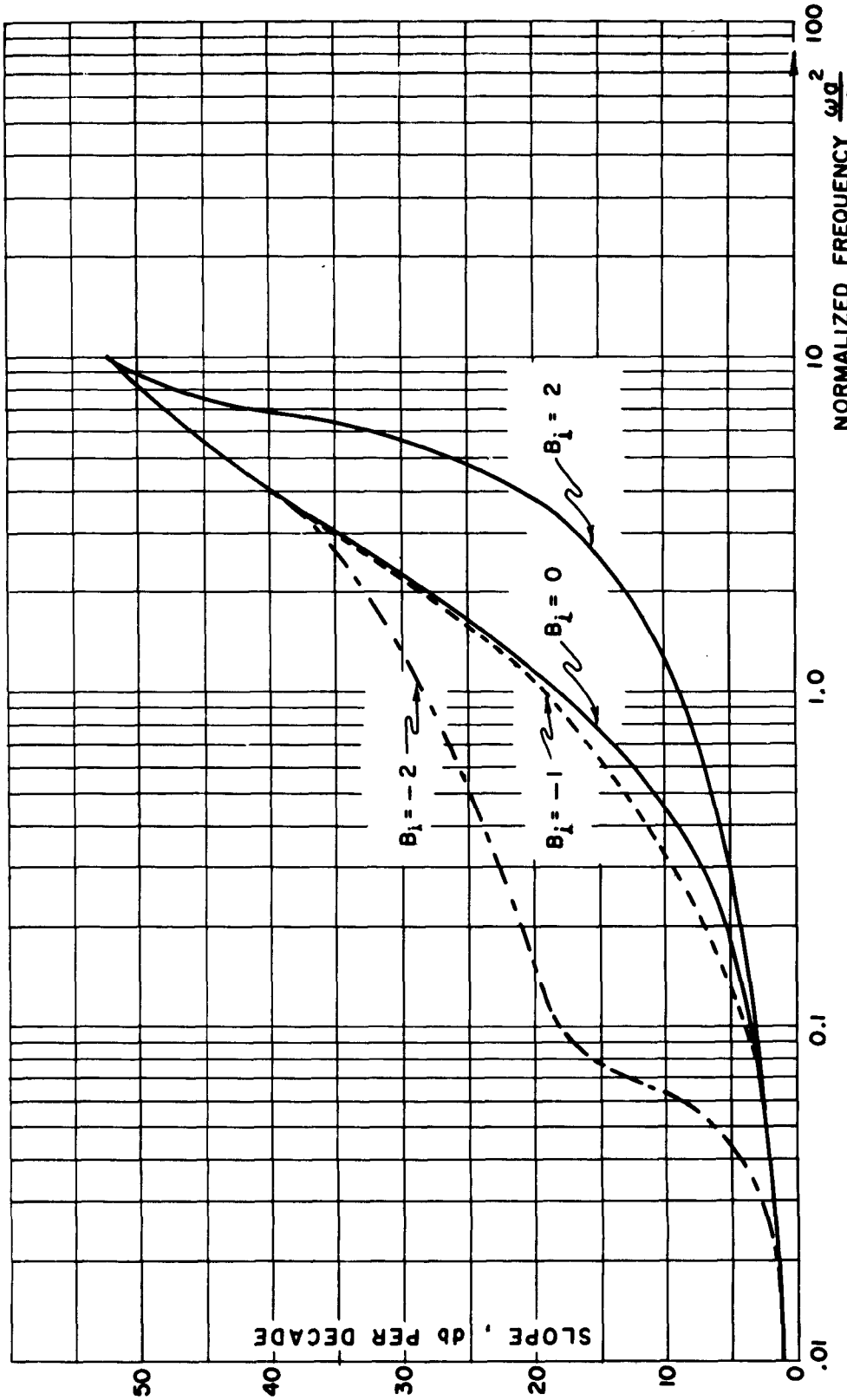

FIG. 6-4

SLOPES OF SECOND ORDER EXPONENTIAL PODYNOMIAL FACTORS

the realizability conditions developed in Chapters Four and Five. Moreover, at the frequency corresponding to the rapid change in slope of the second order polynomials, the functions of Fig. 6-3 are only slowly changing in magnitudes. Thus the second order polynomials may be expected to dominate the frequency characteristics in the band of interest. The plots are frequency normalized, and the break-frequency region may be adjusted by changing the value of $a = 2(RC)^{\frac{1}{2}}$.

6.3 The Design of Low Pass Filters

If a low pass filter characteristic is required to have the sharpest cutoff practically possible for a given number of segments with a monotonically decreasing function, its transfer admittance will lack any second order polynomial factors in the numerator (n=0). In accordance with the realizability conditions stated in Chapter Five, the low pass filter will be of the form

$$-y_{21}(s) = \frac{\sqrt{s}\,(e^{a\sqrt{s}}+1)^{2m-q+1}\,e^{qa\sqrt{s/2}}}{(e^{a\sqrt{s}}-1)\prod_{k=1}^{m}(e^{2a\sqrt{s}}+A_k e^{a\sqrt{s}}+1)} \qquad (12)$$

where q is equal to the number of cascade segments, and no stubs are required. To obtain further quantitative insight, the first eight low pass filters may be listed, with all combinations of q and m, in accordance with Eq. (12).

Number of Sections	q	m	2m-q+1	A_1	A_2	A_3
1	1	0	0	--	--	--
2	2	0	-1	--	--	--
3	3	1	0	-2*	--	--
4	4	1	-1	-2*	--	--
5	5	2	0	-2*	-1.9	--
6	6	2	-1	-2*	-1.9	--
7	7	3	0	-2*	-1.9	-1.85
8	8	3	-1	-2*	-1.9	-1.85

In the above table, blanks indicate that the terms do not occur. The A_1 were chosen as close to -2 as practically possible, realizing that another set of such second order polynomials must be specified which will alternate with these, and will appear in the numerator of the $y_{11}(s)$ function. Choosing the numbers A_1 as above usually requires that calculations in the S plane be carried out to at least five places, since subtraction of almost equal quantities becomes likely with the application of Richard's Theorem.

If the open circuit voltage gain A_V rather than the transfer admittance is the quantity of interest in the filter design, it may be obtained from

$$A_V = -y_{21}/y_{22} \tag{13}$$

Magnitude-normalized y_{22} terms for several values of q are given in (14).

$$q = 1 \qquad y_{22} = \frac{\sqrt{s}\,(e^{a\sqrt{s}} + 1)}{e^{a\sqrt{s}} - 1} \tag{a}$$

$$q = 2 \qquad y_{22} = \frac{\sqrt{s}\,(e^{2a\sqrt{s}} + B_1 e^{a\sqrt{s}} + 1)}{(e^{a\sqrt{s}} + 1)(e^{a\sqrt{s}} - 1)} \tag{b}$$

(14)

$$q = 4 \qquad y_{22} = \frac{\sqrt{s}\prod_{1}^{2}(e^{2a\sqrt{s}} + B_i e^{a\sqrt{s}} + 1)}{(e^{a\sqrt{s}} + 1)(e^{a\sqrt{s}} - 1)(e^{2a\sqrt{s}} + Ae^{a\sqrt{s}} + 1)} \qquad (c)$$

$$q = 8 \qquad y_{22} = \frac{\sqrt{s}\prod_{1}^{4}(e^{2a\sqrt{s}} + B_i e^{a\sqrt{s}} + 1)}{(e^{a\sqrt{s}} + 1)(e^{a\sqrt{s}} - 1)\prod_{1}^{3}(e^{2a\sqrt{s}} + A_i e^{a\sqrt{s}} + 1)} \qquad (d) \qquad (14)$$

For the low pass filter,

$$\begin{aligned} m &= q/2 - 1, \quad (q \text{ even}) \\ m &= (q-1)/2, \quad (q \text{ odd}) \end{aligned} \qquad (16)$$

$$\begin{aligned} 2m - q + 1 &= -1, \qquad (q \text{ even}) \\ 2m - q + 1 &= 0, \qquad (q \text{ odd}) \end{aligned} \qquad (17)$$

Taking the case when q is even, a general expression may be written for the open circuit voltage gain, in terms of s and q:

$$A_V = \frac{e^{q/2\, a\sqrt{s}}}{\prod_{1}^{q/2}(e^{2a\sqrt{s}} + B_i e^{a\sqrt{s}} + 1)} \qquad (18)$$

The sharpness with which the frequency characteristic of A_V may break initially depends primarily on the number of B_i terms which may be clustered about $B_i = -2$. If the original A_i terms of y_{21} are chosen for values of A_i which are close together (but which can not be identical), the values of B_i must alternate with those of A_i according to Theorem VI in Chapter Four. Thus the values of B_i will be very close to those of A_i.

Plots of one, four and eight segment low pass filter characteristics appear in Fig. 6-5, where they are compared with Thompson (Bessel) and Butterworth filters which have been normalized so that they possess the same 3 db points. It is to be noted from this figure, and (18) that $|A_v|$ of the q segment $\overline{URC}$ filter decreases without bound as q approaches infinity. The characteristic, however, can never reach that of the ideal filter, since this would imply an infinity of identical second order exponential polynomials in (18) which is precluded by Theorem VI.

6.4 Example of Low Pass Filter Design With Sharp Cutoff

A synthesis example of the fourth order, frequency and magnitude normalized, low pass filter follows. Theoretical and experimental data are given in Fig. 6-6. The filter was not designed to meet specific requirements, but rather to find how sharp a cutoff might practically be realized by a four-section $\overline{RC}$ filter. From Eq. (14(c)),

$$y_{22}(s) = \frac{\sqrt{s}\prod_{1}^{2}(e^{2a\sqrt{s}} + B_1 e^{a\sqrt{s}} + 1)}{(e^{a\sqrt{s}} + 1)(e^{a\sqrt{s}} - 1)(e^{2a\sqrt{s}} + A_1 e^{a\sqrt{s}} + 1)}$$

Application of the $s \to S$ transformations yields

$$y_{22}(S) = \frac{\left(\left(\frac{1+S}{1-S}\right)^2 - B_1\left(\frac{1+S}{1-S}\right) + 1\right)\left(\left(\frac{1+S}{1-S}\right)^2 + B_2\left(\frac{1+S}{1-S}\right) + 1\right)}{\left(\left(\frac{1+S}{1-S}\right)^2 - 1\right)\left(\left(\frac{1+S}{1-S}\right)^2 + A_1\left(\frac{1+S}{1-S}\right) + 1\right)}$$

$$= \frac{\left(S^2(2-B_1) + (2+B_1)\right)\left(S^2(2-B_2) + (2+B_2)\right)}{4S\left((2-A_1)S^2 + (2+A_1)\right)}$$

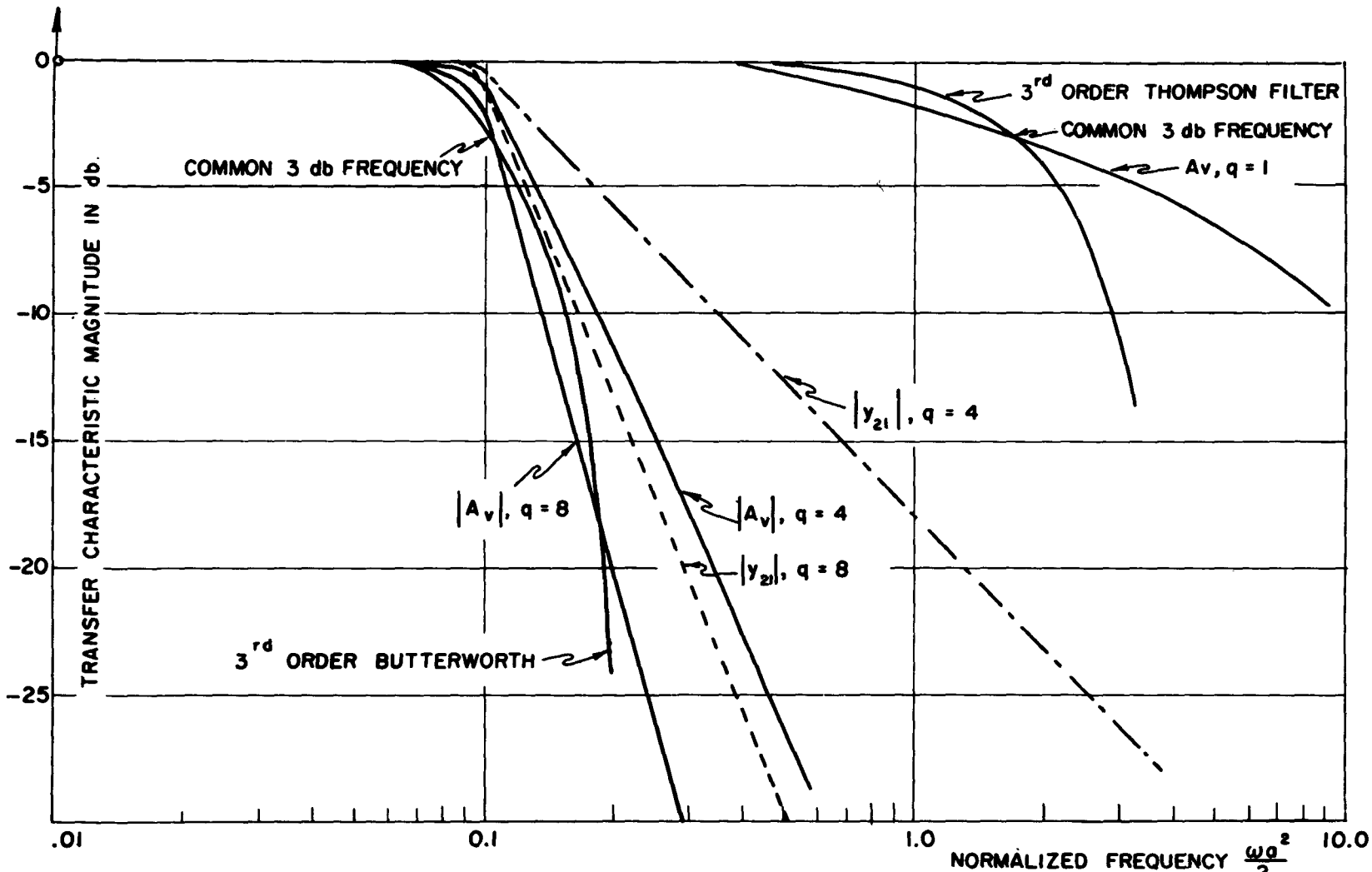

FIG. 6-5

THEORETICAL LOW PASS FILTER CHARACTERISTICS

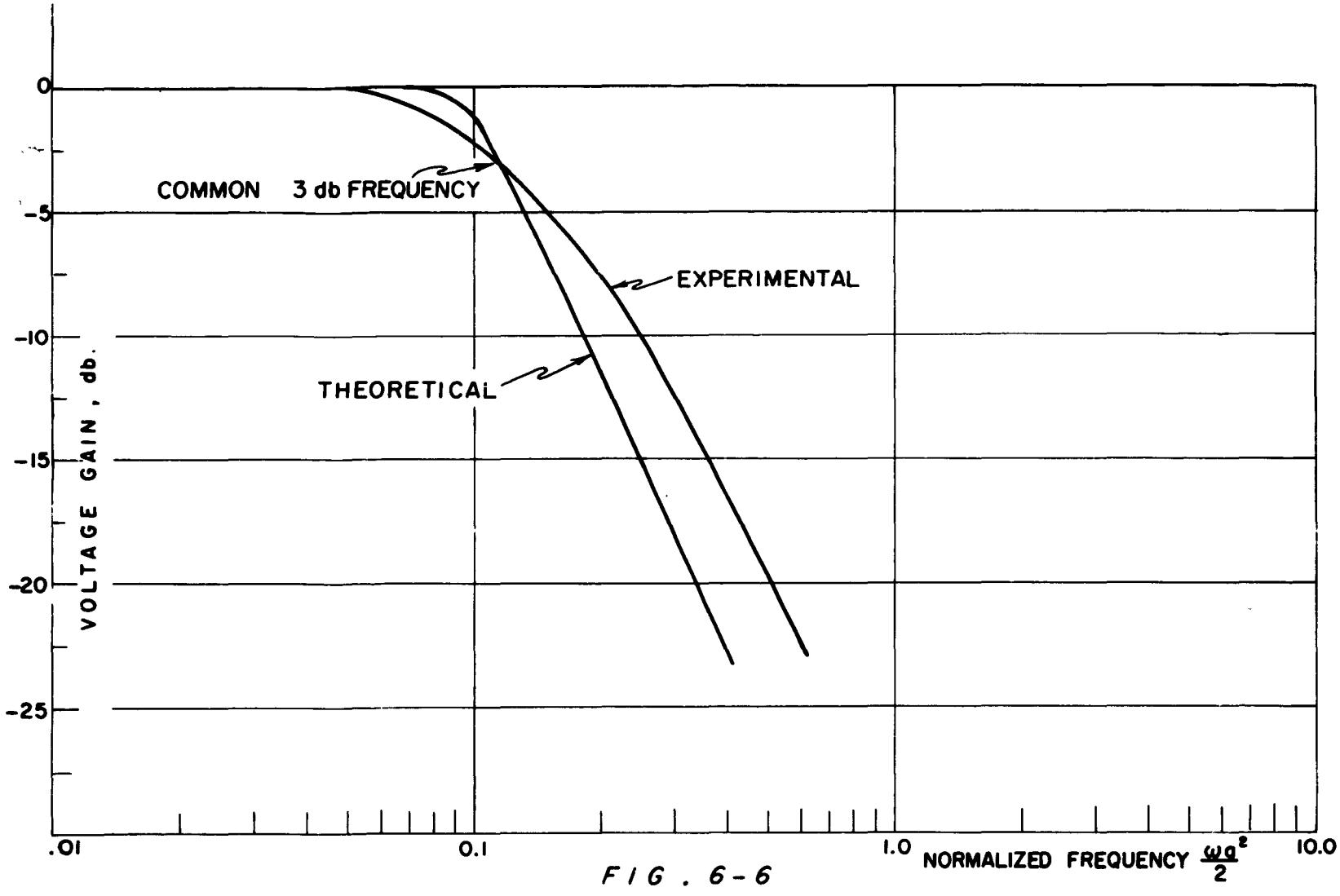

FIG. 6-6

FOUR SECTION FILTER CHARACTERISTICS

Choosing

$$B_1 = -1.9, \quad B_2 = -1.8, \quad \text{and } A_1 = -1.85,$$

$$y_{22}(S) = .96 \left[\frac{(S^2 + .02565)\,(S^2 + .0526)}{S\,(S^2 + .039)} \right]$$

Design the $\overline{RC}$ network for

$$y(S) = \frac{(S^2 + .02565)\,(S^2 + .0526)}{S\,(S^2 + .039)}$$

$$y(1) = 1.03485$$

Application of Richard's Theorem causes

$$y_2(S) = y(1)\,\frac{y(S) - S\,y(1)}{y(1) - S\,y(S)}$$

$$= \frac{.03622}{S} \left[\frac{S^2 + .0359}{S^2 + .04015} \right]$$

$$y_2(1) = .036028$$

$$y_3(S) = y_2(1)\,\frac{y_2(S) - S\,y_2(1)}{y_2(1) - S\,y_2(S)}$$

$$= .036028 \; \frac{\frac{1.0053}{S}\,\frac{S^2 + .0359}{S^2 + .04015} - \frac{S^2}{S}}{1 - 1.0053\,\frac{S^2 + .0359}{S^2 + .04015}}$$

$$= 8.87 \left[\frac{S^2 + .0352}{S} \right]$$

$$y_3(1) = 9.1805$$

$$y_4(S) = y_3(1) \frac{\frac{y_3(S)}{y_3(1)} - S}{1 - \frac{S\, y_3(S)}{y_3(1)}}$$

$$= 9.1805 \frac{\frac{.9648\ (S^2 + .0352)}{S} - S}{1 - \frac{.9648\ (S^2 + .0352)S}{S}}$$

$$y_4(S) = \frac{.321}{S}$$

$$y_4(1) = .321$$

In summary,

$$y_1(1) = \frac{\sqrt{\tau}}{R_1} = 1.035$$

$$y_2(1) = \frac{\sqrt{\tau}}{R_2} = .036$$

$$y_3(1) = \frac{\sqrt{\tau}}{R_3} = 9.18$$

$$y_4(1) = \frac{\sqrt{\tau}}{R_4} = .321$$

From the above calculations, the space-normalized network configuration of Fig. 6-7 may be achieved. Practical difficulties arise in the fabrication of the above network using Teledeltos Paper, in that the

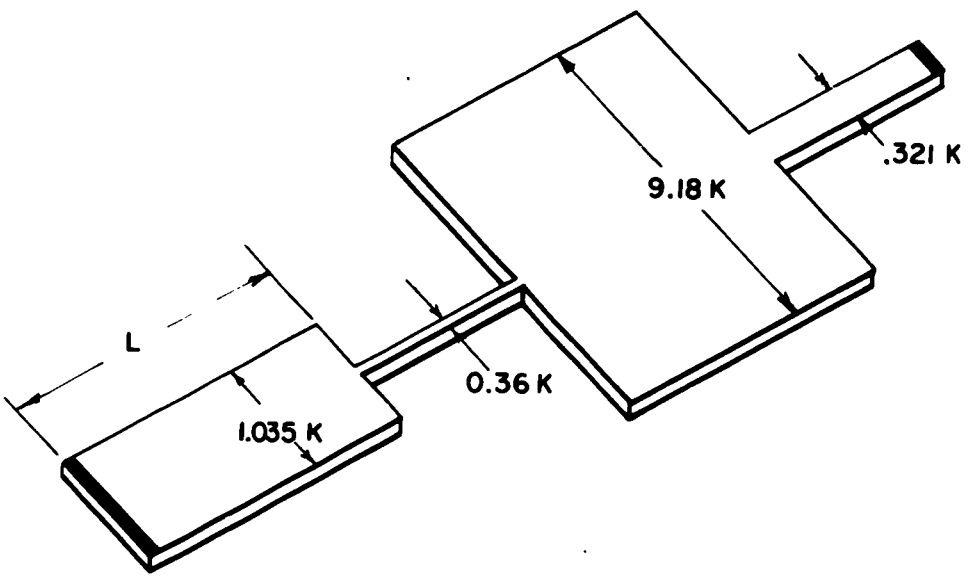

FIG. 6-7

LOW PASS FILTER

segment of width .036 k, which is the narrowest segment, is about 1/250 as wide as the widest segment. If the network were built using masking and deposition techniques, the narrowest segment could practically be made a few mils wide, and the width of the widest segment would still be a practical size. With Teledeltos, 1/32" is a practical lower limit.

As a simple alternative, the narrowest segment was increased in width by a factor of eight over the design value, and poorer cutoff frequency characteristics were accepted. The results are given in Fig. 6-6, where they are compared with expected results.

6.5 Conclusions

This chapter has concerned itself with the actual details of construction of $\overline{RC}$ networks. A low pass filter design problem was employed as the vehicle to illustrate the difficulties of such construction, and to indicate the constraints placed on the physical network realization by the original assumptions in the mathematical models, as well as the design values which are obtained from the synthesis technique. The Teledeltos models used for experimental verification have been illustrated, and were used for all experimental results in earlier chapters.

CHAPTER SEVEN

CONCLUSIONS

The synthesis procedures presented herein are the first simple mathematical techniques applicable to distributed RC networks. The methods introduced here differ significantly from those presently available in that they do not require recourse to a digital computer for their application. Moreover, because the actual synthesis employs an auxiliary complex plane, the calculations may be accomplished with pencil and pad. The synthesis techniques find immediate application in the field of microelectronics.

A contribution to the distributed RC characterization problem has been developed with the introduction of the 'exponential polynomial' approximation of frequency-magnitude characteristics. As was shown in Chapter Two, $\overline{RC}$ networks are described, not by rational functions in the complex frequency variable s, but rather by rational functions in $e^{a\sqrt{s}}$. This property has been exploited by approximating the RC driving point and transfer immittance functions by ratios of polynomial factors which are rational in $e^{a\sqrt{s}}$ and which possess well-behaved magnitudes for values of $s = j\omega$. It is to be emphasized that once the characterization of an immittance by appropriate exponential polynomials is accomplished, the synthesis of the corresponding network function by the methods herein is exact.

The accomplishment of the exact synthesis, which is particularly notable, results from the introduction of the $S \Longrightarrow s$ transformations,

where $e^{a\sqrt{s}} = \frac{1 + S}{1 - S}$. The transformation reduces the synthesis problems associated with the use of $\overline{URC}$ networks to those of lumped, lossless networks. Because of the hyperbolic nature of the distributed network functions, it is no longer practical to think in terms of pole-zero plots, since each $\overline{RC}$ segment contributes an infinity of denumerable poles and zeros, all of which are intimately related.

It has been demonstrated that a practical realization for $\overline{RC}$ networks is a cascade configuration. Such a network is particularly attractive from the fabrication viewpoint, since it minimizes interconnections, network area, and the total number of fabrication properties. Accordingly, Richard's Theorem was applied to develop synthesis techniques which permit the realization of a very wide class of impedances having monotonically decreasing magnitude. Experimental results have confirmed the validity of the theory.

By extending the application of Richard's Theorem, methods have been determined to realize a wide class of transfer immittance and gain functions. Practical network configurations have been suggested, which generally take the form of cascaded $\overline{RC}$ segments using stub (shunt) branches to realize the numerator functions of the transfer terms. Without the stubs, only zeros at infinity are realizable. A specific extraction cycle to determine the stub values and locations, as well as realizability conditions have been given. The theoretical development has been applied to the synthesis of a network to meet specified requirements. Subsequent measurements agree well with those predicted theoretically.

REFERENCES

1. W. Happ and P. Castro. "Distributed Parameter Design Techniques." Lockheed Missile and Space Company Report 6-59-61-1 (November 1961).

2. W. Happ and P. Castro. "Distributed Parameter Circuits and Microsystems Electronics." N.E.C. Proceedings, Chicago, Illinois, vol. 16, pp. 448-460 (1960).

3. C. Holm. "Distributed Resistor-Capacitor Networks for Microminiaturization." Royal Radar Establishment Technical Note 654, Malvern Works, England (August 1959).

4. I. Sugai. "The Solutions of Non-Uniform Transmission Line Problems." Proc. IRE (Correspondence) vol. 48, pp. 1489-90 (August 1960).

5. I. Jacobs. "A Generalization of the Exponential Transmission Line." Proc. IRE, vol. 47, pp. 97-8 (January 1959).

6. F. B. Hilderbrand. Advanced Calculus for Engineers. New York: Prentice Hall, p. 50, 1948.

7. M. Hellstrom. "A New Class of Distributed RC Ladder Networks." IRE Proceedings, vol. 50, no. 9, pp. 1989-90 (September 1962).

8. Joel Ekstrom. "A Theoretical Comparison of Doubly Loaded Distributed Bridge T and Lumped Twin T. RC Notch Filters." Sylvania Engineering Note EN301, Waltham, Massachusetts (January 30, 1962). Given in less detail at IRE Convention, March 1962, with the same title.

9. G. Herskowitz and R. Wyndrum. "Distributed $\overline{RC}$ Networks for Approximately Maximally Flat Narrow Band Amplifiers." Proc. East Coast Conference on Aerospace and Navig. Electronics, Baltimore, Maryland (October 22, 1962).

10. R. Wyndrum. "Distributed $\overline{RC}$ Networks." I.E.E.E. Proceedings (Correspondence) vol. 51, no. 2, pp. 374-5 (February 1963).

11. Manfred Kahn. "Distributed Network Oscillators and Bandpass Amplifiers." Presented at Electronic Components Conference, Washington, D.C., May 9, 1962. Available as Sprague Technical Paper 62-10, Sprague Electric Co., North Adams, Massachusetts.

12. P. Castro. "Design Criteria for a Microsystems Bandpass Amplifier." Lockheed Report LMSD-703112 (August 1960), Lockheed Missile and Space Division, Sunnyvale, California.

13. G. Riddle. "Bandpass Amplifiers Using Distributed Parameter Networks." Proc. ECCANE, Baltimore, Maryland (October 22, 1962).

14. W. M. Kaufman. "Theory of a Monolithic Null Device and Some Novel Circuits." Proc. IRE, vol. 48, pp. 1540-1545 (September 1960).

15. R. Wyndrum. "Microelectronic Active Filters." New York University Technical Report 400-59, College of Engineering, New York (May 1962).

16. P. Richards. "Resistor Transmission Line Circuits." Proc. IRE, vol. 30, no. 2, p. 217-220 (February 1948).

17. M. H. Hellstrom. "Equivalent Distributed RC Networks or Transmission Lines." IRE Transactions, vol. CT-9, no. 3, p. 247 ff (September 1962).

18. F. M. Reza. "On the Schlicht Behavior of Certain Impedance Functions." IRE Transactions, vol. CT-9, no. 3, pp. 231-3 (September 1962).

19. P. Weimer. "The TFT-A New Thin Film Transistor." Proc. IRE, vol. 50, no. 6, pp. 1462-70 (June 1962).

20. A. Van der Ziel. "Shot Noise in Thin Film Transistors." Proc. IRE, vol. 50, no. 9, pp. 1985-6 (September 1962).

21. L. Weinberg. Network Analysis and Synthesis. New York: McGraw Hill, 1961.

22. N. Balbanian and S. Seshu. Linear Network Analysis. New York: John Wiley, 1959, p. 372.

23. Zeev Nehari. Conformal Mapping, New York: McGraw Hill, 1959.

24. M. Van Valkenburg. Modern Network Synthesis. New York: John Wiley, 1961.

25. B. Gross and E. P. Braga. Singularities of Linear Systems. Amsterdam: Elsevier Publishing Co., 1961.

26. H. Ozaki and J. Ishii. "Synthesis of a Class of Strip-Line Filters." IRE Transactions, vol. CT-5, no. 2, pp. 104-109 (June 1958).

27. N. Ikeno. "Design of Distributed Constant Networks." Electrical Communication Laboratory, Tokyo, Japan, July 1955. Translated by Akio Matsumoto, Microwave Research Institute, Brooklyn, New York, while a visiting fellow, as Report PIBMRI-1003-62, dated October 10, 1962 under contract AF-30(602)-2213.

28. P. I. Richards. "A Special Class of Functions with Positive Real Part in a Half-Plane." Duke Mathematical Journal, vol. 14, no. 3, pp. 717-786 (September 1947).

29. W. W. Happ and G. C. Riddle. "Limitations of Film Type Circuits Consisting of Resistive and Capacitive Layers." IRE National Convention Record, vol. 9, pt. 6, pp. 141-65 (1961). See Fig. 1, p. 152.

30. Ruel Burnham. "Design Techniques for Several Molecular-Electronic Circuits with the Controlled Field Approach." Master's Thesis, Air University, Dayton, Ohio (August 1961).

31. H. W. Bode. Network Analysis and Feedback Amplifier Design. Princeton: D. Van Nostrand, 1946.

32. D. E. Thomas. "Tables of Phase of Semi-Infinite Unit Slope of Attenuation." Bell System Technical Journal, vol. 35, pp. 747-9 (May 1956); also Monograph 2550, Bell Telephone Laboratories, New York.

33. E. Weber. Linear Transient Analysis. Vol. II, New York: John Wiley, 1956, p. 112.

34. A. Paige and E. S. Kuh. "Maximum Gain Realization of an RC Ladder Network." IRE Transactions, vol. CT-8, pp. 32-39 (March 1960).

VITA

Ralph W. Wyndrum, Jr. was born in Brooklyn, New York, on April 30, 1937. He attended Columbia College, and Columbia University School of Engineering, from which he received his B.S. and M.S. degrees in electrical engineering in 1959 and 1960, respectively. During the summers 1955 through 1960, and in 1962, he was employed at Grumman Aircraft Engineering Corporation, where his last assignments included microelectronic computer design, thermoelectric generator design and antenna field testing. Mr. Wyndrum has been an instructor at New York University in the Department of Electrical Engineering since September 1961, where he has taught courses in the area of network theory and electronics. Mr. Wyndrum is the author of several papers, and is a member of Eta Kappa Nu, Sigma Xi, The Institute of Electrical and Electronics Engineers, and The American Association for the Advancement of Science. He held the A.M.F. Fellowship in 1962-3, a Regent Fellowship in 1959-61 and was a Grumman Scholar from 1955 through 1959.

APPENDIX I: Proofs of New Theorems in Text

Theorem II: If $Z_{RC}(s)$ is the driving point impedance of a $\overline{URC}$ network composed of segments with $RC = (a/2)^2$, then $Z_{LC}(S_1) = \sqrt{s}\, Z_{RC}(s)$ with $S_1 = \tanh(a\sqrt{s}/2)$ is the driving point impedance of a lumped LC network.

Proof: If $Z_{RC}(s)$ is the driving point impedance of any RC network, $\sqrt{s}Z(s)$ will be an LC function in the $\sqrt{s}$ plane.[21,22] Moreover, a positive real transformation for which $\mathrm{Re}\sqrt{s} = 0 \rightarrow \mathrm{Re}\ S = 0$ (i.e., $S_1(\sqrt{s})$) of an LC function is again an LC function, so that $Z(S_1)$ is in fact LC. To show that it is lumped and LC, consider the two possibilities in Fig. 2-2 (b) and (c). The $\overline{URCS}$ and $\overline{URCO}$ driving point impedances become $S_1\sqrt{R/C}$ and $(1/S_1)\sqrt{R/C}$ respectively, which are indeed lumped impedances in the S plane.

Theorem III: If $Z_{RC}(s)$ is the driving point impedance of a $\overline{URC}$ network composed of segments with $RC = (a/2)^2$, $Z_{LC}(S_2) = \sqrt{s}\, Z_{RC}(s)$ with $S_2 = \coth(a\sqrt{s}/2)$ is a lumped LC driving point impedance in the S_2 plane.

Proof: Since $S_2(\sqrt{s})$ is positive real with $\mathrm{Re}\sqrt{s} = 0 \rightarrow \mathrm{Re}\ S = 0$, the proof follows as above to show that $Z(S_2)$ is LC. To show that $Z(S_2)$ is lumped, apply S_2 to the two networks of Fig. 2-2 (b) and (c). The resulting impedances are $(1/S_2)\sqrt{R/C}$ and $S_2\sqrt{R/C}$ respectively.

Theorem IV: $Z(s)$ may be realized as the driving point impedance of a finite number of elemental $\overline{URCS}$ and $\overline{URCO}$ networks using (4-7) (and similarly (4-8)) if and only if

a) $Z(s)$ may be expressed as

$$Z(s) = \frac{k_\infty}{\sqrt{s}} \tanh \frac{a\sqrt{s}}{2} + \frac{k_o}{\sqrt{s} \tanh \frac{a\sqrt{s}}{2}} + \sum_{i=1}^{n} \frac{2 k_i \tanh \frac{a\sqrt{s}}{2}}{\sqrt{s} \left[\tanh^2 \frac{a\sqrt{s}}{2} + \Omega^2_i\right]}$$

b) where k_∞, k_o, and $k_i \geq 0$

Proof: $Z(s)$, under (4-7) (and similarly, under (4-8)), is transformed to

$$Z(S) = k_\infty S + \frac{k_o}{S} + \sum_{i=1}^{n} \frac{2k_i S}{S^2 + \Omega_i^2}$$

which is an LC driving point impedance if k_∞, k_o, and $k_i \geq 0$.

Theorem V: $Z(s)$ may be realized as the driving point impedance by a finite number of elemental $\overline{URCS}$ and $\overline{URCO}$ networks of constant RC product using (4-7) or (4-8) if and only if

a) $\sqrt{s}\ Z(s)$ is a rational real function of $e^{a\sqrt{s}}$, a real and positive.

b) Re $(\sqrt{s}\ Z(s)) = 0$ for $\sqrt{s} = jq$, q real

or $s = -q^2$, q real

c) Re $(\sqrt{s}\ Z(s)) \geq 0$, Re$\sqrt{s} \geq 0$

Proof: $Z(S)$, using either (4-7) or (4-8), must be a reactance function in S. Hence, since either (4-7) or (4-8) are positive real, (a), (b), and (c) follow as necessary conditions. Re $Z(j\omega) \to 0$ as $\omega \to \infty$, since the $\overline{URC}$ shunt capacitance has zero impedance as $\omega \to \infty$. The sufficiency of (a) - (c) is shown by noting that, under (4-7) and (4-8), $\sqrt{s}\ Z(s)$

must be transformed into an LC function in the S plane, of the form of Theorem IV.

Theorem VI: Z(s) may be realized as a URC network under (2-7) if and only if $\sqrt{s}\ Z(s)$ may be expressed as

$$\sqrt{s}\ Z(s) = \frac{(e^{a\sqrt{s}} + 1)^{2(m-n)+1}}{(e^{a\sqrt{s}} - 1)} \frac{\prod_1^n (e^{2a\sqrt{s}} + B_k e^{a\sqrt{s}} + 1)}{\prod_1^m (e^{2a\sqrt{s}} + A_k e^{a\sqrt{s}} + 1)}$$

or its inverse, where $A_k > B_k$, $|A_k| < Z$, $|B_k| < Z$, and $m = n$ or $n - 1$.

Proof Case 1:

$$\sqrt{s}\ Z(s) = \frac{(e^{a\sqrt{s}} + 1)}{(e^{a\sqrt{s}} - 1)} \prod_1^n \left[\frac{e^{2a\sqrt{s}} + B_k e^{a\sqrt{s}} + 1}{e^{2a\sqrt{s}} + A_k e^{a\sqrt{s}} + 1} \right]$$

$$Z(s) = \frac{1}{S} \prod_1^n \left(\frac{2 - B_k}{2 - A_k} \right) \frac{S^2 + \dfrac{2 + B_k}{2 - B_k}}{S^2 + \dfrac{2 + A_k}{2 - A_k}}$$

$$= \frac{1}{S} \prod_1^n \left(\frac{2 - B_k}{2 - A_k} \right) \left(\frac{S^2 + D_k^2}{S^2 + C_k^2} \right)$$

For Z(S) to be LC in the S plane, pole zero alternation demands that $A_k > B_k$. Since D_k^2 and C_k^2 are positive and real, $|A_k| < 2$ and $|B_k| < 2$.

Case 2:

$$\sqrt{s}\,Z(s) = \frac{1}{(e^{a\sqrt{s}} - 1)(e^{a\sqrt{s}} + 1)} \frac{\prod_{1}^{n} (e^{2a\sqrt{s}} + B_k e^{a\sqrt{s}} + 1)}{\prod_{1}^{n-1} (e^{2a\sqrt{s}} + A_k e^{a\sqrt{s}} + 1)}$$

$$= \frac{1}{4S} \frac{\prod_{1}^{n} (2 - B_k)\left(S^2 + \frac{2 + B_k}{2 - B_k}\right)}{\prod_{1}^{n-1} (2 - A_k)\left(S^2 + \frac{2 + A_k}{2 - A_k}\right)}$$

Again, for Z(S) to be LC, $A_k > B_k$, $|A_k| < 2$, $|B_k| < 2$.

Theorem XI: Using a cascade and stub $\overline{RC}$ network, $y_{12}(s)$ may be realized together with $y_{11}(s)$ within a constant if

a) $y_{11}(s)$ fulfills the conditions of Theorem VI and possesses the same A_i polynomials as $y_{12}(s)$

b) $-y_{12}(s)$ may be expressed as

$$-y_{12}(s) = \frac{\sqrt{s}\, e^{qa\sqrt{s}/2}}{e^{a\sqrt{s}} - 1} \frac{\prod_{1}^{n} e^{2a\sqrt{s}} + B_i e^{a\sqrt{s}} + 1}{(e^{a\sqrt{s}} + 1)^{2(n-m)+q-1} \prod_{1}^{m} (e^{2a\sqrt{s}} + A_i e^{a\sqrt{s}} + 1)}$$

where (1) $|B_i|$, $|A_i| \leq 2$, $A_{i+1} > A_i$, $B_{i+1} > B_i$.

(2) $B_i > A_m$, $i = 1,2,3, \ldots n$.

(3) $B_n > C_n$, where C_n is the largest C_j of the numerator polynomial factors of y_{11}

(4) $m \geq n + (q/2) - 1$.

(5) $q/2 \geq n$.

Proof: Under the transformation $e^{a\sqrt{s}} = \frac{1+S}{1-S}$, the following hold:

$$e^{qa\sqrt{s}/2} = \left(\frac{1+S}{1-S}\right)^{q/2} \quad , \quad \frac{e^{a\sqrt{s}}-1}{e^{a\sqrt{s}}+1} = S \quad , \quad e^{a\sqrt{s}}+1 = \frac{2}{1-S} \quad ,$$

and

$$e^{2a\sqrt{s}} + A\, e^{a\sqrt{s}} + 1 = \frac{S^2(2-A_i)+(2+A_i)}{(1-S)^2}$$

Then (b) above becomes

$$y_{21}(S) = \frac{\left(\frac{1+S}{1-S}\right)^{q/2}}{S} \frac{\prod_1^n \frac{S^2(2-B_i)+(2+B_i)}{(1-S)^2}}{\prod_1^m \frac{S^2(2-A_i)+(2+A_i)}{(1-S)^2} \frac{(2)^{2(n-m)+q-1}}{(1-S)^{2(n-m)+q}}}$$

$$= \frac{(1+S)^{q/2}(1-S)^{q/2}}{S} \frac{\prod_1^n S^2(2-B_i)+(2+B_i)}{\prod_1^m S^2(2-A_i)+(2+A_i)}$$

$$= k \frac{(1-S^2)^{q/2}}{S} \frac{\prod_1^n (S^2+\beta_i^2)}{\prod_1^m (S^2+\alpha_i^2)}$$

This expression satisfies the conditions of Corollary III if (a) thru (c) of Corollary III are met; i.e.,

1) is a statement of the fact that all transmission poles, and transmission zeros not at $S = \pm 1$, lie on the imaginary axis of the S plane.

2) is a direct consequence of (b)

3) is a direct consequence of (c)

APPENDIX II: Derivation of the Basic Field Equations for the $\overline{URC}$ Segment

Consider the structure of Fig. A-2-1. Let $V(x,y,t)$ be the potential between the resistive layer and the conductor. Assume an ideal conductor, and a lossless dielectric of negligible thickness. Then the surface current density and potential are given by

$$\nabla \cdot \bar{J}_s = -C \frac{\partial V}{\partial t} \tag{A2-1}$$

$$\nabla V = -R\bar{J}_s \tag{A2-2}$$

where R is the resistance per square, and C is the capacitance per unit area. Then (1) and (2) imply

$$\nabla^2 V = \nabla \cdot \nabla \quad V = RC \frac{\partial V}{\partial t} \quad . \tag{A2-3}$$

The general solution for e^{st} excitation is

$$V(x,y,t) = (Ae^{-\gamma_x x} + Be^{\gamma_x x})\ (Ce^{-\gamma_y y} + De^{\gamma_y y})e^{st} \tag{A2-4}$$

$$\gamma_x^2 + \gamma_y^2 = sRC \tag{A2-4a}$$

Similarly the current components are (for $\bar{J}_s = J_x\hat{a}_x + J_y\hat{a}_y$)

$$J_x e^{st} = \frac{\gamma_x}{R}\ (Ce^{-\gamma_y y} + De^{\gamma_y y})\ (Ae^{-\gamma_x x} - Be^{\gamma_x x})e^{st} \tag{A2-5}$$

and

$$J_y e^{st} = \frac{\gamma_y}{R}\ (Ae^{-\gamma_x x} + Be^{\gamma_x x})\ (Ce^{-\gamma_y y} - De^{+\gamma_y y})e^{st} \tag{A2-6}$$

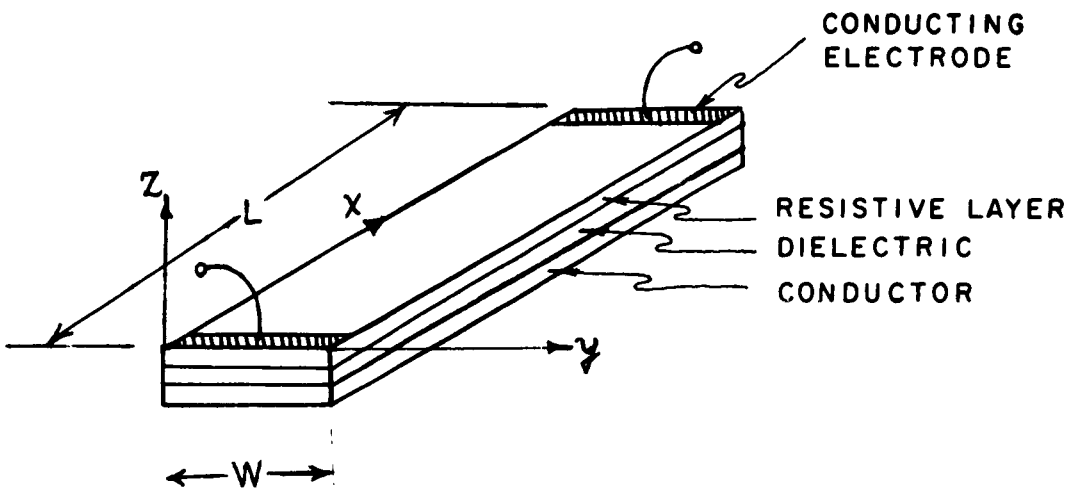

FIG. A 2 - 1

$\overline{URC}$ SEGMENT

The solution of these equations may be made from the conditions. For the uniform rectangular $\overline{URC}$ section, such that $0 \leq x \leq L$ and $0 \leq y \leq W$, with a conducting strip across the edges where the voltage is applied, the boundary conditions are

$$V = V_1 e^{st} \quad \text{for } x = 0 \quad \text{and} \quad V = V_2 e^{st} \quad \text{for } x = L \tag{A2-7}$$

$$J_y = 0 \quad \text{for } y = 0 \quad \text{or } y = W. \tag{A2-8}$$

Under these boundary conditions (4) leads to

$$V_1 = V(0,y) = (A + B)\ (Ce^{-\gamma_y y} + De^{\gamma_y y}) \tag{A2-9}$$

and clearly $\gamma_y = 0$ since V_1 is independent of y.

Thus $\gamma_x = \sqrt{SRC}$ from (4a).

Hence (4) and (7) may be combined to

$$V_2 = (Ae^{-\gamma_x L} + Be^{\gamma_x L})M \qquad \text{when } M = C + D \tag{A2-10}$$

and

$$J_x = \frac{\gamma_x}{R}\ (M)\ (Ae^{-\gamma_x x} - Be^{\gamma_x x}) \tag{A2-11}$$

since $M \neq 0$

$\gamma_x \neq 0$

and $J_y\Big|_{y=0} = 0$ since $\gamma_y = 0$. (A2-12)

In summary, then, $V(x)$ and $J_x(x)$ are functions of x only, and $J_y(x) = 0$.

$$V_1 = (A+B)M \tag{A2-13}$$

$$V_2 = (Ae^{-\gamma_x L} + Be^{\gamma_x L})M \tag{A2-14}$$

or, letting $\alpha = MA$, $\beta = MB$

$$V_1 = \alpha + \beta \tag{A2-15}$$

$$V_2 = \alpha e^{-\gamma_x L} + \beta e^{\gamma_x L} \tag{A2-16}$$

Thus

$$V_2 = (V_1-\beta)\, e^{-\gamma_x L} + \beta e^{\gamma_x L} \tag{A2-17}$$

$$\beta(e^{\gamma_x L} - e^{-\gamma_x L}) = V_2 - V_1\, e^{-\gamma_x L} \tag{A2-18}$$

$$\beta = \frac{V_2 - V_1\, e^{-\gamma_x L}}{2 \sinh \gamma_x L} \tag{A2-19}$$

$$\alpha = \frac{V_1\, e^{\gamma_x L} - V_2}{2 \sinh \gamma_x L} \tag{A2-20}$$

Therefore (A2-21)

$$V(x,y,t) = \left[\left(\frac{V_1\, e^{\gamma_x L} - V_2}{2 \sinh \gamma_x L} \right) \left(e^{-\gamma_x x} \right) + \left(\frac{V_2 - V_1\, e^{-\gamma_x L}}{2 \sinh \gamma_x L} \right) \left(e^{\gamma_x x} \right) \right] e^{st}$$

$$J_x e^{st} = \frac{\gamma_x}{R} \left[\left(\frac{V_1\, e^{\gamma_x L} - V_2}{2 \sinh \gamma_x L} \right) \left(e^{-\gamma_x x} \right) - \left(\frac{V_2 - V_1\, e^{-\gamma_x L}}{2 \sinh \gamma_x L} \right) e^{\gamma_x x} \right] e^{st} \tag{A2-22}$$

where $\gamma_x = \sqrt{sRC}$

$$J_y \equiv 0 \tag{A2-23}$$

The Y and thus the Z parameters (Eqns. 1-5 and 1-6) are rapidly derived from (A2-22). If a load termination, Z_L, provides the terminal condition at x = L, alternate forms of (A2-21) and (A2-22) are

$$I(x,s) = \frac{V_1(s)\left(Z_L + \frac{\gamma_x}{sC}\right)e^{\gamma_x(L-x)} - \left(Z_L - \frac{\gamma_x}{sC}\right)e^{-\gamma_x(L-x)}}{\left(\frac{\gamma_x}{sC}\right)\left(Z_L + \frac{\gamma_x}{sC}\right)e^{\gamma_x L} + \left(Z_L - \frac{\gamma_x}{sC}\right)e^{-\gamma_x L}} \qquad \text{(A2-24)}$$

$$V(x,s) = V_1(s)\frac{\left(Z_L + \frac{\gamma_x}{sC}\right)e^{\gamma_x(L-x)} + \left(Z_L - \frac{\gamma_x}{sC}\right)e^{-\gamma_x(L-x)}}{\left(Z_L + \frac{\gamma_x}{sC}\right)e^{\gamma_x L} + \left(Z_L - \frac{\gamma_x}{sC}\right)e^{-\gamma_x L}} \qquad \text{(A2-25)}$$

Higher order modes might be possible solutions if a finite segment dielectric thickness were considered in the previous analysis. The $\overline{URC}$ segment may be considered as a waveguide with one highly lossy wall (the resistive sheet), a lossless dielectric of thickness "a", and one lossless wall. A thorough library search has failed to uncover any analysis of such a structure from the waveguide point of view, except where the lossy wall is characterized by very small loss. In this case, perturbation techniques have been employed to compute the power dissipated in the lossy wall, assuming a small variation of the TE or TM mode. In such a case, the cutoff frequency is assumed to be that of the lossless case. For the dimensions of practical $\overline{URC}$ segments used in this synthesis technique, the dielectric thickness is of the order of 10^{-2} cm, and the corresponding cutoff frequency for the TE_{10} mode of the lossless case would be of the order of several kilomegacycles, far above our intended operating frequency. Experimental data confirms the use of the two-port parameters derived in Chapter 1, up to hundreds of kilocycles.

DISTRIBUTION LIST

List A

Code	Organization	No. of Copies
AF 5	AFMTC (AFMTC Tech Library-MU-135 Patrick AFB, Fla.	1
AF 18	AUL Maxwell AFB, Ala.	2
AF 32	OAR (RROS, Col. John R. Fowler) Tempo D 4th and Independence Ave, Wash 25, D. C.	3
AF 33	AFOSR, OAR (SRYP) Tempo D. 4th and Independence Ave, Wash 25, D. C.	4
AF 43	ASD (ASAPRD-Dist) Wright-Patterson AFB, Ohio	5
AF 124	RADC (RAALD) Griffiss AFB, New York Attn: Documents Library	6
AF 139	AF Missile Development Center (MDGRT) Holloman AFB, New Mexico	7
AF 314	Hq. OAR (RROSP, Maj. Richard W. Nelson) Wash 25, D. C.	8
Ar 5	Commanding General USASRDL Ft. Monmouth, N. J. Attn: Tech. Doc. Ctr. SIGRA/SL-ADT	9
Ar 9	Department of the Army Office of the Chief Signal Officer Wash 25, D. C. Attn: SIGRD-4a-2	10
Ar 50	Commanding Officer Attn: ORDTL-012 Diamond Ordnance Fuze Laboratories Wash 25, D C.	11
Ar 87	Redstone Scientific Information Center U. S. Army Missile Command Redstone Arsenal, Alabama	12
	State University of New York Dept. of Electrical Engineering Stony Brook, Long Island, New York	13

Code	Organization	No. of Copies
G 2	Defense Documentation Center (DDC) Arlington Hall Station Arlington 12, Virginia	14-33
G 31	Office of Scientific Intelligence Central Intelligence Agency 2430 E Street, N.W. Wash 25, D. C.	34
G 68	Scientific and Technical Information Facility Attn: NASA Representative (S-AK/DL) P.O. Box 5700 Bethesda, Maryland	35
G 109	Director Langley Research Center National Aeronautics and Space Administration Langley Field, Virginia	36
M 6	AFCRL, OAR (CRXRA - Stop 39) L. G. Hanscom Field Bedford. Mass.	37-56
M 83	Hq. AFCRL, OAR (CRTPM) L. G. Hanscom Field Bedford, Mass.	57
N 9	Chief, Bureau of Naval Weapons Department of the Navy Wash 25, D.C. Attn: DLI-31	58-59
N 29	Director (Code 2027) U.S. Naval Research Laboratory Wash 25, D.C.	60-61
I 292	Director, USAF Project RAND The Rand Corporation 1700 Main Street Santa Monica, California THRU: AF Liaison Office	62
G 75	Director National Security Agency Fort George G. Meade, Maryland Attn: G3/TDL	63
	Syracuse University, Dept. of Electrical Engineering Syracuse, New York	64

Code	Organization	No. of Copies
AF 253	Technical Information Office European Office, Aerospace Research Shell Building, 47 Cantersteen Brussels, Belgium	65
AF 318	Aero Res. Lab. (OAR) ARCL Lib. AFL 2292, Bldg. 450 Wright-Patterson AFB, Ohio	66
Ar 107	U. S. Army Aviation Human Research Unit U. S. Continental Army Command P. O. Box 428, Fort Rucker, Alabama Attn: Maj. Arne H. Eliasson	67
G 8	Library Boulder Laboratories National Bureau of Standards Boulder, Colorado	68-69
M 63	Institute of the Aerospace Sciences, Inc. 2 East 64th Street New York 21, New York Attn: Librarian	70
M 84	AFCRL, OAR (CRXR, J. R. Marple) L. G. Hanscom Field Bedford, Mass.	71
N 73	Office of Naval Research Branch Office, London Navy 100, Box 39 F.P.O. New York, N. Y.	72-81
U 32	Massachusetts Institute of Technology Research Laboratory Building 26, Room 327 Cambridge 39, Mass. Attn: John H. Hewitt	82
U 431	Alderman Library University of Virginia Charlottesville, Virginia	83
G 9	Defence Research Member Canadian Joint Staff 2450 Massachusetts Avenue, N.W. Wash 8, D. C.	84-86
	Hq. AFCRL, OAR (CRB, K. Haase) L. G. Hanscom Field, Bedford, Mass.	87-96

Air Force Cambridge Research Laboratories, Office of Aerospace Research, United States Air Force, Bedford, Massachusetts.

Rpt Nr AFCRL-63-157. THE EXACT SYNTHESIS OF DISTRIBUTED RC NETWORKS. Third Scientific report, May 1963, 134 + viii pp. incl illus., 34 refs.

Unclassified Report

The research reported in this thesis is devoted to the development of network synthesis techniques which are exact and applicable to distributed RC functions. Complex Variable transformations are introduced which greatly simplify the representation and use of the hyperbolic complex frequency functions of distributed RC structures. Realizability conditions are given for the existence of distributed RC driving point and transfer functions, and the actual synthesis techniques are described in detail. Examples of the methods introduced herein are verified by experimental data.

1. Network realizability

I. Project 5628, Task 562801
II. Contract AF19(628)-379
III. New York University, College of Engineering, Department of Electrical Engineering, Laboratory for Electroscience Research, University Heights, New York 53, New York
IV. Wyndrum, R.W., Jr.
V. NYU Technical Report 400-76
VI. Aval fr OTS
VII. In DDC collection

Air Force Cambridge Research Laboratories, Office of Aerospace Research, United States Air Force, Bedford, Massachusetts.

Rpt Nr AFCRL-63-157. THE EXACT SYNTHESIS OF DISTRIBUTED RC NETWORKS. Third Scientific report, May 1963, 134 + viii pp. incl illus., 34 refs.

Unclassified Report

The research reported in this thesis is devoted to the development of network synthesis techniques which are exact and applicable to distributed RC functions. Complex Variable transformations are introduced which greatly simplify the representation and use of the hyperbolic complex frequency functions of distributed RC structures. Realizability conditions are given for the existence of distributed RC driving point and transfer functions, and the actual synthesis techniques are described in detail. Examples of the methods introduced herein are verified by experimental data.

1. Network realizability

I. Project 5628, Task 562801
II. Contract AF19(628)-379
III. New York University, College of Engineering, Department of Electrical Engineering, Laboratory for Electroscience Research, University Heights, New York 53, New York
IV. Wyndrum, R.W., Jr.
V. NYU Technical Report 400-76
VI. Aval fr OTS
VII. In DDC collection